Alma Mater Studiorum – Università di Bologna

DOTTORATO DI RICERCA IN

Ingegneria Civile, Chimica, Ambientale e Materiali

Ciclo XXXI

Settore Concorsuale: 03/B2 – Fondamenti Chimici delle Tecnologie

Settore Scientifico Disciplinare: CHIM/07 – Fondamenti Chimici delle Tecnologie

Development of innovative processes for the transformation of polymeric thermoplastic materials based on compression molding at high rates

Presentata da: Alberto Marcolongo

Coordinatore Dottorato

Prof. Luca Vittuari

Supervisore

Prof. Maurizio Fiorini

Co-Supervisore

Dott. Fiorenzo Parrinello

Esame finale anno 2019

Abstract

Poly(lactic acid) possesses many desirable properties, above all biodegradability an compostability. PLA can be either amorphous or semicrystalline depending on its stereochemistry and thermal history.

A high crystallinity degree is desirable to increase the heat resistance of PLA but it is rather difficult to reach high values during injection and compression moulding due to its very slow crystallization kinetics. Therefore, two different approaches can be carried out. The first concerns the synthesis and use of a PLA stereocomplex by mixing PLLA and PDLA, because this blend has shown higher crystallization rates and higher melting temperature than the single homopolymers. The second approach regards the adding of a nucleating agent that favours the formation of the PLA spherulites. In my thesis project, funded by SACMI Imola, an innovative process for the processing of PLA by compression moulding was developed.

The study was focused on two different aspects. The first regarded the formation and crystallization of the stereocomplex by means a Rheo-Raman instrument. The second aspect regarded the investigation of some operative parameters for the compression moulding process for the production of coffee-pods.

The results regarding the stereocomplex have shown that its formation is strongly affected from two different parameters that are the temperature of the experiment and the shear rate applied. By means the Rheo-Raman analysis it was also possible to monitor on line the formation and crystallization of the stereocomplex, that takes place in relatively short time (1-2 minutes).

As far as the processing of PLA by means compression moulding is concerned, the attention was focused on the thermal treatments after the formation of the coffee pod. This thermal treatment, carried out by means a post-mould device, favours the post crystallization process of the polymer leading to reach the target value requested for the application in the coffee machines.

Summary

1. Introduction

Manufacturers traditionally have not concerned themselves with the impact on the environment of using various feedstocks. The products of the future must be designed "from conception to reincarnation" or "cradle to cradle" using holistic life-cycle concepts. The noble aim of economy circular together with petroleum deficit, fluctuating oil prices and the enormous increase in the use of polymers in areas of great demand, such as packaging, have intensified the development of new cost-effective, greener alternatives. The challenge is to adopt some new design criteria to produce materials with the necessary functionalities during use, but which undergo degradation under the stimulus of an environmental trigger after use. For these reasons there is great interest in the so-called green polymer materials to offer an answer to sustainable development of economically and ecologically attractive technologies, contributing to the preservation of fossil-based raw materials, reducing the volume of garbage through compostability in the natural cycle leading to climate protection and reduction of carbon dioxide footprint [1]. In recent years, green movements, initiatives, and regulations are pushing almost every developed country to reduce the volume of solid polymers waste generated by consumers in order to protect the environment [2]. For instance, the production of plastics in Europe reached 49.9 million tons in 2016, mostly divided between polyethylene, polypropylene, poly(vinyl chloride), polystyrene and poly(ethylene terephthalate) production[3]. From 2006 to 2016 the volumes of plastic waste collected for recycling increased by 79%, energy recovery increased by 61% and landfill decreased by 43%(Figure 1.1).
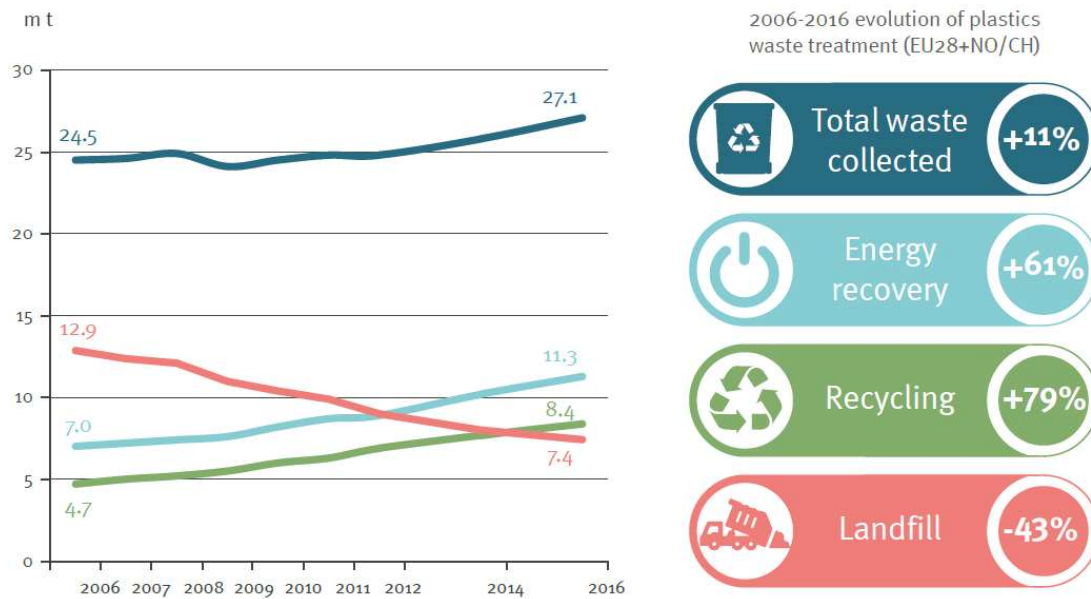
Figure 1.1: Plastic recovery in Europe from 2006 to 2016[3].

Therefore a huge benefits to the environment and will contribute to reduced dependence on fossil fuels came from the development of bio-sourced materials. These biopolymers produced from alternative resources will capable of substituting the currently existing family of oil-based polymers, as they become cost- and performance-wise competitive. Nevertheless, the properties of these biomaterials are often behind those of common thermoplastics and some improvements are needed in order to make them operative for their industrial use. The development of biopolymer matrices and their use in common applications is the subject of increasing interest by numerous research groups. The reasons for this increase in the number of studies on these materials reside more in the circular economy even.

In this direction, it has moved SACMI – international group that leads the world in machines for packaging including Beverage and Closures & Containers. The cap-making compression technology, for which SACMI is so renowned, has been able to take full advantage of the unique physiochemical behaviour of the molten material, polyl(actid acid) (PLA). SACMI group aim to conceptualize the integration of economic activity and environmental wellbeing in a sustainable way of the consumer goods, as well as to strict governmental regulations in the use of non-degradable thermoplastics.

1.1   Biopolymers

In recent years the use of products made from both natural renewable resources and fossil resources that decompose into environmentally friendly constituents, is increasing steadily and rapidly. Moreover it is grew in the consumer the desire for products that are environmentally friendly while providing the same results with products made from synthetic material. On the other side, the higher cost and inferior properties of these products as compared to common thermoplastic bring consumer distrustful.

It is important to understand what biodegradable and bio-based means. According to the standard ASTM D5488-94de1 , biodegradable polymers refer to polymers that are "capable of undergoing decomposition into carbon dioxide, methane, water, inorganic compounds, or biomass in which the predominant mechanism is the enzymatic action of microorganisms that can be measured by standard tests, over a specific period of time, reflecting available disposal conditions"[4].

"Bio-based" is a term focused on the raw materials basis, and it is applied to polymers derived from renewable resources. Raw materials are defined as renewable if they are replenished by natural procedures at rates comparable or faster than their rate of consumption [5]. To be exact, a biobased material is "an organic material in which carbon is derived from a renewable resource via biological processes". Bio-based materials include all plant and animal mass derived from carbon dioxide previously fixed via photosynthesis.

It is important to clarify what biopolymers are because also not-biodegradables biopolymers exist. In fact, exist two criteria underline the definition of a biopolymer: first, the source of the raw materials and second the biodegradability of the polymer. Here, a second differentiation is made between[4]:

1. Biodegradable bio-based biopolymers can be produced by biological systems like microorganisms, plants, and animals; or chemically synthesized from biological starting materials such as corn, sugar, starch, etc. The most used bio-based biodegradable biopolymers are starch and poly(hydroxyl acids).

2. Non-biodegradable bio-based biopolymers are synthetic polymers produced from biomass or renewable resources such as polyamides from castor oil (polyamide 11), polyesters based on biopropanediol, biopolyethylene (bio-LDPE, bio-HDPE), biopolypropylene (bio-PP), or biopoly(vinyl chloride) (bio-PVC) based on bioethanol from sugarcane, and also natural occurring biopolymers such as natural rubber or amber.

3. Biodegradable fossil fuel based biopolymers are synthetic aliphatic polyesters made from crude oil or natural gas that are certified biodegradable and compostable. Polycaprolactone (PCL), poly(butylene succinate) (PBS), and certain "aliphatic/aromatic" copolyesters are at least partly fossil fuel-based polymers, but they can be degraded by microorganisms.

Actually, the properties of the renewable resources are inferior compared to synthetically derived products. But the real difference is that the cost of bio-resourced are much higher than common. In order to decrease this two gap, the research and innovation are focusing to develop new synthetic routes and new processes for obtain environmentally friendly products with similar performances and price to fossil resources based materials.

It is clear that the most interesting biopolymers are the biodegradable bio-based biopolymers, due to their zero carbon dioxide emission that characterize their life cycle.

One of the main well known and in large quantity produced bio-based biodegradable biopolymer is polylactic acid. Polylactic acid is a poly(α-hydroxyalkanoic acid) largely produced by fermentation of renewable resources such as starch and sugarcane.

1.1.1 Introduction to polylactic acid

Polylactic acid was synthetized by Théophile-Jules Pelouze in 1845 throw polycondensation of lactic acid [5]. In 1932, Wallace Hume Carothers et al. developed a method to polymerize lactide into PLA and subsequently Du Pont in

1954 patented this method [6]. In the first years since its discovery PLA and its copolymers were originally developed as biomedical materials until 1970s, this since this polymers are bioabsorbable and biocompatible[7][8]. In the early 1990s Cargill Inc. managed to obtain high-molecular-weight poly(L-lactic acid) (PLLA) by ring-opening polymerization (ROP) of L-lactide [9]. In 1997, a joint venture between Cargill Inc. and The Dow Chemical Company formed NatureWorks, the major landmark in PLA's history. It marked the beginning of a large-scale use of this bio-based polymer, transforming PLA from a specialty material to a commodity thermoplastic. In particular, PLLA polymers having high L-contents and stereo-complex PLA polymers showing high melting temperatures are now expected to be candidates for high performance materials.

1.2 Lactic Acid

Lactic acid was discovered in 1780 by the experimental chemist Carl Wilhelm Scheele, who isolated "acid of milk" from sour whey [10]. A further description of the history of lactic acid by Holten and Benninga shows that industrial production of lactic acid started in the United States in the 1880s [11]. Avery patented and applied a fermentation process of vegetable sugars [12]. In 1950, the first commercial production of synthetic lactic acid started in Japan [13]. For some decades, synthetic lactic acid competed with lactic acid obtained by fermentation, but currently almost all lactic acid is produced by fermentation.

1.2.1 Chemical structure of Lactic Acid

Lactic acid is a simplest 2-hydroxycarboxylic acid (or α-hydroxy acid) with a chiral carbon atom. The chirality in alpha position to the carbonyl permits the existence of two optically active stereoisomers, namely L-lactic acid and D-lactic acid (Figure 1.2). By chemical method rather than fermentation is conveniently synthesized racemic DL-lactic acid. It consisting of the equimolar mixture of D- and L-lactic acids shows characteristics different from those of the optically active ones.
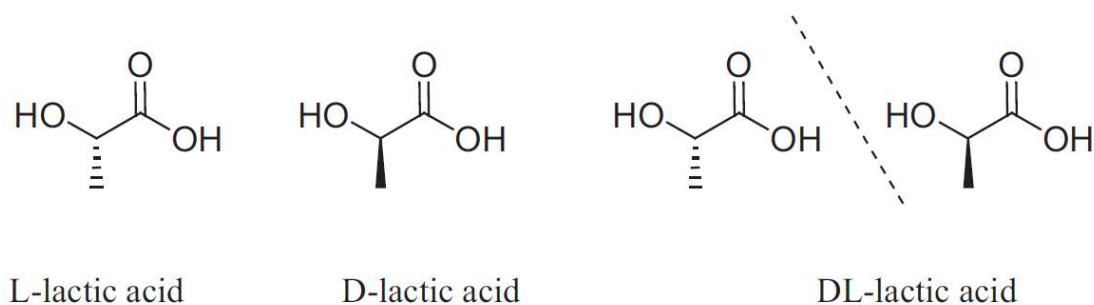
Figure 1.2: Enantiomer species of lactic acid[14].

In the structure of the lactic acid molecule are present hydroxyl and acid functional group, these groups can react together through an intermolecular esterification reactions, leading to the formation of a linear dimer (lactoyl lactic acid). This condensation reaction can proceed to higher oligomers and it is promoted by the water removal. Also the cyclic dimer, lactide, is formed in small amounts by intramolecular esterification of lactoyl lactic acid or by cyclization of higher oligomers (Figure 1.3)[15].
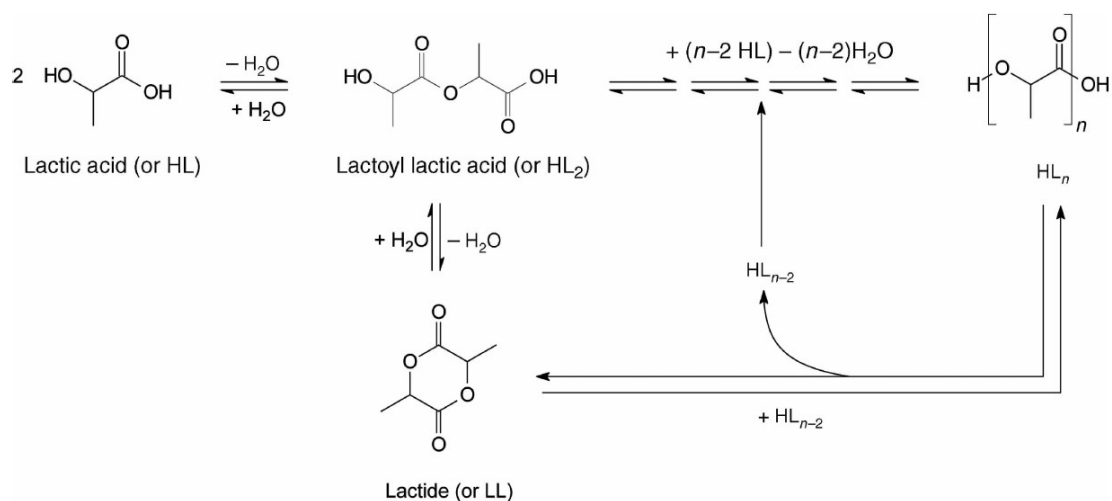

Figure 1.3: Lactic acid condensation reaction[15].

Due to these reactions, a solution of lactic acid at equilibrium consists of monomeric lactic acid, dimeric lactic acid or lactoyl lactic acid, higher oligomers of lactic acid, and lactide. The ratios between all substances depend on the amount of water present[11]. The condensation reactions are also the reason that it is quite difficult to obtain enantiopure solid lactic acid. For this pourpose, crystallization is a suitable technique [16].

1.2.2 Production of lactic acid

Lactic acid fermentation is one of almost bacterial reaction a long available on the market to produce it. The lactic acid bacteria that operate in this field are different. Some classes of microorganism are able to convert suitable carbohydrates to lactic acid[17].

For example the reaction of the sugar conversion into lactic acid is made with homofermentative lactic acid bacteria (LAB) . The reaction involves several enzymatic steps inside the microorganism cells, the sugar is first converted to pyruvate, then the pyruvate is reduced to lactic acid. In this way, the microorganism generates energy in the form of ATP that uses in several processes, for example, cell growth, maintenance, and sometimes even motility. In other words, lactic acid is mainly produced to keep the cellular processes going[15].
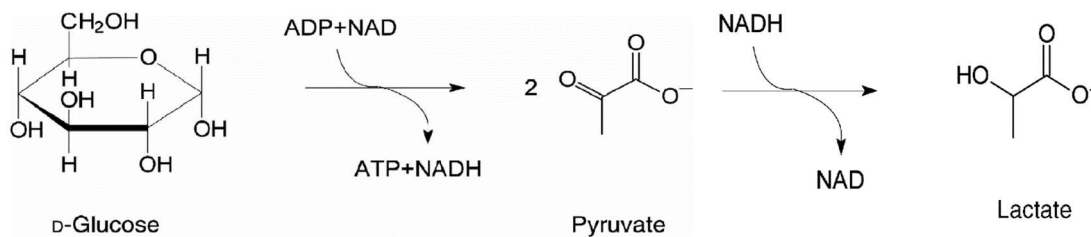
Figure 1.4: Lactate biosynthetic route in homofermentative bacteria[15].

The yield of this reaction is exclusively lactic acid, with this microorganism, glycolysis reactions splits a C6 into two C3 molecules. Lactic acid can be produced also by heterofermentative bacteria that produce a mixture of lactic acid, acetate, CO_2, and ethanol [15].

At the industrial level the fermentation process can be run in batch [18] or in continuous mode[19]. In all scenarios, microorganisms produce lactic acid together with various impurities such as un-reacted raw materials, cells and culture media-derived saccharides, amino acids, carboxylic acids, proteins and inorganic salts. The first step to separate lactic acid is the filtration of microorganism and raw material residue.

Then, the generated lactic acid is neutralized in situ with calcium oxide o ammonia. With the first base the products, a crude calcium lactate, is filtered off and acidified

with sulfuric acid. Subsequently filtering off the calcium sulphate, and evaporating to obtain a crude viscous lactic acid. When ammonia is used for the neutralization, the ammonium lactate is formed and directly converted into butyl lactate by esterification with n-butanol [14] .

In the industries of food, pharmaceutical and polymer synthesis, the lactic acid require a high purity. This can be obtained in different ways such as:

• active carbon treatment and/or ion exchange process; in order to remove impurities and salts;

• esterification/saponification;

• crystallization; this method can lead to an excellent lactic acid grade, but the yield is generally low.

• distillation; lactic acid can be distilled under low vacuum in order to separate it from higher molecular weight components such as sugar and protein that remain as residue. Lactic acid is obtained as the top product, but the formation of oligomers limit an overall high distillation yield.

• extraction; an extraction and back-extraction process with tertiary amine systems can be a suitable way to purify lactic acid [19].

The use of more efficient raw materials and more performing purification processes that involve lower costs, are the key to reduce the overall cost of lactic acid and mainly, the lactide and PLA commercial costs.

Two of the biggest PLA producers in the world have moved in this direction, Natureworks and Corbion. In 2015, Corbion became the first company to successfully produce, on lab scale, PLA from alternative feedstocks – and therefore the first to make PLA from non-food biomass [20]. While Natureworks, in these years, program to commercialize a fermentation process for transforming methane, a potent greenhouse gas, into lactic acid, the building block of Ingeo™ biopolymer.

To summarize all the traditional lactic acid production process including fermentation, a simplified block scheme is shown in Scheme 1.1.
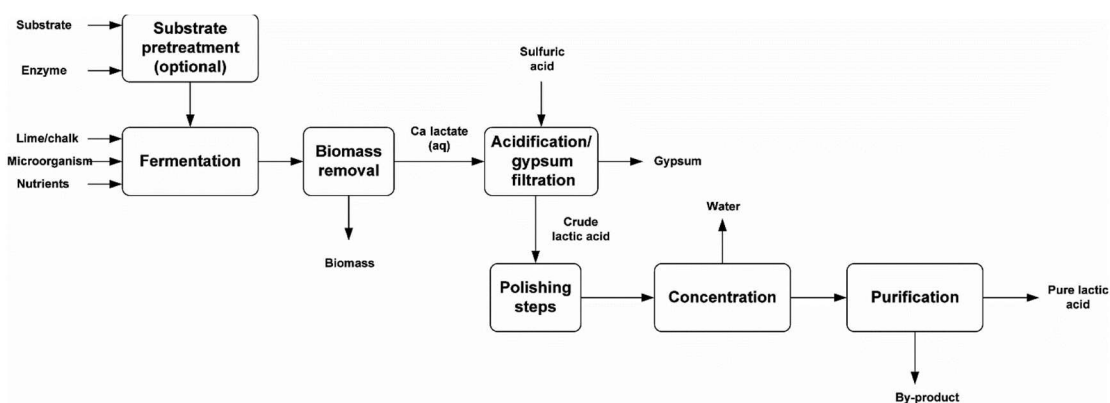
Scheme 1.1: Bock scheme of traditional lactic acid production process [15].

1.3 Lactide

1.3.1 Lactide structures

The dehydrated, cyclic dimer of lactic acid is commonly known as lactide (3,6-dimethyl-1,4-dioxane-2,5-dione). Due to the two asymmetric carbon atoms in the molecule, lactides exists in three different stereoisomeric lactic acid units. L- and D-lactides consist of two L- and D-lactic acids, respectively,

while meso-lactide consists of both D- and L-lactic acids. In addition to the three diastereomeric structures also a racemic lactide is commercially available: rac-lactide or DL-lactide (Figure 1.5).
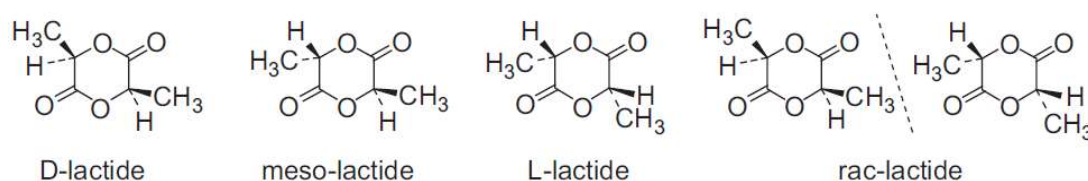

Figure 1.5: Lactide diastereoisomeric species[14].

1.3.2 Production of lactide

The synthesis of lactide was described for the first time by Pelouze in 1845 [21] studying the self-esterification of lactic acid by heating and distilling off water. Later, in 1914 Gruter and Pohl [22] patented an improved procedure where lactic

acid was self-esterified at 120-135°C and water removed using an air flow. Then the lactic acid oligomers obtained were converted in lactide adding zinc oxide as cyclization catalyst. One of the main reaction problem is the equilibrium reaction that limit the conversion from oligomer to lactide, so in order to pull the reaction toward the products, the lactide produced was distilled off under vacuum at 200°C. A modern lactide production processes involve two main reaction step, the prepolymerization process and the lactide synthesis (Scheme 1.2). Both step can be drown in a batch or in a continuous process.
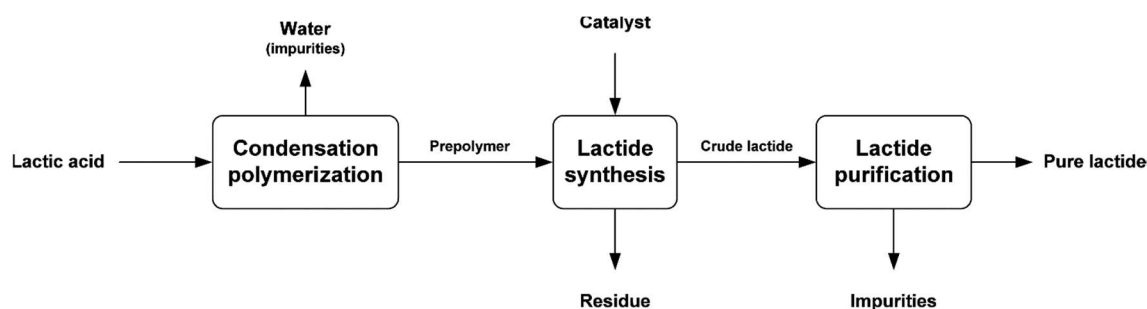
Scheme 1.2: General scheme of lactide manufacture and purification route[15].

In the last two decades, several papers have appeared on lactide manufacture [23], the major step forward was the use of a tin catalyst as coordinating catalyst. Tin catalyst can be considered the best compared to other catalysts and showed the lowest levels of racemization. The catalyst increases the rate of lactide formation catalysing the backbiting reaction of the oligomer hydroxyl end chains group [24].

Tin octoate (stannous 2-ethylhexanoate) was and actually is still the most used catalyst for lactide production, moreover is a liquid catalyst that can be handled easily, is food grade, and is widely available.

In batch processes, the depolymerisation rate is initially constant, but during the synthesis, polyesterification also occurs, and the degree of polymerization of the polyester rises concomitantly. For this reason the melt viscosity of the reaction mixture increases during the reaction and at the end of the batch process, mixing the highly viscous residue becomes very difficult. The mass transfer of lactide from the liquid to the gas phase decreases limiting the lactide separation.

Gruber et al. described a continuous lactide synthesis in 1992 [25]. In this process the prepolymer is continuously fed inside the reactor, crude lactide is evaporated

under vacuum pressure at 4 mbar, temperature 213°C, and using 0.05 wt% tin octoate as catalyst. The process has a residence time of about 1 h.

In both processes, continuous and batch, the lactide synthesis reactor produces a crude lactide stream that contains lactic acid, lactic acid oligomers, water, meso-lactide, and further impurities.

Different separation methods for lactide purification are currently employed:

• Distillation: this process was well described in Gruber et al. patent in 1993 [26]. This technique permit to split the multicomponent mixture of lactide, water, lactic acid, and its oligomers into pure fractions. The boiling points of all compounds are in the range of 200–300°C, thus low pressures are used. Since the difference in boiling temperature of lactide and meso-lactide is quite small, this distillation requires a lot of theoretical plates (>30).

• Solvent crystallization; this method is commonly used in laboratory and involves the lactide purification trough recrystallization from mixtures of toluene and ethyl acetate [24]. To obtain high purity of Lactide is possible by repeated crystallization with different toluene / ethyl acetate ratios.

• Melt crystallization; this method is preferred for large-scale process. Lactide crystallizes easily when melt is cooled down, but the presence of impurities limit the maximum yield [27]. In patents, the use of different types of equipment is mentioned: static equipment, falling film crystallizers, vertical column with scraper to remove crystal mass from the cooled wall, and scraped heat exchanger coupled to a wash column [27][28][29].

In order, the stereochemical purity of the product, the choice is between distillation, crystallization, or novel separation methods such as absorption or membrane separation. Distillation equipment don't fully remove all meso-lactide, and consequently, a mixture of lactic units are obtained during the polymerization. Instead, crystallization yields highly pure lactide, suitable for high molecular weight PLA homopolymer.

1.4 Polylactic Acid

Exist different synthetic routes to PLA polymers [15], but the mainly are two: direct polycondensation of lactic acid and ring-opening polymerization (ROP) of lactide. Industrial production of PLA mostly depends on the latter route.

1.4.1 Polycondensation of lactic acid

Lactic acid can be polymerized to polylactic acid by polycondensation, the condensation reactions occur between the hydroxyl groups and the carboxylic acid groups. The removal of the water formed during this reaction is essential to converts oligomers into polymer (Figure 1.6).
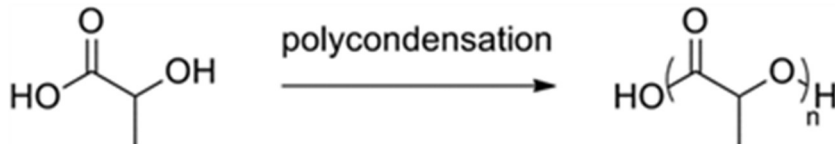
Figure 1.6: Polycondensation of lactic acid.

This direct polycondensation involve different phases, in a first step the lactic acid is dried removing the water contained in the feedstock. Then, a condensation step produces oligomers. The rate determining step in this stage is usually the chemical reaction, which is significantly affected by the catalyst used [30]. Traditional polycondensation catalysts are strong Lewis acids and organometallic compounds. The last step is characterized by melt polycondensation in which oligomers condense generating the polymer chains. The removal of water becomes more difficult and can be rate determining when producing a higher molecular weight polymer. To enhance the polycondensation reaction rather than the transesterification reactions, the water formed in the reaction mixture is removed under vacuum in inert atmosphere conditions.

To improve mass and heat transfer, the melt polycondensation reaction should be carried on in an apparatus having an efficient renewal of phase boundary layers and systems that can handle high-viscosity mass are required such as rotating disk type reactor.

The preparation of a high molecular weight PLA by a direct dehydration condensation reaction is not practicable due to the equilibrium reaction towards high molecular weight polymer. Generally, this type of polymerization is used for obtaining a polymer with low molecular weight, and usually the reaction is stopped when the polymer reach a molecular weight of about few thousands. PLA prepared from polycondensation possessing low molecular weight has poor mechanical properties and therefore is not suitable for many applications. Polymers whit high

molecular weight can also be obtained, but the conversion remains low. As example the results of different catalyst tested shown SnO as the most efficient catalyst in terms of molecular weight but the maximum yield obtained at 180°C after 20 hour of reaction is below 40% [31]. Moreover, side reactions occur and they give a negative influence on the properties of the polymer. Indeed the formation of cyclic structures, such as lactide, lowers the overall molecular weight. Furthemore, the lactide is removed with the water under vacuum lowering also the yield of the process even if it is recycled.

1.4.2 Ring-opening polymerization of lactide

Ring opening polymerization of lactide is usually the most preferred route for preparing high molecular weight polylactide, this due to the fact that the repetitive unit is composed essentially of two condensed molecules of lactic acid (Figure 1.7). In addition, this catalysed process not involves water formation during the polymerization, so most of the problems related to water removal and hydrolysis of polymer are avoided.
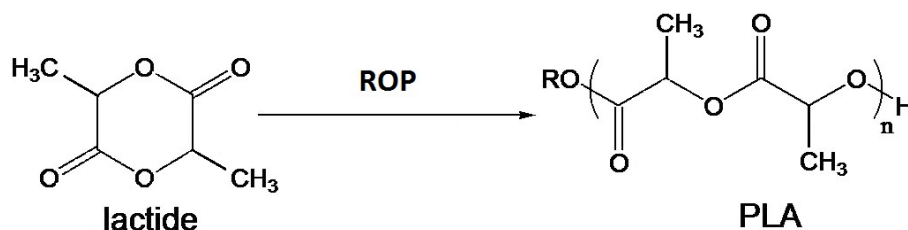

Figure 1.7: Ring-opening polymerization of lactide.

Moreover this type of synthesis permits an accurate control of the polymer stereochemistry, using a pure lactide stereoisomer or a mixture of them is possible to obtain semicrystalline or amorphus polylactic acid and also stereopolymers.

Lactide can be polymerized by melt, bulk, solution, and suspension polymerization. Each of these methods has its own advantages and disadvantages, but melt polymerization is generally considered the most simple and reproducible method [32].

A large number of catalysts have been studied in the ROP of lactide, the most used are the carboxylates and alkoxides of Sn [33] [34]and Al [35] [36].

As has proposed by Kowalski et al [37] lactide is polymerized in bulk with Sn(Oct)2—a Lewis acid—and that seems to be the main mechanism involved. The polymerization mechanism involves a catalyst activation step, in which tin 2-ethylhexanoate is converted to a tin alkoxide by reaction with a hydroxyl compound, such as aliphatic alcohol or water. In the next stage, one of the exocyclic carbonyl oxygen atoms of the lactide temporarily coordinates with the tin atom of the catalyst having the alkoxide form. This coordination enhances the nucleophilicity of the alkoxide part of the initiator as well as the electrophilicity of the lactide carbonyl group. Then the cleavage of the lactide ester bond makes the lactide open and insert into the alkoxide tin-oxygen bond of the catalyst. In this way, the lactide alkoxide group formed by the ring opening, coordinates tin and the latide opened carbonyl group forms a new ester bond with the alkoxides compound that coordinated tin in the previous catalyst activated species. Subsequently propagation is induced by identical coordination and insertion mechanism of additional lactide molecules into the tin-oxygen bond making the polymer chain grow (Figure 1.8).
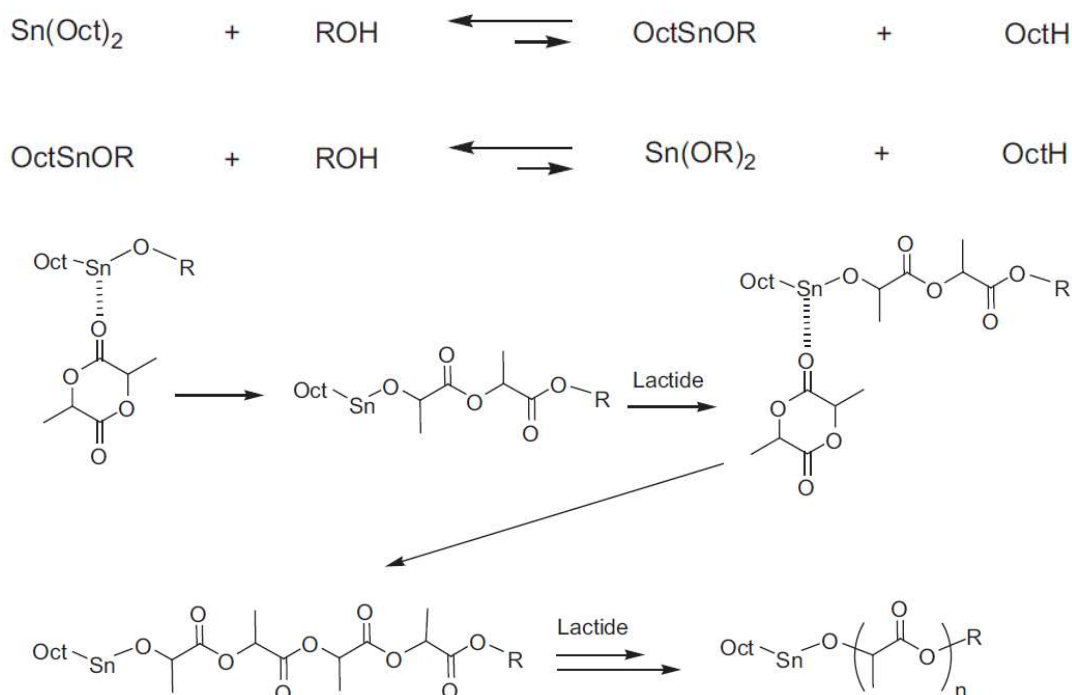
Figure 1.8: Coordination-insertion mechanism in ROP of lactide with tin octoate [14].

Every initiating molecule is covalently bonded as an end group to each polymer chain, transesterification reactions between polymer and the 2-ethylhexanoate ligands of the catalyst will also give octanoic ester end groups in the polymer.

The most common reactor system used for lactide ROP consist on one or more mixed reaction vessel, the number of vessels can vary depending on the desired polymerization conditions. A combination of this type of reactor and a static mixer has also been developed, plug-flow reactor columns are used for a continuous polymerization process. In this type of reactors agitation blades are used in order to ensure appropriate mixing.

ROP can also be performed by reactive extrusion, in this process the residence time and catalyst efficiency are essential to achieve the right polymer molecular weight.

At the end of the PLA polymerization process, low molecular weight oligomers unreacted, lactide and the lactide generated by side reaction like back biting and intramolecular cyclization, need to be removed. This process is carried on by distillation under vacuum in the presence of an inert gas current. During this final step, the catalyst deactivation also occurs. Deactivator agents can be various such as phosphorous containing compounds, antioxidants, acrylic acid derivatives, and organic peroxides.

A solid state-state polymerization can be also used in order to reduce the lactide content, and increase the molecular weight of the polymer.

The final polymer product must be dried at 60°C under vacuum or with dry air before storage or before future processing, in order to avoid hydrolysis due to the presence of moisture.

1.4.3 Chain Configuration

As we said above starting from different types of lactides or from a mixture of them is possible to synthetize PLA with various stereoregolarity (Figure 1.9).
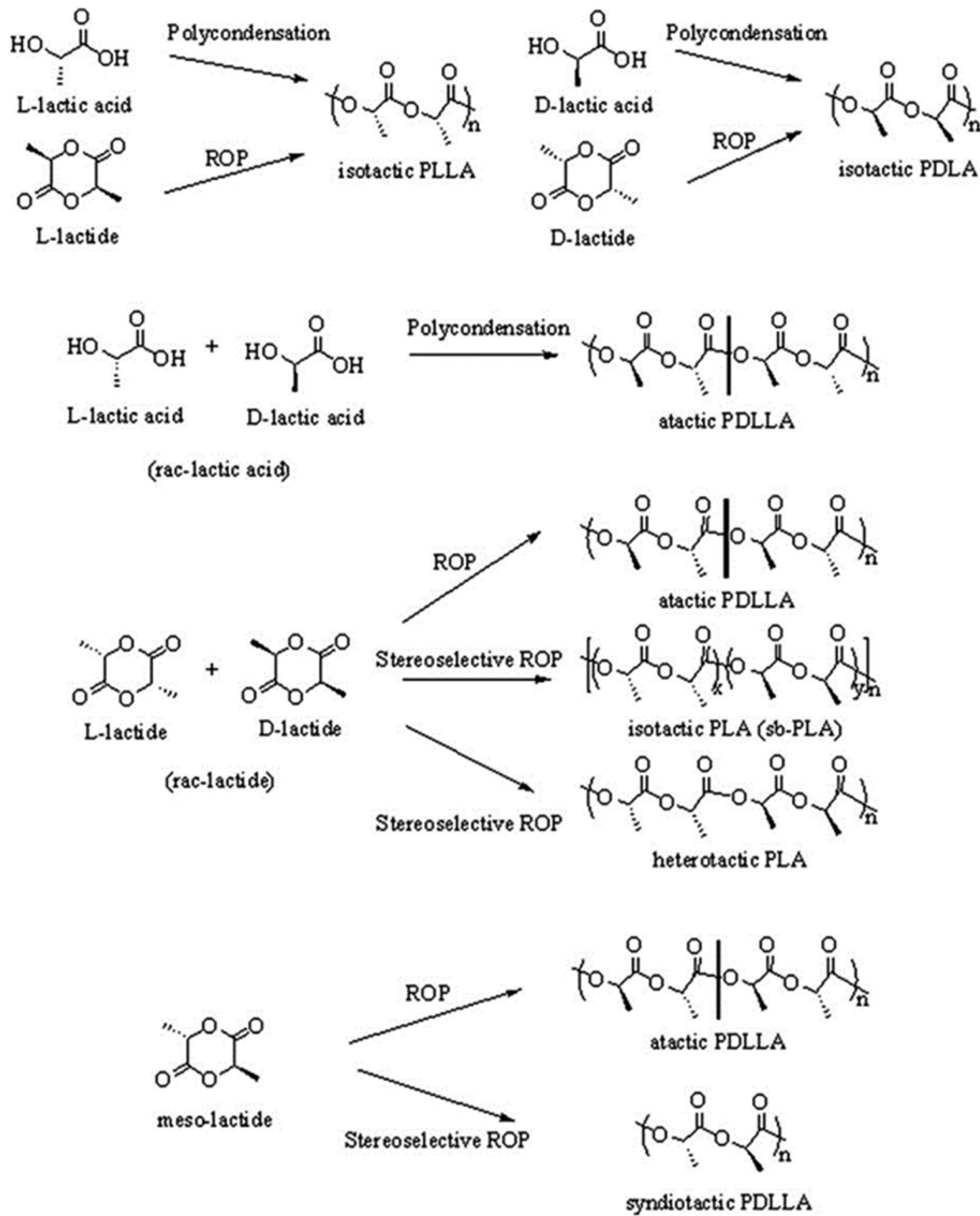
**Figure 1.9**: A variety of microstructures of lactides and PLAs [14].

Four different stereoisomers of PLA can be distinguished:

• Isotatic PLAs; they are formed from pure L-lactide or pure D-lactide obtaining a polymer with the same stereoconfiguration in all repeting unit, poly(L-lactide) (PLLA) or poly(D-lactide) (PDLA).

• Syndiotactic PLA; it has alternating configurations of the sequential stereocenters L and D of meso-lactide obtaintaing from stereoselective ROP, poly(meso-lactide) (mesoPLA).

• Atactic/Heterotactic PLA; the atactic has a random distribution of configurations about the stereocenters, while its heterotactic counterpart has regions of stereo-homogeneity, poly(rac-lactide) (PDLLA, racPLA).

• Isotactic stereoblock PLA; it consist on a block copolymer of PLLA and PDLA, poly(l-lactide-co-d-lactide) (PLDA).

At this different classification we can add the stereocomplex PLA (scPLA) [38]. Pure PLLA and PDLA macromolecules can crystallise together into a stronger crystalline structure. The alternation of PLLA and PDLA molecules in the crystal lattice permit the formation of a structure where the macromolecules are closer. In fact, in this particular stereoconfiguration the two polymer chains are less hindered when align in the crystals leading to an increase of the intermolecular interaction energy compared to the crystalline structure obtained in both homopolymers alone [39]. A schematic representation of all PLA family is given in Figure 1.10.
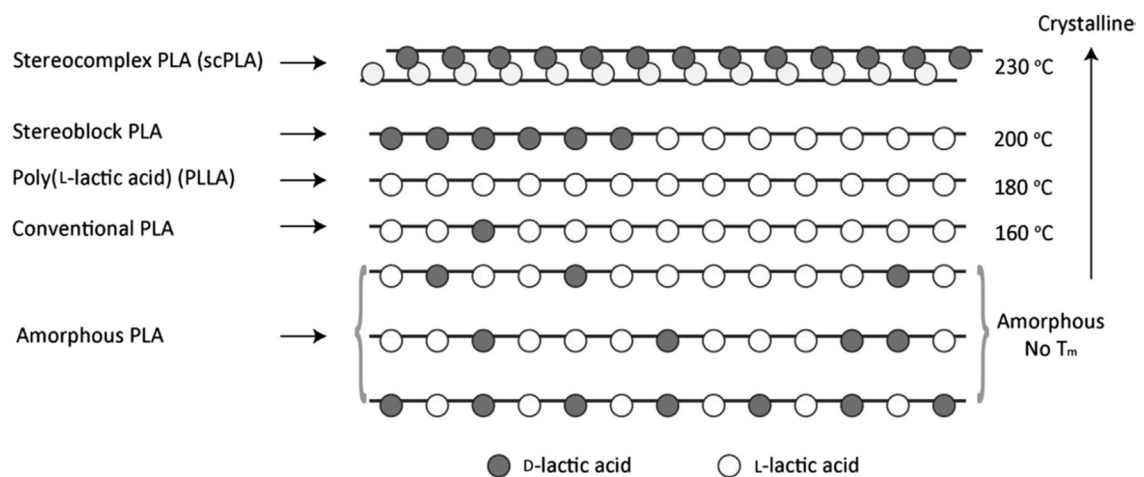
Figure 1.10: Schematic representation of all PLA family[4].

As reported in Figure 1.10 , and in Table 1.1, the melting point and the glass transition temperature change depending on the molecular weight, the degree of crystallinity, and possibly the proportion of comonomers on the chain stereoregularity.

Table 1.1: Transition Temperatures of different stereoisomers of PLA.

Transition temperatures	PLLA	racPLA	mesoPLA atac. / synd.	scPLA	sbPLA
Tg (°C)	53-63	50-55	40-45 / 34	70-90	50-55
Tm (°C)	160-185	-	- /153	200-230	185-195

PLLA is semicrystalline with a Tm of 160-185°C, a Tg of 53-63°C, and a crystallization temperature Tc of 100-120°C.

Syndiotactic PLA can be produced from the polymerization of meso-lactide using a stereoselective catalyst. It is semicrystalline with a Tm of 153°C and a Tg of 43°C, however, its thermal properties are poorer compared to PLLA.

Atactic PLA (PDLLA or racPLA) can be prepared from rac-lactide. It has a Tg of 50-55°C but it has no Tm because it is amorphous, it shows the lowest mechanical properties. Atactic PLA can also be prepared from the random copolymerization of meso-lactide or from polycondensation of rac-lactic acid.

PDLA is prepared from D-lactide, it is very expensive and produced only in small quantities.

Stereoblock PLA (sbPLA) can be prepared by solid-state polycondensation of PLLA and PDLA. It has a Tm of 185-195°C and a Tg of 50-55°C.

Stereocomplex PLA (scPLA) by mixing PLLA and PDLA in solution state or in molten state. It has a Tm of 200-230°C and a Tg of 80-90°C. The melting temperature and enthalpy of fusion of the stereocomplex drop, however, sharply with the overall isotacticity of the sample, no stereocomplexation occurring when the optical purity of the polylactide is below 72% [40].

1.4.4 PLA crystalline structures

Different crystal structures have been reported for PLA, the formation of which depends on the crystallization conditions. PLA can crystallize into three forms (a, b, and c), generally refered to as polymorphism. Polymorphism in materials science refers to the existence of more than one form of crystalline structure in a solid material with the same chemical composition[15].

De Santis and Kovacs was the first that reported the most common α-form occurring in conventional melt and solution crystallization conditions [41]. Subsequently, other studies followed to investigate its structure [42][43]. Based on WAXD and IR data, Zhang et al. reported the slightly different α′-form for PLA crystallized below 120 °C [44]. Moreover, it was discovered that the α′ crystal is formed at crystallization temperatures below 100 °C while crystallization between 100 and 120 °C gives rise to the coexistence of α′ and α crystal structures [45]. The results of this disordered structure influenced the properties of products in PLA. In particular, the α′ crystal leads to a lower modulus and barrier properties and to higher elongation at break compared to α crystal [46].

The conformation of α-form is characterized by two antiparallel chains in a left-handed 10_3 helix packed in an orthorhombic (or pseudoorthorhombic) unit cell (Figure 1.11) [47].
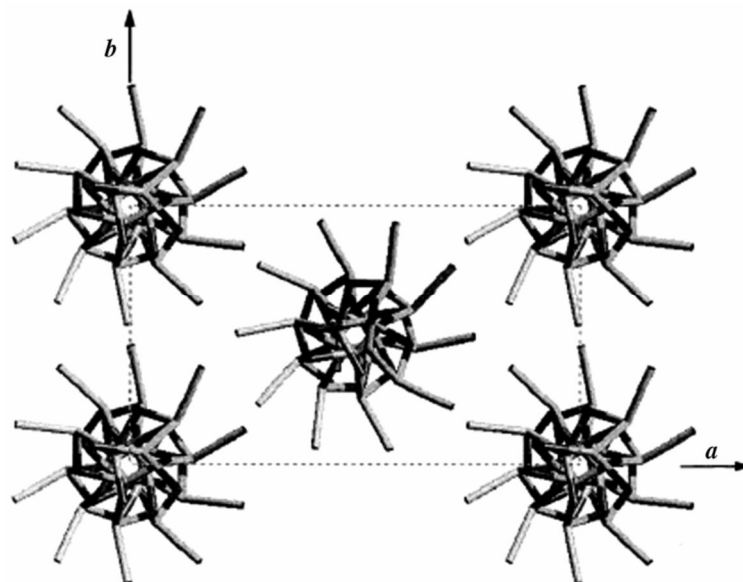
Figure 1.11: Schematics of the a-phase of PLLA assuming regular 10_3 helix conformation and parallel helices[47].

The study of Aou and Hsu [48] confirmed that the 10_3 helix provided a better description of the PLA structure.

The β-form crystals are generally created by stretching of α-form at high temperature and high draw ratio [49]. The β structure presented a melting temperature about 10° C lower than the α structure . Later, Puiggali et al. [50] suggested that β-form crystal is a frustrated structure with a trigonal cell containing three chains which are randomly oriented up and down.

A new crystal modification, γ-form, was produced via epitaxial crystallization of

PLA on hexamethyl benzene, two antiparallel helices were packed in an orthorhombic unit cell [47].

The ability to control the stereochemical architecture allows precise control over the rate and degree of crystallinity.

1.5 Properties

Before its introduction as a packaging and commodity material, specialty grades of PLA had been developed for biomedical uses. The commercial introduction of bio-based PLA in 2003 has opened the way for more common applications. In particular, PLA has been finding an increasing number of applications in the packaging industry due to its good mechanical properties, is weather resistence, transparency and compostability. Its methilic side groups give to the material a hydrophobic behaviour. PLA is soluble in many organic solvents like chloroform, dichloromethane or THF. It is a high modulus thermoplastic polymer with properties in between polystyrene (PS) and polyethylene terephthalate (PET). Similarly to polyethylene terephthalate, polylactic acid has slow crystallization rate. The highest rates of crystallization occur in pure PLLA in the temperature range of 110–130°C with the formation of spherulitic crystals. The polymers obtained from optically active monomers (L-lactide and D-lactide) are semicrystalline while the optically inactive monomers (racemic D,L-lactide and meso-lactide) give amorphous polymers.

PLLA and PDLA are semicrystalline polymers due to optically active monomers and the stereoregularity of the polymer chain. Conversely, PDLLA, which is an equimolar randomcopolymer of L- and D-lactic acid (or L- and D-lactide), is fully amorphous because of its irregular structure. The stereochemical configuration of PLLA (or PDLA) and PDLLA is analogous to that of isotactic polypropylene and atactic polypropylene.

As I said before PLA properties depend on the molecular weight, on the degree of crystallinity, and also on the polymer chain stereochemistry. A higher molecular weight raises Tg, as well as Tm, tensile strength, elastic modulus, and lowers the elongation at break. In the same way an increase in crystallinity increase the tensile strength, the elastic modulus and lower the elongation at break.

The stereochemistry is very easily controlled by the polymerization with D-lactide,

L-lactide, D,L-lactide, or meso-lactide, to form random or block stereocopolymers, while the molecular weight is directly controlled by the addition of hydroxylic compounds such as lactic acid, water, alcohols. The ability to control the stereochemical architecture allows precise control over the rate and degree of crystallinity.

Usually commercial PLA grades are based on an L-rich mixture due to purification issues, they typically comprise a minimum of 1-2% D units. Since the two repeating units are optically active, they rotate polarized light in opposite directions. Commonly, in the literature is used for 100% pure PLLA and PDLA, a specific optical rotation values in chloroform at 25°C ([α]25) equal to -156° and +156 °, respectively [51][52]. A higher content of one repeating unit in polymer chain results in a higher rotation angle in that direction. Thus, the molar fraction of D units (XD) in PLA could be calculate by employing the following equation 1.1:

$$X_D = \frac{[\alpha]^{25} + 156}{312}$$ **Equation 1.1**

Based on the molar fraction and source of D units in PLA chains, i.e., DD-lactide or meso-lactide, another important parameter called the average isotactic sequence length ($\bar{\zeta}$) is defined for L-lactide rich PLA as:
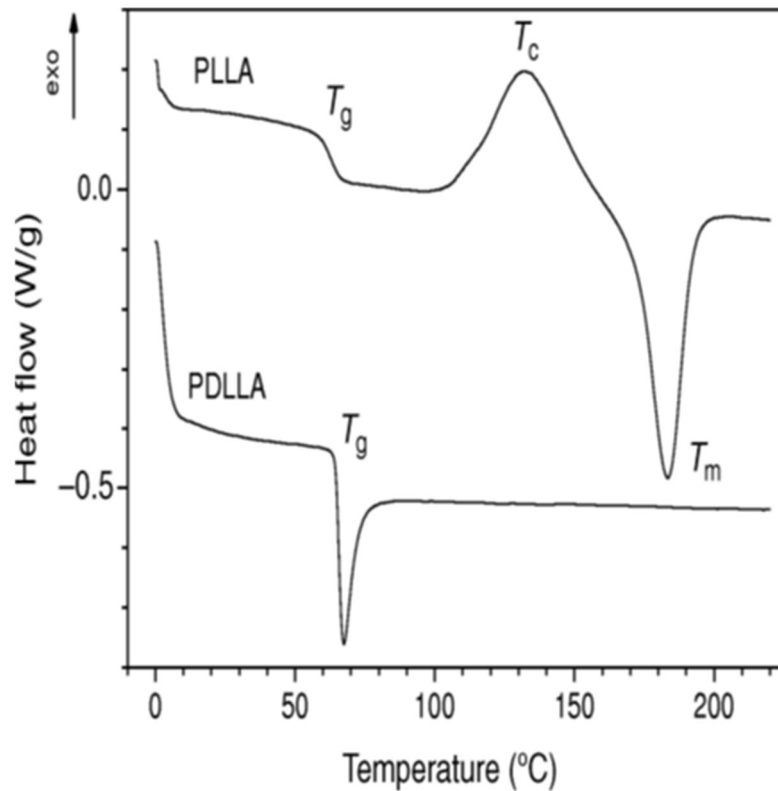
$$\bar{\zeta} = \frac{a}{X_D}$$ **Equation 1.2**

where *a* is a coefficient that depends on the source of D units in polymerization feed. It is equal to 1 if all D units are incorporated via meso-lactide, equal to 2 if they are all comprised of DD-lactide and between 1 and 2 depending on the ratio of meso and DD-lactide in the polymerization feed.

A higher value means a higher level of chain order. Therefore, this parameter influences directly the crystallization behavior of PLA. It can be controlled by adjusting the ratio of LL, DD and meso-lactide in the monomer feed for PLA polymerization.

1.5.1 Melting and Glass Transition Temperatures

Figure 1.12 shows a typical differential scanning calorimetry (DSC) analysis of thermal behaviour of two amorphous PLAs, that is, a PDLLA (Mw 70 kg/mol) sample that is intrinsically amorphous and PLLA (Mw 200 kg/mol) that was quenched to the amorphous state by fast cooling at -100°C/min after melting. In both cases, the Tg is evident and is located at about 65 °C.

Figure 1.12: Differential scanning calorimetry thermograms of amorphous PLLA and PDLLA (heating rate 10°C/min).

The crystallinity content (Xc) has been evaluated from the DSC data according to the following equation:

$$\mathbf{Xc(\%) = 100\ (\Delta H_m - \Delta H_C)/\Delta H_m^0}$$ **Equation 1.3**

where ΔH_m and ΔH_c are the melting and the crystallization enthalpies, respectively, and ΔH_m^0 is the melting enthalpy of 100% crystalline PLA (93.0 J/g) [53]. Molecular weight has a considerable influence on the melting temperature (Tm) of polymeric crystals. Figure 1.13a shows a compilation of literature data that clearly

22

demonstrates how Tm values increase with number average molecular weight (Mn). For M_n > 100 kg/mol, an asymptotical Tm value is achieved. However, Tm is also a function of optical purity of PLA. Pure PLLA (0% D-lactide) exhibits the maximum melting temperature, between 175 and 180 °C depending on authors. The melting point decreases linearly with the D-lactate content, as shown in Figure 1.13b.
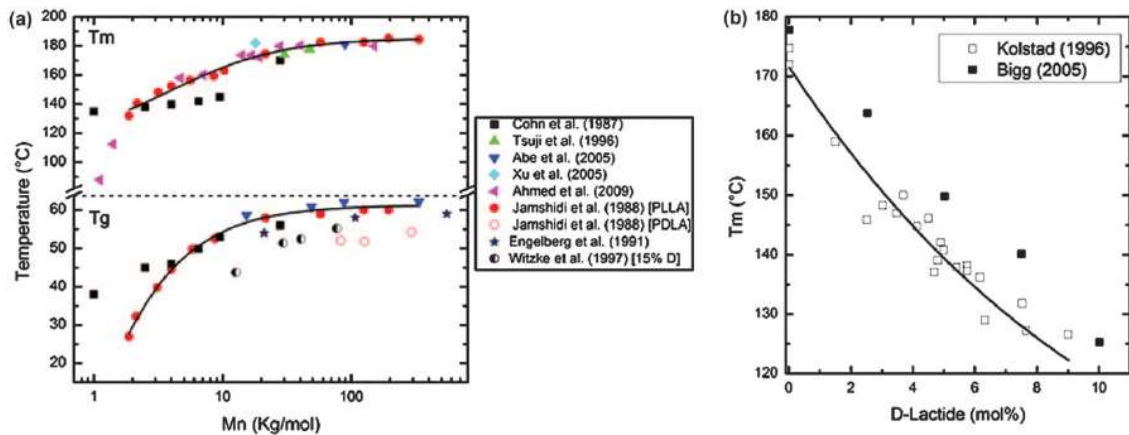
Figure 1.13: a) melting and glass transition temperature versus molecular weight of PLLA,18–25 b) melting temperature versus D-lactide content [14].

Figure 1.14 shows how Tg values also depend on the molecular weight. In fact, the Tg increases rapidly when the molecular weight is increased but then arrives a constant value. At a given molecular weight, an increase D-lactide content decreases the glass transition temperature to some extent but its effect on Tg is not as significant as on Tm.
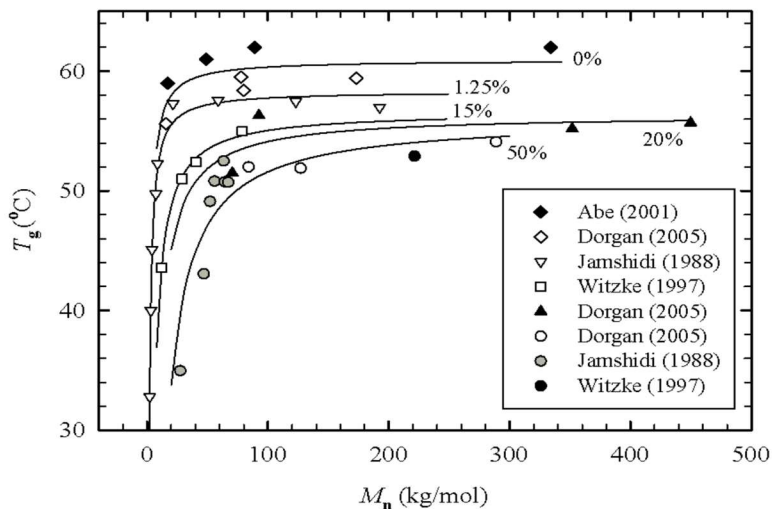
Figure 1.14: Tg vs. Mn for different D-lactate concentrations [54][55][56][57].

The physical, mechanical and barrier properties of PLA are dependent on the morphology, crystalline form and crystallinity degree. PLA can be either amorphous or semicrystalline at room temperature, depending on the molecular weight, its stereochemical architecture, thermal history and content of L, D or meso-lactide in the main chain. PLA can be totally amorphous or up to 40% crystalline. PLA resins containing more than 93% L-lactic acid can crystallize. However, high molecular weight can reduce the crystallization rate, and therefore the crystallinity degree.

1.5.2 Crystallization kinetics

A semicrystalline polymer like PLA can develop a crystalline structure when cooled from the melt or heated from the glassy state, either under isothermal or under nonisothermal conditions. Two competing factors affect the crystallization behavior: cooling/heating rate and crystal nucleation and growth rates. The resulting microstructure has a significant effect on the ultimate properties of the product, such as elasticity, permeability, transparency, and stiffness.

Typically, the crystallization kinetics considered two independent phenomena: initial crystal nucleation and of subsequent crystal growth. The technique that study these two event is optical microscopy. In particular a polymer films is used to determine the nucleation density and spherulite growth rates in isothermal conditions. The crystal growth process is normally studied by measuring the spherulite radius (r) as a function of the crystallization time (t). The spherulite radius increases linearly with crystallization time at isothermal condition.The growth phenomenon is evaluated by measuring spherulite radius with time. The crystal growth rate (G) is simply equal to the slope of the r vs. t curve. Therefore, G is a constant value at a given crystallization temperature (Tc) [58].

The relation between the growth rate and the crystallization temperature for various molecular weights of PLLA is illustrated in Figure 1.15.
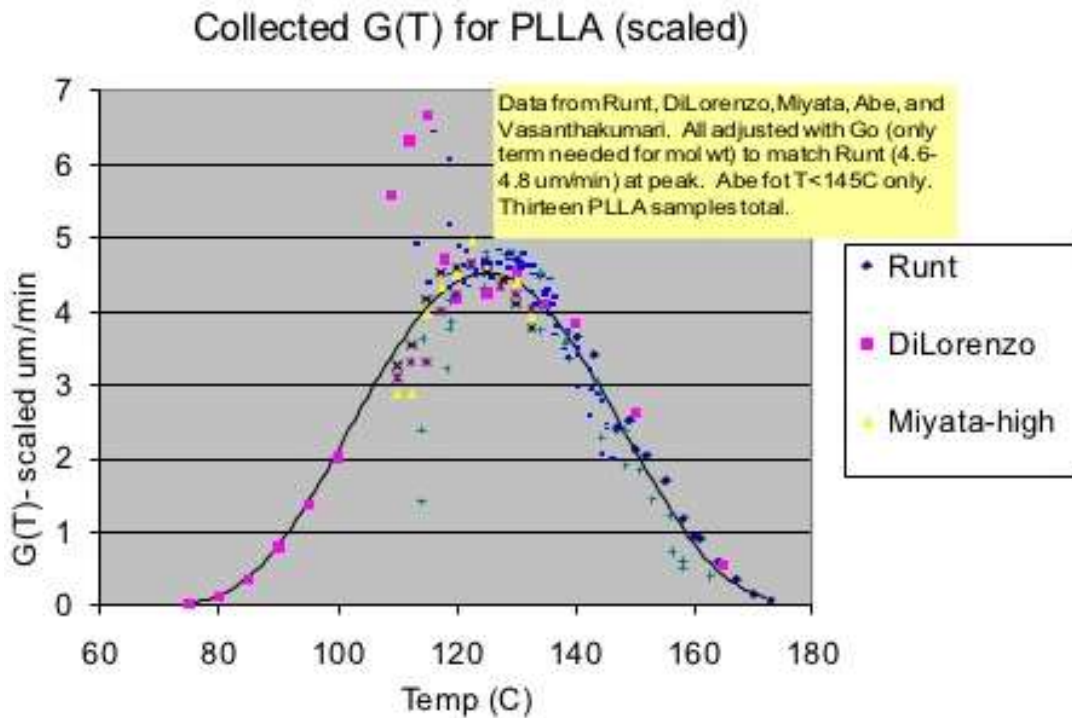
Figure 1.15: Radial crystal growth rate, G(T) for PLLA (0-0,3 %D) [59][60][58].

The spherulite growth rate increases with a crystallization temperature and a maximum value is limited at around 115-140 °C. After this temperature G decrease with Tc. As supercooling increases, the thermodynamic driving force for secondary nucleation also increases causing a general improvement in G (right-hand side of the bell-shaped curve). However, as temperature decreases the melt-viscosity also increases limiting chain diffusion to the growth front and causing a decrease in G (left-hand side of the bell-shaped curve).

Another technique used to study the crystallization kinetics is the calorimetry. It enables quantification of enthalpies and transition temperatures in isothermal and non-isothermal modes. For isothermal characterizations, after initial quenching below the glass transition temperature or directly from the melt state, the amorphous polymer is rapidly brought to the selected crystallization temperature. Heat flow is then measured as a function of time until crystallization is completed. This data it can be curve-fitted with the Avrami model:

$$X_t = 1 - \exp\left[-(kt)^n\right]$$

Equation 1.4

where k is a kinetic rate constant and n is the Avrami exponent. But to compare the crystallization rates of materials is used crystallization half-time ($t_{1/2}$). It is defined as the time required to attain half of the final crystallinity ($X_t = 0.5$). The half-time is typically reported as a function of temperature enabling the determination of the optimal temperature window. For example, in figure 1.16 $t_{1/2}$ is plotted versus Tc for PLA having different molecular weights (M_n in kg/mol) and different percentage of D-lactate [61].
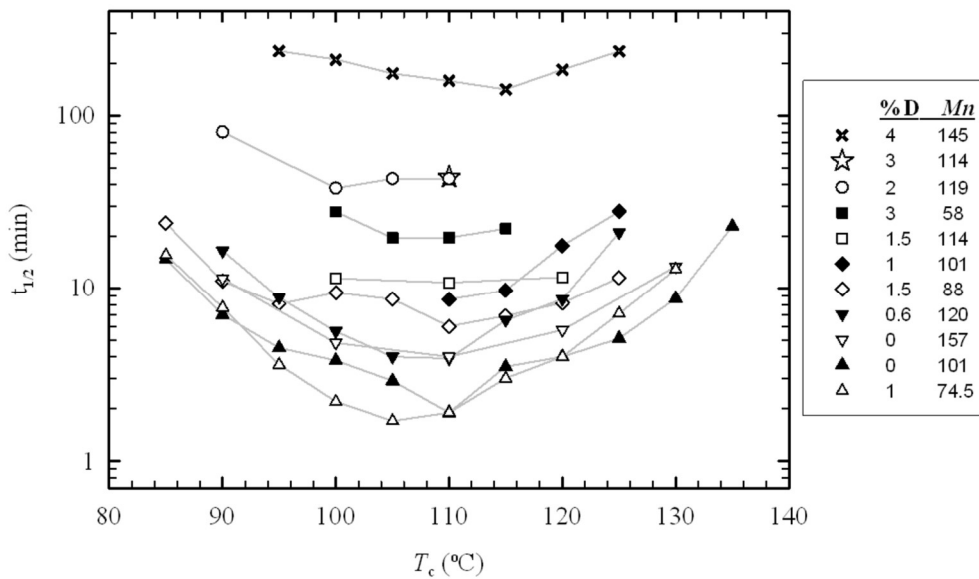
Figure 1.16: t1/2 versus Tc for PLA having different molecular weights and different percentage of D-lactate [61].

For all curves, even though the materials varied in terms of molecular weight and D-lactide concentration there is a minimum. The D-contents effect is describe by the half-time increasing and the shifted up of typical U-shaped curves. The minimum half-time, was reached in the 105-110 °C range. This illustrates the fact that the overall crystallization rate measured by calorimetry takes into account the increased number of crystallization sites emerging by reducing the temperature. It is also in agreement with the trend observed in Figure 1.15 where spherulite density sharply decreases above 110 °C. Therefore, at temperatures lower than the optimal growth rate temperature, the crystal growth rate decrease was compensated by a larger number of crystallization sites (higher nuclei density) due to increased driving force for nucleation.

1.5.3 Rheological properties

PLA is made into useful items using thermal processes, such as extrusion, compression/injection moulding. Therefore, PLA materials required a preliminary study of rheological properties in order to understand its processability behaviour. Rheology is the science that studies the behaviour of matter when it undergoes an stress or strain. It relates the viscosity with temperature and shear rate, and is consequently linked to the processability of a polymer.

During the polymer-forming process the polymer chains flowed easly past one another into narrow cavities in order. The shear rates perform an important role and usually at high shear rate the number of entanglements between the polymer chains decreases. These phenomena are classified as shear thinning fluids and it characterize most polymer melts. The viscosity also decreases at elevated temperatures due to the higher kinetic energy of the molecules. Rotational and capillary rheometers are instruments that can be employed to gain data on the shear viscosity of polymers.

The viscosity, η, is often described as the resistance of a material to flow; the greater the viscosity, the greater the force needed to deform the fluid. That is, viscosity relates the measurable shear stress to the imposed shear rate (or visa versa). For Newtonian fluids, the viscosity is independent of shear rate and the stress may be written as follows:

$$\tau = \eta\,\dot{y}$$
<div align="right">**Equation 1.5**</div>

For polymer melts and solution, the equation must be modified in function of shear rate. While for solid material the relationship between stress (τ) and strain (γ), is governed by the shear modulus, G.

$$\tau = G\,\gamma$$
<div align="right">**Equation 1.6**</div>

For such elastic materials, there is no rate dependence. An elastic material

subjected to an extensional deformation is characterized by a Young's modulus, E.

Consider the case of a time-varying shear deformation, the strain (ɣ) is given by a sine wave of frequency ω and amplitude A(ω).

$$\gamma(\omega) = A(\omega)\sin(\omega t)$$

the corresponding shear rate is

$$\dot{\gamma}(\omega) = \omega A(\omega)\cos(\omega t)$$

For a viscous material the stress would be

$$\tau(\omega) = \eta\,\dot{\gamma}(\omega) = \eta\omega A(\omega)\cos(\omega t)$$

Whereas for an elastic material the stress would be

$$\tau(\omega) = A(\omega)[G'\sin(\omega t) + G''^{(\omega)}\cos(\omega t)]$$

That is, for an elastic material, the stress would be in phase with the imposed strain; in contrast, the viscous material shows that the stress would be 90° out of phase with the strain.

For viscoelastic materials the dynamic viscosity , the stress contains both in-phase and out-of-phase components. In the small deformation limit where the stress remains linear with respect to the amplitude of the applied strain, the response may be written as:

$$\tau(\omega) = G\gamma(\omega) = GA(\omega)\sin(\omega t)$$

where the frequency (i.e., rate of deformation)-dependent moduli G'(ω) and G"(ω) are known as the storage and loss moduli, respectively. The storage modulus

represents the elastic or in-phase response of the material and the loss modulus reflects the viscous or out-of-phase response. Due to their rate dependence, these are known as the dynamic moduli.

From the dynamic moduli, it is possible to construct a complex viscosity, the magnitude of which is given:

$$|\eta^*(\omega)| = \sqrt{\left(\frac{G'(\omega)}{\omega}\right)^2 + \left(\frac{G''(\omega)}{\omega}\right)^2}$$
Equation 1.12

The empirical Cox–Merz rule simply states that the magnitude of the dynamic viscosity as a function of the frequency is equal to the steady viscosity as a function of shear rate.

For linear architectures, the Cox–Merz rule relating complex viscosity to shear viscosity is valid for a large range of shear rates and frequencies. The branched architecture deviates from the Cox–Merz equality and blends show intermediate behavior. Both the zero shear viscosity and the elasticity (as measured by the recoverable shear compliance) increase with increasing branched content. For the linear chain, the compliance is independent of temperature, but this behavior is apparently lost for the branched and blended materials. These authors use the Carreau–Yasuda model, Equation 1.13, to describe the viscosity shear rate dependence of both linear and branched PLAs and their blends:

$$\eta = C_1[1 + (C_2\dot{y})^{C_3}]^{\left(\frac{C_4-1}{C_3}\right)}$$
Equation 1.13

where g is the viscosity, c_ is the shear rate, and C1–C4 are material-dependent parameters. C_1 determines η_0 that decreases with increasing linear content.C_2 is the relaxation time corresponding approximately to the reciprocal of frequency for the onset of shear thinning. C_3 determines the shear thinning that increases with increasing linear content; that is, branched PLA shear thins more strongly than the linear material.

The molecular weight of a polymer is a fundamental parameter to determine the

final and process characteristics of final product. From a process point of view, molecular weight is the main factor controlling the viscosity of the melt.

In general, at shear rates for film extrusion, it was study that low molecular weight PLA (40,0000 g/mol) behave like Newtonian fluid, while high molecular weight PLA like a pseudoplastic (non-Newtonian fluid). Under the same processing conditions, semicrystalline PLA (highly isotactic) tends to possess higher shear viscosity than its amorphous (low tacticity) counterpart. Moreover, as shear rates increase, the viscosities of the melt reduce considerably, i.e. the polymer melt exhibits shear-thinning behaviour [62]. This phenomena was observed even by Fang and Hanna [63]. The semicrystalline PLA tends to possess higher shear viscosity than its amorphous counterpart. In their view, this due to semicrystalline PLA are arranged in an organized structure, which provides a relatively large resistance to flow. Conversely, amorphous PLA is in a random distribution, which, in turn, exhibits less resistance to flow.

A temperature increase was found to cause a reduction in the shear viscosities for both semicrystalline and amorphous PLA. This condition is observed even for other polymer, and happened because the high temperature induce a weaker effect to connections between the molecular chains.

Temperature, molecular weight and shear rates have significant consequences on the rheological properties of polymer melt. Cooper-White and Mackay [64] studied with a parallel plate rheometer these three effects. The dynamic viscoelastic behaviour, of three commercial grades of PLLA (molecular weights ranging from 40,000 to 360,000 g/mol) have been measured over a broad range of frequencies, shear rates and temperaures.

Figure 1.17 shows a plot of complex viscosity (η^*) as a function of frequency and molecular weight for the series of PLLA polymers when subjected to both dynamics and steady shear. It was observed that only for low a medium molecular weight there was good agreement between dynamic and steady viscosity. For high molecular weight PLA (Mw 360,000 g/mol), even at very low frequencies, is was not possible to observe due to notable sample edge fracture and degradation. The Newtonian viscosity plateau is observed for low molecular weight PLA. The "knee" point, i.e. the shear rate value at which the viscosity begins to decrease, move towards lower values with increasing molecular weight. This is due to the progressive increase in relaxation time. All curves tend to a single straight line at

high shear rates. This is due to the progressive alignment (and possible extension) of the chains polymer. This effect, due to the flow, becomes dominant at high shear rates, making the tangential stress independent of the number of entanglements present.
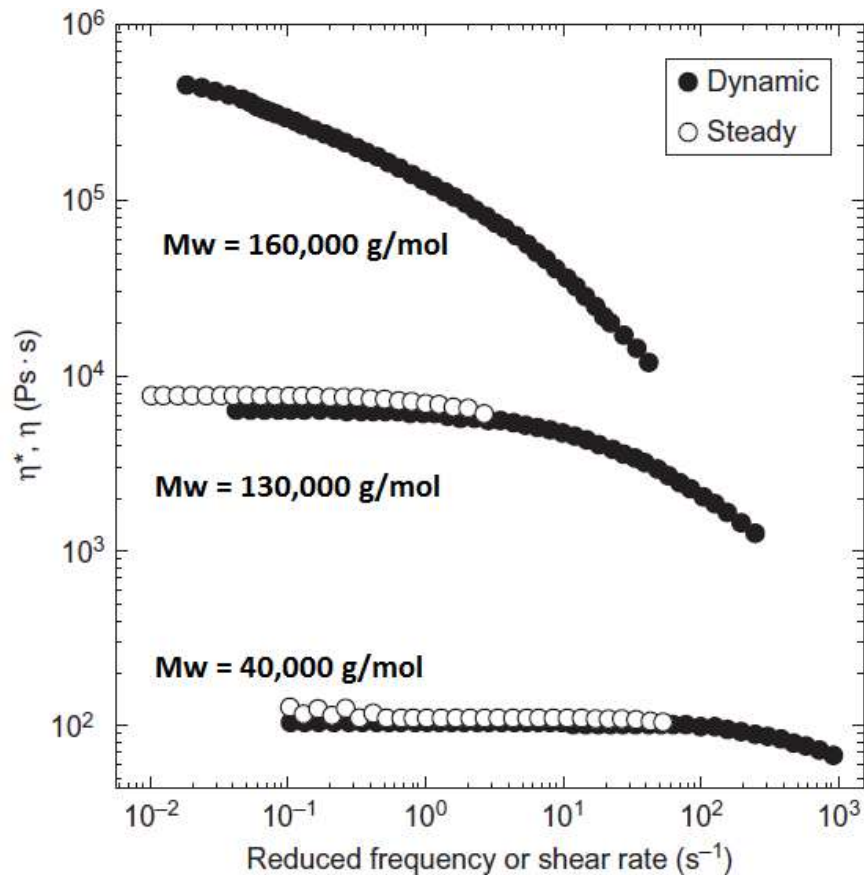
Figure 1.17: Effect of molecular weight on viscosity [64].

1.5.4 Annealing

As reported by Tsuji [65]. the Xc (cristallization degree) of quenched PLLA is generally around 3%, while PLLA annealed at 25-100°C can reach Xc around at 50%.

PLLA specimens annealed at 100°C maintain high the value of the storage modulus above Tg due to the presence of more cristallinity that contributes to the mechanical properties.

These data agree with others reported in the literature and in general, the

annealing of PLLA is accompanied by increase in tensile and flexural strengths, as well as impact resistance and thermo-mechanical properties.

1.5.5 Nucleation and Plasticization

PLA in homogeneous conditions present relatively low nucleation and crystallization rates. This has prompted the scientific community to look for improvement of PLA crystallization kinetics by nucleating agents to increase its nucleation density and plasticizers to improve chain mobility. It is noteworthy that the compounding of PLA with nucleants and plasticizers may lead to molecular weight reduction by hydrolytic or thermal degradation. Therefore care must be taken in distinguishing between nucleation, plasticization and molecular weight reduction effects.

Plasticization increased chain mobility in the amorphous phase unto the existing crystal surface, especially at lower temperatures. Consequently, it has contrasting effects on the crystallization behavior. On one hand, the Tg depression, a measure of plasticization efficiency, will shift the crystallization temperature window to lower temperatures [61].

One of the most investigated plasticizer is Polyethylene glycol (PEG) [66][67][68][69]. It is available in a wide range of molecular weights. Martin and Avérous [67] studied the addition of PEG (Mw 400 kg/mol) at PLLA. Their research discover that the Young's modulus of a pure PLLA decreased from an initial value of 2050 to 1488 MPa at a PEG concentration of 10% and to 976 MPa at 20%.Furthermore the elongation at break increases considerably.

In general, the storage modulus drops in plasticized PLA, the Tg decreases almost linearly with increasing plasticizer concentration, from 67°C for pure PLA to 54 and 46°C with 10% and 20 % of PEG content. Martin and Avérous tested also oligomeric lactic acid (OLA) as plasticizer, the results obtained show a reduction of the elastic modulus of PLLA from 2050 to 1256 MPa with 10% plasticizer and to 744 MPa with 20% plasticizer, while elongation at break increases to 32% and 200%, respectively.

It was discover that PEG in the intra-spherulitic region crystallized much faster than the inter-spherulitic amorphous region [61].

Nucleation is used to increase the crystallization rate during the cooling of the material. In particular nucleation agents increase the temperature of melt crystallization, so during industrial process where the cooling rate are rapid in order to maintain high the productivity of the process, the material starts to crystalize at higher temperature and the final product is more crystalline with respect the material nucleating agent free. In a general classification, nucleation can be either chemical or physical (mineral, organic and mineral-organic hybrids) [61].

- Chemical: chemical nucleating agents operate through a chemical reaction mechanism. For example, Legras [70] studied the nucleating effect of organic salts of sodium on the crystallization of polyesters such as PET and polycarbonate (PC). In the case of PLA, sodium salts such as sodium stearate have been studied for nucleating PLA crystallization but failed to provide significant improvement of the crystallization rate [71].

- Physical: Talc is an efficient nucleating agent for PLLA increasing the polymer crystallization rate. Kolstad at al. [72] showed that for PLLA with 6% of talc the polymer half-time crystallization at 110°C was reduced from 3 minutes to approximately 25 s. For PLLA copolymerized with 3% meso-lactide and with the same percent of talc, the half-time was reduced from about 7 minutes to about 1 minute.

  In another study, Li and Huneault [71] compared the crystallization kinetics of talc and montmorillonite Closite Na+ added to PLLA with 4.5% of D-content. They reported that the lowest crystallization induction period and maximum crystallization speeds were observed around 100°C. By adding 1 wt% of talc, the crystallization half-time of PLA was decreased from a few hours to 8 min. In contrast, the montmorillonite tested was less effective as a nucleating agent achieving 30 min as lowest half-time.

  Organic compounds such as calcium lactate, N,N-ethylenebis(12-hydroxystearamide), benzoylhydrazide compounds, or sodium stearate are also been studied [73][74]. For example, in the L-lactide/meso-lactide copolymer containing 10% meso-lactid the addition of 1% calcium lactate increase the crystallization rate[74].

  Ke and Sun also reported the detailed thermal behaviors of the starch/PLA

blends studied by differential scanning calorimetry [40]. For comparison, talc was also incorporated into PLA at 1%. Starch effectively increased the crystallization rate of PLA, even at just 1% content, but the effect was less compared to talc.

As we said above mixture of PDLA and PLLA can lead to the formation of a complex whose properties are usually very different from those of the parent homopolymers. The melting temperature of the stereocomplex is 230 °C, approximately 50 °C above that of the corresponding homopolymer (179 °C). This different temperature leads to small concentrations of PLA stereocomplex suitable for nucleating PLA homo-crystallization.

Brochu et al. [75] reported that in presence of the PLA stereocomplex, the spherulite density was increased and the homopolymer crystalline fraction was higher than that in the pure polymer, implying the nucleating effect of stereocomplex crystals. They concluded that PLLA crystals can form epitaxially on stereocomplex lamellae that were previously formed at higher temperatures.

In another study Anderson and Hillmyer [76] quantified the effect of PDLA molecular weight (Mn equal to 5.8, 14 and 48 kg mol^{-1}) and concentration (0.5-3 wt.%) on the nucleating efficiency of the stereocomplex. They discovered that only 3 wt% of the 14 kg mol^{-1} PDLA, nucleation efficiencies near 100% could be obtained. In addition, the final crystallinity of PLLA were observed in isothermal crystallization experiments at 140 °C. By contrast, the compared to addition of talc, a common nucleating agent. The effect of the stereocomplex and talc on the crystallization rate of PLA at 140 °C is descrived in Figure 1.18. For the lower and high molecular weight PLLA, $t_{1/2}$ was reduced from 17 min to 1 min and 70 min to 10 min, respectively. In both cases, the half-time for PDLA nucleated samples was one order of magnitude smaller than the corresponding PLA nucleated with 6% talc.
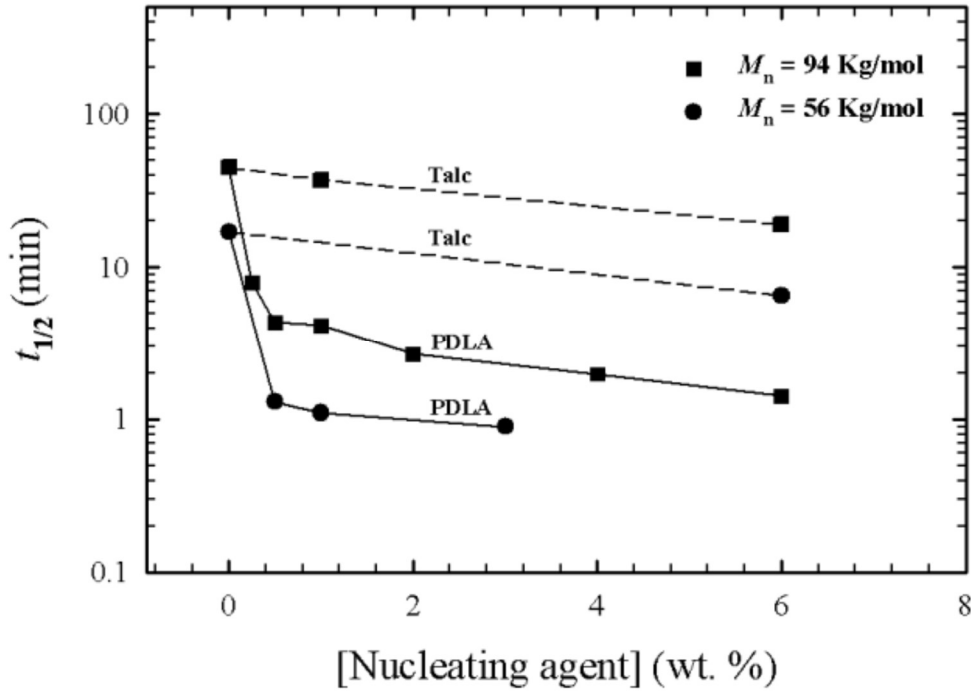
Figure 1.18: t1/2 as a function of PDLA and talc concentration for two PLLAs [61].

Schmidt and Hillmyer [77], they found that crystallinity of PLLA increased when the PDLA content was very low, but tended to plateau at higher PDLA concentrations. It is noteworthy that when cooling from 200 ° C the stereocomplex crystals are already present and those formed by PDLA with higher molecular weight provide a larger surface area for the crystallization of PLLA. On the other hand, when the samples are cooled by 240 ° C, the stereocomplex must be created within the limited time period of the cooling process, therefore a lower molecular weight PDLA is preferable because the stereocomplex is produced at a higher speed.

From the study of Hillmyer at al. [76][77] it was compared the effect of different cooling rates (Φ in °C min^{-1}) with PDLA concentration. In Figure 1.19 two distinct trends arise from the stereocomplex formation route. For samples, in the solid trend lines (pre-crystallized stereocomplex) the Tc increased with PDLA concentration up to a plateau. While in the dash trend lines (direct stereocomplex formation from the melt), the nucleation effects were not observed until the PDLA concentration reached about 5%. There is an insufficient time to form the stereocomplex nucleation sites. Furthermore, Tc shifted to lower values when the molecular weight of PDLA or cooling rate was increased.
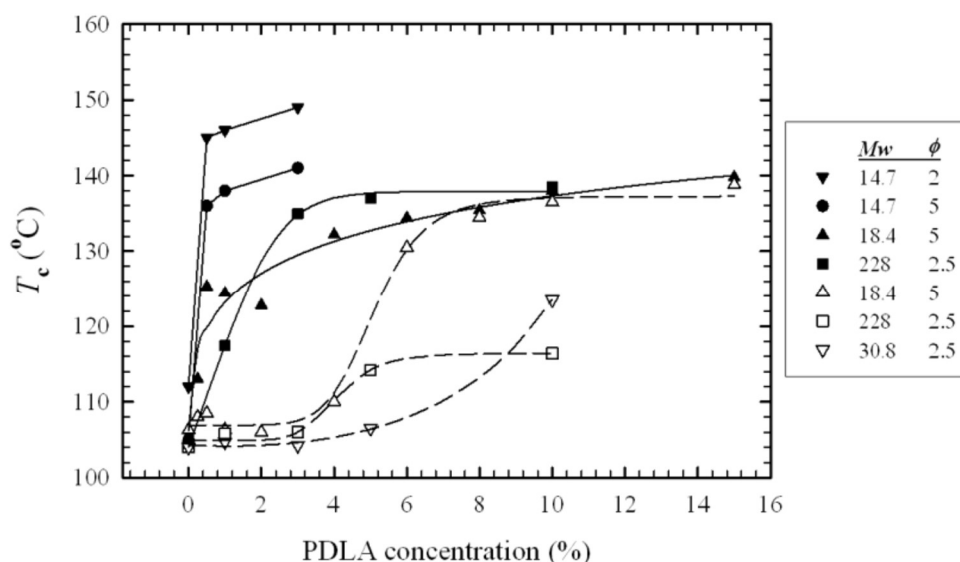
Figure 1.19: Effect of PDLA concentration on peak crystallization temperature for various molecular weight and cooling rate [61].

Tsuji et al. [78] compared the spherulite growth rates of stereocomplex-nucleated PLA with the stereocomplex growth rate observed in their previous study. They concluded that the spherulites contained only PLLA crystallites because the growth rate was independent of the PDLA content. If the spherulites had contained stereocomplex crystallites other than nucleating sites, the growth rate should have increased due to the high stereocomplex growth rate. In addition, increasing the PDLA content did not have a significant influence on the induction time.

1.6   Polylactide Acid Stereocomplex

PLA stereo-complexation derives from stereoselective interactions between the two complementing stereo-regular L- and D- polylactic acid. The result of this interlock is a polylactide acide stero-complex (PLAsc) with altered physical properties in comparison with the homo-polymers.

The first that reported stereo-complexation between PLLA and PDLA was Ikada et al. in 1987 [38]. He observed that X-ray diffraction pattern is different from homopolymer crystals; however, the crystal structure was discovered. Only by previously investigation of De Santis and Kovacs it was possible formulate the crystal structure of stereocomplex [41]. They reported that the crystalline structure

of poly(L-lactide) consists of left-handed helical chains. Since poly(D-lactide) must have a right-handed helical crystalline structure, it is believed that the Van der Walls forces such as dipole-dipole interactions are responsible for the stereocomplexation. Specifically, Van der Waals forces between the hydrogen atoms of methyl group and the oxygen of carbonyl in PLA chains with opposite configurations. The crystalline structure was studied by Okihara et al. [79] based on X-ray measurements and energy calculations. They suggested that chains' conformation is 3_1 helix, each unit cell containing a PLLA and a PDLA chain with the same number of L and D units. It means that in stereocomplex crystals, chains are more extended compared to PLLA α crystal in which chains are 10_3 helices. Moreover, based on energy calculations, they discovered that 3_1 helix chain conformation in stereocomplex is more stable than a 10_3 helix in α-form crystal. Figure 1.20 is a schematic illustration of the stereocomplex crystal structure.
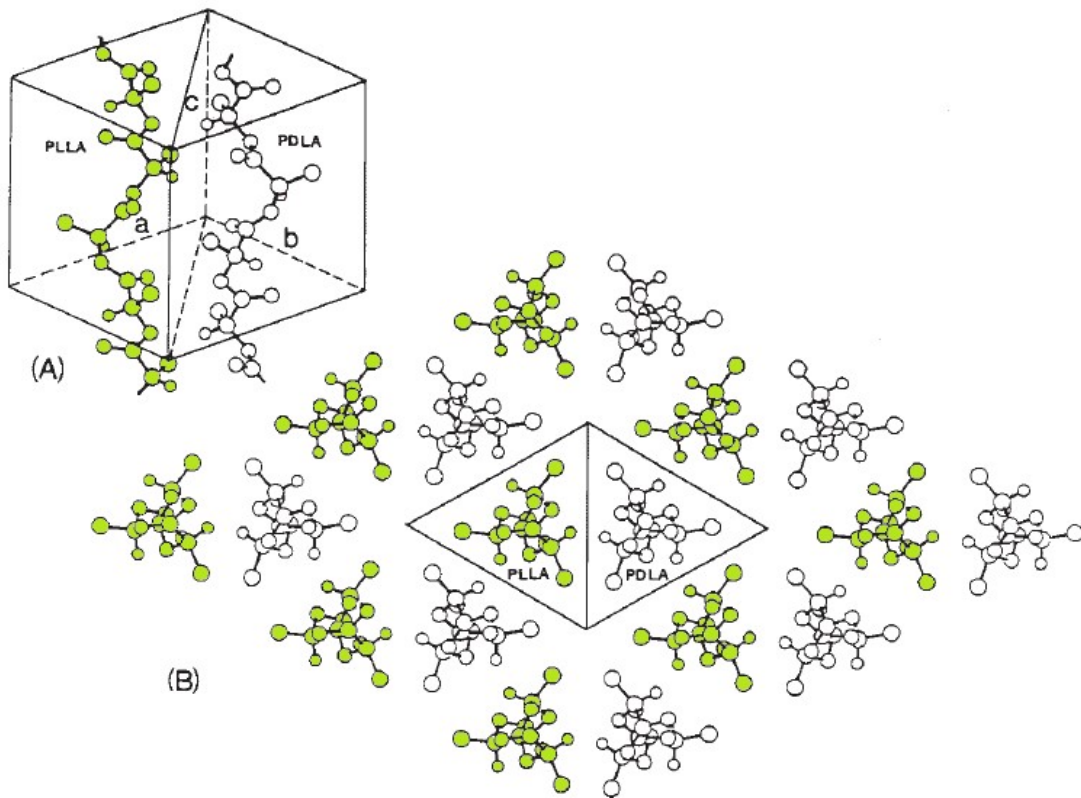
Figure 1.20: Crystal structure of PLA stereocomplex [80].

Brizzolara et al. [81] propose a model of stereocomplex crystal growth, which explains the triangular shape of single crystals. The triangular type of crystallizing offers favorable position for the polymer loops during the crystal growth.

As I reported in the Table 1.1, the most interesting characteristic of PLA stereocomplex is to have a T_m around 230 °C. The difference between the melting point of the homocrystal is about 50 °C and this gives the opportunity to evaluate the existence and amount of stereocomplex in blends of PLLA and PDLA or stereo-block copolymers, simply by DSC analysis.

DSC analysis by Ikada et al. [82], [83] revealed that the optimum blending ratio for PLLA and PDLA is 1:1. At this ratio, only stereocomplex was formed with the procedure they used for blending and by deviating from equimolar ratio, PLA homocrystallization occurred simultaneously. Considering the previously stereocomplex crystalline structure in Figure 1.20 it is reasonable to say that equimolar blending ratio is the optimum ratio for efficient production of stereocomplex.

Tsuji et al. [84][85] investigated how much the PDLA fraction (XD) affected in the stereocomplex formation. He demonstrated the only stereocomplex was detected for XD between 0.4 to 0.6. While was observed melting peaks of both homocrystal and stereocomplex for PDLA fraction (XD) between 0.1 to 0.3 and 0.7 to 0.9.

 Morphology and conformation of PLA stereocomplex was studied by Kister et al. [86] with IR and Raman spectroscopy. They observed spectral changes in peak shapes and wavelengths upon PLA stereocomplexation. Later, by the use of FT-IR, Zhang et al. [87] during stereocomplex crystallization from the melt found that a very small low-frequency shifts of the bands of the methyl and carbonyl groups. This confirmed the interaction between the chains of PLLA and PDLA is attributable to the CH3···O=C hydrogen bonding. Moreover, the peak shift of the v(C=O) band already occurs in the induction period, which indicates that the CH3···O=C interaction is the driving force for the racemic nucleation of the PLA stereocomplex.

Stereocomplexation takes place in bulk during non-isothermal or isothermal crystallization from the melt or the glass and in solution. Considering the efficiency, solution precipitation and solution casting are employed mostly for facility of production and required time for the stereocomplex. Instead, in industry direct melt blending is the preferred route due to higher production capacity and the appeal for solvent-less processing. However the bulk route is less reported in

literature [39], this probably due to the high cost and limited availability of PDLA which made it unpractical for more material-consuming processes.

Tsuji et al. [82][83] compared stereocomplexation by solution precipitation or solution casting and its competition with homocrystallization. The comparison is done with equimolar PLLA/PDLA blends (Figure 1.21).
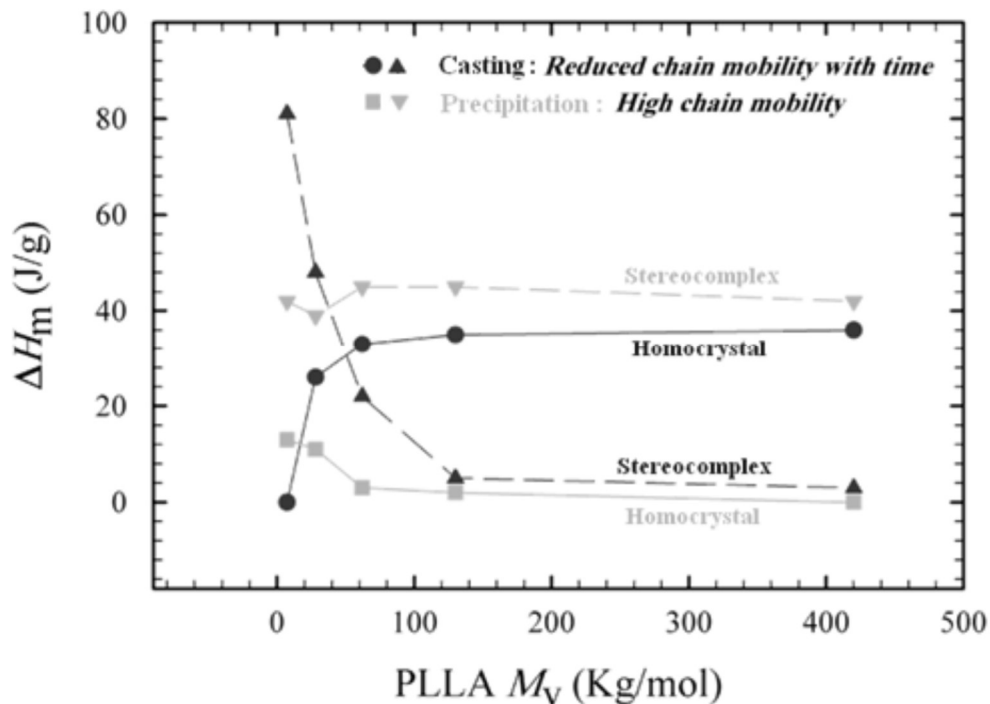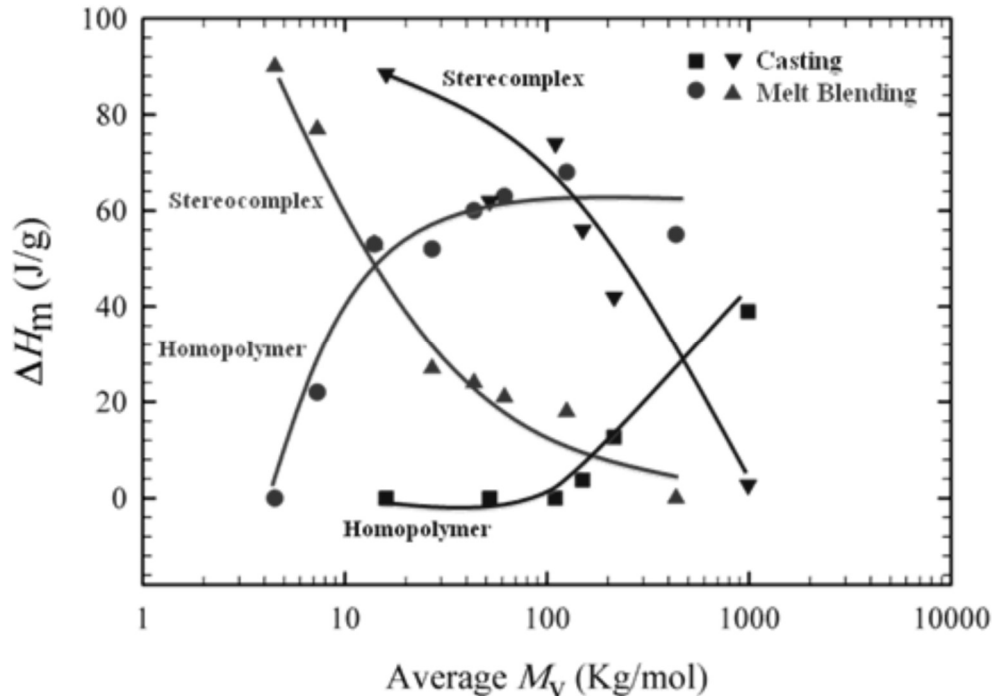

Figure 1.21: Competition between stereocomplex and homocrystal formation in solution casting and precipitation methods [82][85].

As shown in this figure, when precipitation is employed, for a wide range of molecular weights only stereocomplex is formed. Contrarily, in the casting route, the amount of stereocomplex decreased rapidly and gave place to homocrystallization, due to co-crystallization of the chains that could not participate. Increasing polymer concentration and molecular weights, by decreasing chain mobility, prevented co-crystallization.

Regarding stereocomplexation from the melt it was found that stereocomplexation proceeded rapidly after cooling the melt while homocrystallization required much longer induction time [88]. This may be the consequence of higher under-coolings as the equilibrium melting point of the stereocomplex is higher than that of the homocrystals. At the blending ratio of 50:50, homocrystallization increased as

molecular weights are increasing but it is reduced stereocomplex formation (Figure 1.22).

Figure 1.22: Competition between stereocomplex and homocrystal formation in solution casting and from the melt [88][83].

The degree of stereocomplexation is therefore affected by the formation conditions and chain structure, particularly by the molecular weights of PLLA and PDLA and mixing level. With polymers having high molecular weights, the stereocomplexation is hindered by homopolymer crystallization, while complete stereocomplexation can be attained with polymers having sufficiently low molecular weights.

1.7 Biodegradability

Plastics biodegradation could be aerobic or anaerobic, depending upon the environment in which they are degrading, and biodegradation is measured by the amount of carbon by-products that are produced by the biodegradation process in which the sum of all the carbon by-products is equal to the total amount of carbon

in the non-degraded material.

PLA like other bio-based polymer, containing hydrolysable linkages, that are generally susceptible to biodegradation by microorganism enzymatic catalysis. Usually biodegradation reactions occur in aqueous media. More polar are the polymers and more readily can be biodegraded. Also the crystallinity and chain flexibility are important characteristics that affect the polymer degradation.

Biodegradation is a composite effect of different mechanisms that proceed simultaneously or consecutively on the polymer. This process include disintegration, dispersion, dissolution, erosion, hydrolysis, and enzymatic degradation. Generally microbial reactions are sequential, the metabolism end product of a one organism becomes the substrate for another organism. Biodegradation involves the microorganism growth on the surface of the polymer and the secretion of enzymes able to break down the chains into oligo- or monomeric units such as hydroxyacids in case of aliphatic polyesters. Then the microorganism consumes these hydroxyacids as carbon sources in order to produce energy. In aerobic environment the carbon dioxide and water are the main degradation products, whereas in anaerobic environment the degradation products are carbon dioxide and methane.

The whole biodegradation process can take from days to months to years, and it depends on the type of polymer. PLA breaks down slowly in the soil and, if composted, high temperatures are required to decompose it.

PLA is initially degraded by a nonenzymatic catalysed hydrolysis mechanism. Its hydrophobicity nature and the presence of crystalline region act as barriers for the diffusions of enzymes. Therefore at the beginning of the biodegradation the process is slow. Enzymatic involvement can produce pores and fragmentation, making more polymer regions accessible to the enzymes. Subsequently, soil bacteria and fungi microorganism are able to hydrolyse the shorter polymer chain formed, consuming these oligomers with their enzymatic catalysed reactions [74].

1.8 PLA Application

1.8.1 Agricultural

The biodegradability of PLA can begin to be exploited in agricultural applications such as sandbags, weed prevention nets, vegetation nets and pots etc. These applications are very interesting because the materials can be left in the ground to decompose without needing to remove it. For this reason, the complete decomposition in the ground is essential but at the same time, a structural integrity during their use is compulsory. Moreover, PLA needs to possess properties that permit manufacture on an automatic loom. Tight binding, abrasion resistance, and branching prevention are required. The use of monofilament, yarn, and nonwoven fabric made from PLA loaded with inorganic fillers are example used to satisfy this request.

1.8.2 Electronics

Over the past 20 years, the electronics industry as well as make great strides in technology has also undertaken efforts to improve its environmental profile. In particular, optimizing the energy efficiency of products and devices and the sustainability of the materials used. Biodegradable polymers can reduce the amount of waste electrical and electronic equipment.

In order for a biodegradable polymer to be used in electrical and / or electronic devices, this must have high mechanical and thermal strength. However, the thermomechanical and electrical properties of these polymers remain inadequate for electrical and electronic because good flame resistance properties are required. Another good alternative is the use of biocomposites that include materials containing a biopolymer in combination with structural reinforcing materials such as carbon, plant or wood fibber.

PLA based materials are the greatest promise to replace polycarbonate /acrylonitrilebutadiene-styrene (PC/ABS) blends that are actually the most used in the electronic device. However, PLA is brittle, and more difficult than PC/ABS to make flame resistant. The solution was compounding PLA with various additives

or PLA blends with other polymers were studied to overcome these drawbacks. NEC developed a flame-retardant PLA composite with durability that exceeds flame-retardant used in conventional consumer electronic devices such as personal computers (PCs).

The recent applications are the Bioserie iPhone 5 cover and the Telecom Italia's Eco-cordless telephone made of PLA Ingeo® NatureWorks Bioserie [89].

1.8.3 Packaging

Poly(lactic acid) is a thermoplastic polyester characterized by mechanical and optical properties similar to polystyrene (PS) and polyethylene terephthalate (PET).

The thermoplastic nature of polylactic acid permits to process it with different techniques like extrusion, thermoforming, injection moulding, compression moulding, blow moulding and film blowing. The range of objects obtainable goes from fibres, films, bottles and printed items, making the PLA packaging applications various. The applications of packaging materials are in functions of the use period of the materials and function of it. It is short and they are disposed after use, such as food packaging, while for applications like packaging of electronic items, cosmetics containers, etc were required that the initial properties of the polymers can be maintained for a longer period.

The industry that plays a fundamental and strategy role in the use of non-renewable and non-biodegradable materials is the food packaging industry. This is because it is one of the largest producers of waste disposal. Therefore, the replacement of the current commodities by biopolymers is desirable, particularly PLA. But the industry of food required a rigid legislation against health risck for consumers, particularly when the product was used at temperature above Tg. The use of PLA in contact with food is considered safe by the European Commission and the US Food and Drug Administration [90]. In fact the degradation pathway of PLA leads to the formation of lactic acid, which is considered safe in many applications. One of the main goal of food packaging is maintain unaltered the food organoleptic and nutritional properties. Hence, material should be chosen with outstanding characteristics in terms of barrier properties against radiation, water vapour, atmospheric gases and organic compounds, preventing food

degradation and oxidation while preserving aromas and flavours [91]. The other key point is light-sensitive food due to the degradation of product when exposed to radiation and oxygen. This condition is important because UV radiation is increasingly utilized in food sanitization, as an alternative method to chemical preservatives. From this point of view, PLA shows better behaviour than classical materials like polystyrene, cellophane, PET or LDPE [92].

The least but not the last aspect for PLA is the light coloration imparted by the polymer. In fact, PLA presented a natural yellowish coloration and this aesthetic aspect can create a consumer perception of ''old stuff''. The problem was solving with colorizing agents that changing the visual aspect of the final articles.

1.9   Processing PLA

1.9.1 Drying and extrusion

Typically the processing of PLA start with drying the pellets to prevent excessive hydrolysis, that can compromise the physical properties of the polymer. Natureworks LLC, one of the main suppliers for PLA polymers, recommended that polymer should be dried to 250ppm (0.025%, w/w) moisture content or below before extrusion. As reported in the Figure 1.23 to perform an effective drying, the dew point of the drying air should be −40 ∘C or lower. Commercial grade PLA resin pellets are usually crystallized, which permits drying at higher temperatures to reduce the required drying time.
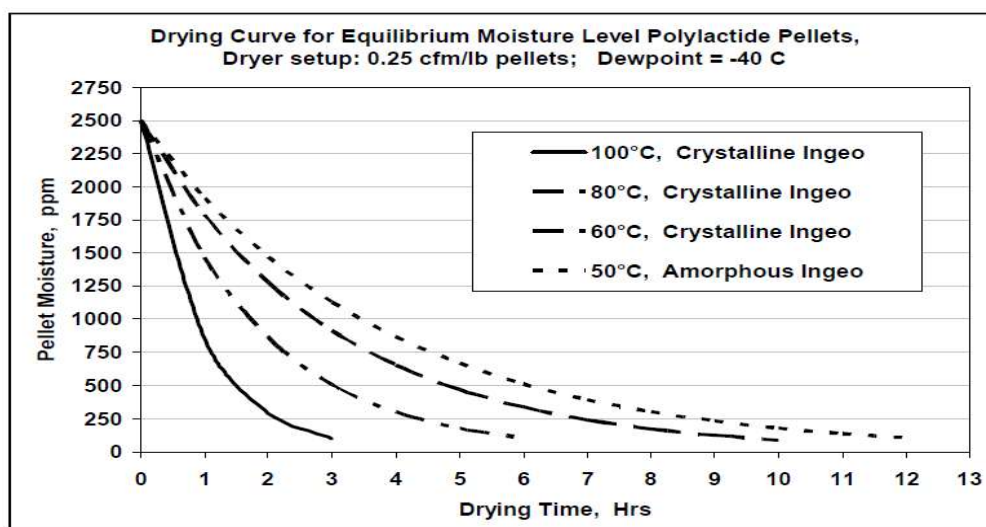
Figure 1.23: Drying Curve for Equilibrium Moisture Level Polylactide Pellets.

In industry drying of PLA is commonly achieved using a closed loop dual-bed regenerative desiccant-type dryer. In this type of dryer, the resin pellets are contained in a hopper that is purged with dry air at elevated temperature.

Extrusion is the most important technique for continuously melt processing of PLA. The plasticizing extruder can be part of the forming machine systems for injection moulding, compression moulding, film blowing and melt spinning. Figure 1.24 shows a schematic representation of the major components of an extruder screw.
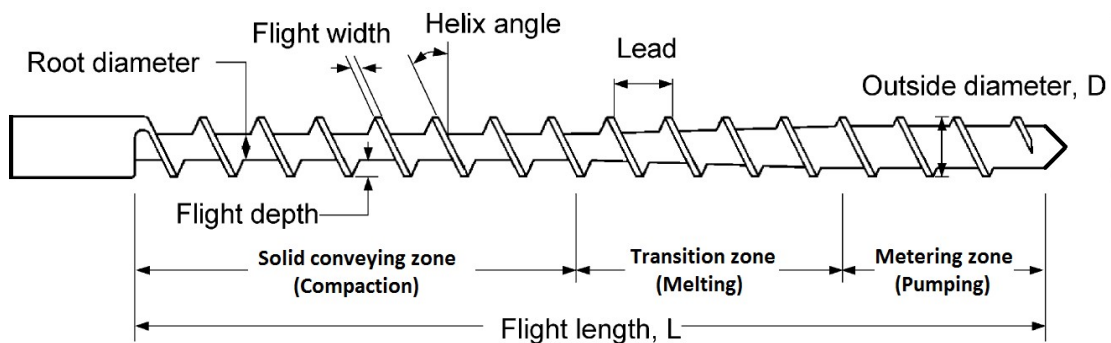
Figure 1.24: Component of extruder screw.

A typical screw consists of three zone:

1. Solid conveying zone – the flight depth is maximum and constant while the root diameter is minimal in order to be able to easily transport and compact the solid polymer.

2. Transition zone (also known as compression or melting sections) – flight depth decreases gradually in the direction of advancement of the material, while the root diameter increases in order to compress the polymer. The ratio between the cross-section of the polymer at the beginning and the end of this area is called compression ratio (RC). The greater the compression ratio a screw possesses, the greater the shear heating it provides

3. Metering zone – flight depth is again constant and is minimal while the root diameter is maximum, in order to mix and pressurize the required quantity of molten polymer.

The L/D ratio, which is the ratio of flight length of the screw to its outer diameter, determines the shear and residence time of the melt. Screws with large L/D ratio provide greater shear heating, better mixing, and longer melt residence time in the

extruder. Commercial grade PLA resins are typically processed with a screw of L/D ratio of 24–30. Moreover, is used screws for processing PET, which are typically low-shear for gentle mixing to minimize resin degradation and acetaldehyde generation [93].

1.9.2 Compression moulding

Compression moulding is historically the first form of plastic moulding ever developed. The principle behind this technology is the application of force, in the form of moulding pressure, on a polymer contained in a mould of the shape of the final product to be obtained. There are two different technologies based on the concept of compression: the discontinuous process and the continuous process. Discontinuous compression moulding is usually used to produce thermosetting polymers or rubber moulding. In the first case, the polymer is compressed inside a heated mould; the temperature and the pressure causes a natural movement of the polymer to fill all the mould. Due to the heat, the process of transformation of the plastic material continues until it is completely hardened; in a second time, the object can be removed from the mould (Figure 1.25). With this technique, it is possible to obtain objects of mass between a few grams and a few kilograms.
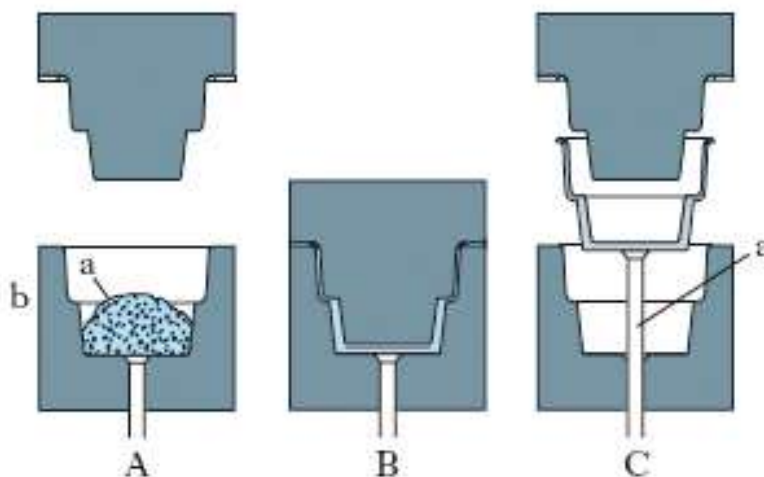
Figure 1.25: Discontinuous compression moulding for thermosetting polymers.

Compression moulding is the traditionally most used method for moulding rubber technical articles. The raw rubber in the form of semi-finished product loaded in

the open and thermally conditioned mould. When the press surfaces are closed, the material flows into the mould and vulcanizes due to the temperature and pressure in the post. After a certain time (which depends primarily on the type of material used and the volume of the piece to be produced) the mould is opened and the pieces are removed. Usually follows a process of trimming artefacts.

In the continuous compression moulding, the material is first extruded and then it is inserted into a cooled rotary moulding. This type of technology is particularly efficient for the realization of small axisymmetric objects. It is not hard to believe that this technique has been widely used in the production of plastic caps. It is estimated that about 50% of plastic closures are printed by compression and the remaining 50% is produced by injection moulding.

The compression moulding press is composed of several units:

- Extrusion
- Portion insertion system and capsule extraction
- Rotary moulding

The task of the extruder is to plasticize the compound; that means melting, mixing and preparing the melt correctly for the lining process.

As reported in the extrusion paragraph at the head the screw is positioned a volumetric pump that has a dual purpose: keeping the pressure constant and regularizing the flow of melt material. At the end the melt reaches a nozzle whose diameter can vary depending on the weight of the capsule and the productivity (usually it is between 10 mm and 25 mm). The possibility of extruding by a nozzle allows using materials with a lower Melt Flow Index and working at lower temperature. Lower extrusion temperatures mean less energy needed to bring the material to extrusion temperature and, since the material is colder, less energy to cool it is needed (Figure 1.26).
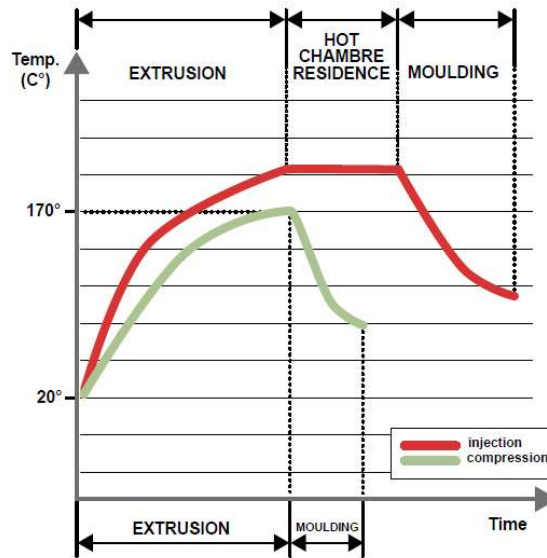
Figure 1.26: Cycle time differentiation between compression and injection moulding.

Once the melt polymer passes through the nozzle, a rotating system of shearers cuts the melt into pellet portion that are transported inside the cavities of the rotary mould (Figure 1.27). The setting of the insertion system depends on both the weight of the portion and the physical characteristics of the melt itself. For example, it needs to be considered the rheological phenomena like die swelling or melt strength.
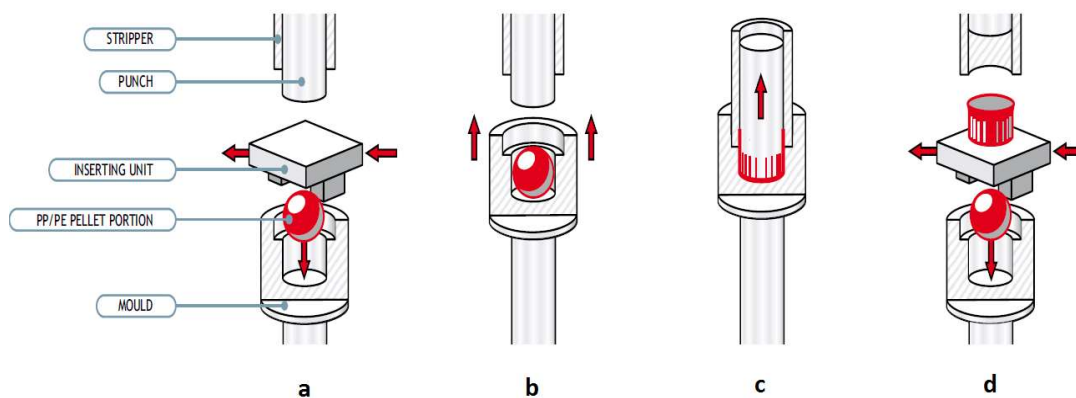
Figure 1.27: Continuous compression moulding phases: a) cut/transport dose; b) dose insertion; c) moulding; d) extraction.

On the rotary moulding, there are individual independent moulds, which allow the moulding and cooling of the material. According to the dimensions of the capsule and the rotary mould, it is possible to obtain a variable number of moulds between

8 and 80. Each moulds are equipped with an independent cooling system between the upper and lower units. During the work cycle, the mould remains open during the insertion of the dose and the extraction of the capsule and closed during the actual moulding phase (Figure 1.28). When the mould is closed, is applied a pressure to flow the material into the mould and form the capsule; in the meantime the plastic is cooled to have the mechanical properties necessary for the extraction phase.
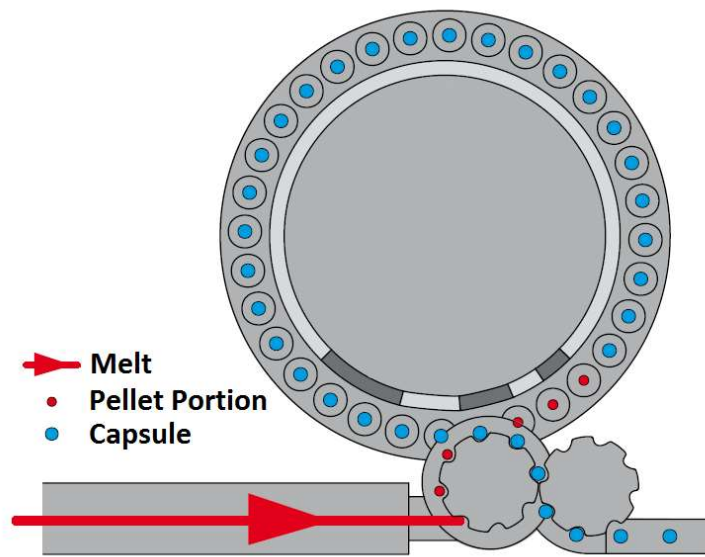
Figure 1.28: Rotary moulding.

2. Aim

Although Poly(lactic acid) (PLA) possesses many desirable properties, above all biodegradability an compostability, a high crystallinity degree is desirable to increase the heat resistance of PLA. It is rather difficult to reach high values during injection and compression moulding due to its very slow crystallization kinetics.

Thus the increase of temperature above PLA glass transition during the further processing steps (e.g. in the packaging of hot products) or during the use of the material, can enable cold crystallization, resulting in undesired shrinkages leading to dimension instability and deformation of the items. In order to improve these properties, two different approaches can be carried out:

The first concerns the synthesis and use of a PLA stereocomplex (PLA$_{SC}$) by mixing PLLA and PDLA, because this blend has shown higher crystallization rates and higher melting temperature than the singles homopolymers. The goal of this strategy was defined, at laboratory scale, how the parameters (molecular weight, temperature, shear rate, induction time, and viscosity) affect the formation and crystallization of the PLA stereocomplex. To study the formation and crystallization of the PLASC, an innovative technique has been used, by means the coupling Rheometer and Raman Spectrometer. Combining Rheo-Raman provides simultaneously information on both the chains interaction and viscoelastic properties that influence the PLA$_{SC}$ formation and crystallization.

The second approach regards the possibility of post crystallization of the molded articles by heating route and hence increase the properties. In particular was studied the effect of different PLA molecular weight and nucleating agent that favours the formation of the PLA spherulites. The focused of this post-crystallization treatment is increased the crystallinity up to a level at which coffee pods may resist thermo-mechanical stress in coffee-making machine. A final step is to introduce an industrial oven for post-crystallization of coffee pods in the final step of production chain.

3. **PLA-stereocomplex**

The widespread applications of PLA are lacking due to its poor thermomechanical properties, as the low thermal stability (above Tg), low crystallization rate and brittleness of the final manufacture [4][93]. In order to improve these properties, different approaches are investigated [3][4]. One of these solution concerns on the formation PLA stereocomplex by means a mixing of PLLA and PDLA chains.

Two aspects of stereocomplex formation can be useful in the process of crystallization of the PLA:

1. It was found that stereocomplexation proceeded rapidly after cooling the melt while homocrystallization required much longer induction time. This may be the consequence of higher under-cooling as the equilibrium melting point of the stereocomplex is higher than that of the homocrystals [88].

2. In presence of the PLA stereocomplex, a higher crystallinity and the spherulite density was observed during the PLA homopolymer crystallization process; suggesting then the possible use of PLA$_{SC}$ as nucleating agent [75].

As reported in chapter one, stereocomplex formation between PLLA and PDLA can occur by blending of these two polymers mainly in solution [95][96][97] or in melt [39][80]. Both processes presents pro and con's, for example with the solvent casting process it is possible control the exact ratio between the two homopolymers, while the main coin's regards the use of chlorinated solvent (with their problems regarded their recyclability) and the necessity to work with a discontinuously process (batch). On the other hand, the main pro of the melt compounding is correlated the possibility to work under continuously condition (extrusion), The main con's regards the necessity to work with a tight control of the operative parameters as temperature, shear rate and the thermal history during the process.

The studies on the melt-blending process [98][99][100] have shown that the complete stereocomplex crystallization occurs in a shorter period than the pure PLLA and PDLA systems. Several methods have been reported for tracing PLA stereocomplex formation [95][96][100][101]. Unfortunately, all of these studies focused the attention only on the characterization of PLLA/PDLA already blended

(both in solution and in melt). During the mixing process of the two homopolymers, that lead the formation of the blend, new entanglements/interaction are formed between the polymer chains. The formation of these interactions is strictly correlated both the operative parameters and to the specific features of the homopolymers mixed. The thermal treatments above the melting point of the PLA stereocomplex (PLA$_{SC}$) don't remove the already generated interactions because these latter occur between the PDLA and PLLA chains (the link between the homopolymer chains are already present). A deeply investigation on the main parameters that can be affect the stereocomplex formation process will be shown in the following paragraphs. In particular, the influence of pre-shear rate of the initial mixing, the temperature and the molecular weight of the two homopolymers are investigated.

The tests were carried out monitoring the rheological properties of the mixture during all the phase of the process by a rheometer equipped with a Raman spectrometer, in order to follow all the crystallization formation.

Both PDLA and PLLA with high and low molecular weights were tested with PDLA:PLLA ratio equal to 1:1 wt, in order to maximize the yield and the properties of the stereocomplex [97][100][101] and emphasize also the Raman signals of the species [102][86][103].

The temperatures of the mixing were fixed to 190 and 200°C in order to melt completely the homopolymers (their T$_m$ is 175-180 °C) and also to work at temperature close to the onset of melt of the stereocomplex. While, regarding the shear rate, values from 0 to 220 s^{-1} were applied for 15 seconds. The stereocompelx formation process was followed by a time sweep test and Raman acquisition in order to monitor the formation and crystallization of PLAsc.

3.1 Experimental section

3.1.1 Material

As reported in Table 3.1, different grades of Poly (lactic acid) were applied for the stereocomplexation. PLA pellets were supplied by SULZER.

Table 3.1: Properties of PLA grades available from SULZER.

	Sample ID	T_m [°C]	Mw [Kg/mol]	PDI	MFR [g/10 min]	D–Isomer [%]	Crystallinity [%]
L100-M	PLLA_HW	180	73 *	1,72	15 **	< 0.3	45 - 55
L99-L	PLLA_LW	173	62 *	1,78	30 **	< 1	40 - 45
D100-M	PDLA_HW	175	72 *	1,74	15 **	> 99.7	40 - 50
D100-LL	PDLA_LW	175	32 *	1,75	40 **	> 99.7	45 - 60

* Absolute values measured by GPC with light scattering detector
** 190 °C / 2.16 Kg [104]
HW = High Molecular Weight
LW = Low Molecular Weight

3.1.2 Sample preparation

To avoid degradation due to hydrolysis and prevent the formation of voids during processing, PLLA and PDLA pellets were dried at 80 °C under vacuum overnight. The pellet of each homopolymer was cryogenic grinded with an M 20 Universal batch mill by IKA. To obtain the correct diameter of the powder (1 mm), sieves with different diameters were used. Finally, the powder was dried at 80°C under vacuum overnight.

3.1.3 Test Methods

Rheo-Raman Coupling

In Figure 3.1 and 3.2 the instrument setup are depicted. It represents a novel integration of commercial instrumentation: a Raman microscope (Thermo Scientific DXR Raman Microscope) and rotational rheometer (Thermo Scientific

HAAKE MARS III) are coupled through an optically transparent base modified from the Thermo Scientific HAAKE. The primary modification to commercial instrumentation is the close optical path to guide laser light from the Raman to the sample through the transparent rheometer base and bench to the detector. The rheological and Raman data collection was started simultaneously through their respective software.
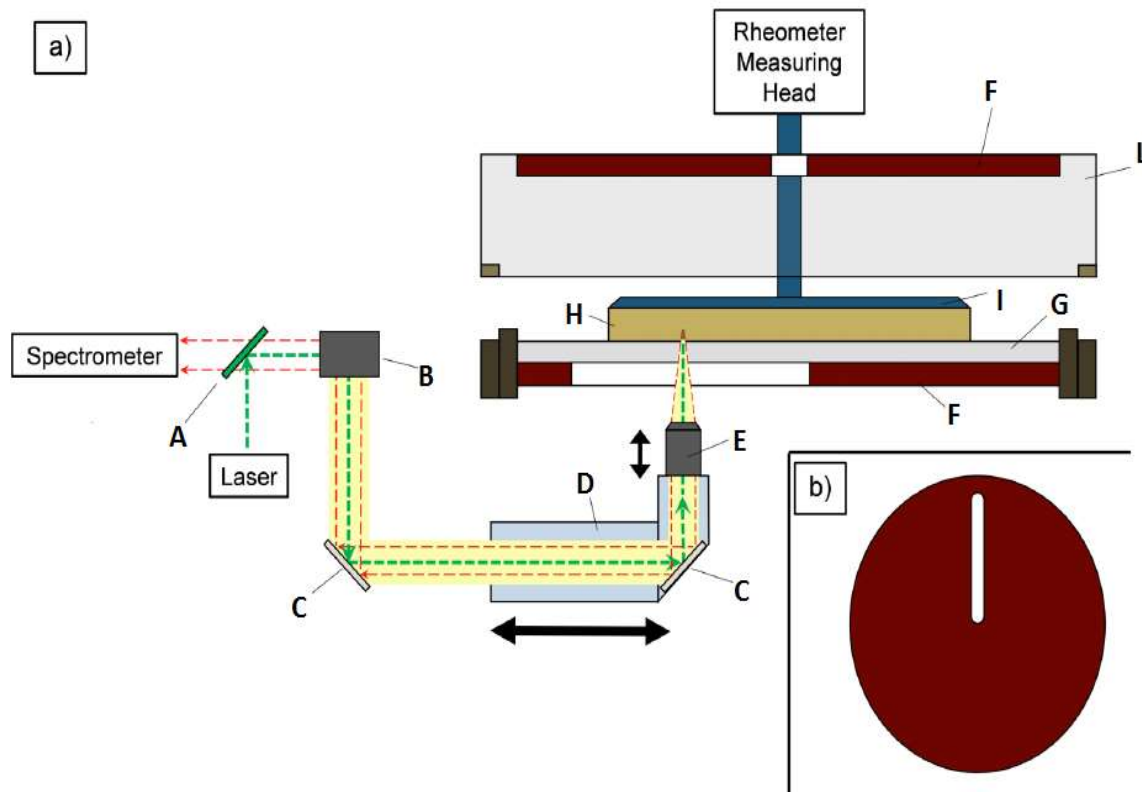
Figure 3.1: 1. Schematic diagram of the experimental apparatus. (a) Side view cutaway of the coupled Raman-rheology system: A, edge filter; B, movable mirror; C, mirror; D, lens tube; E, objective 25x; F, electric heating element; G, glass plate; H, sample; I, upper plate; L, heating enclosure. (b) Top view of the bottom heating element F showing the geometry of the opening for optical measurement [105].

The slit on the botton heating element (Figure 3.1 section b) allows to focus the laser on different points of the sample. Unlike the cone plate geometry, where the shear rate is uniform throughout the radial position (R), the parallel-plate geometry is sensitive to meccanical changes near the outer edge of the sample. This behaviour is correlated to the R^4 dependence for the tourque [106]. It is for these reasons that the objective used for Raman spectroscopy is positioned to probe a region that is 9.5 mm from the center of the plate.
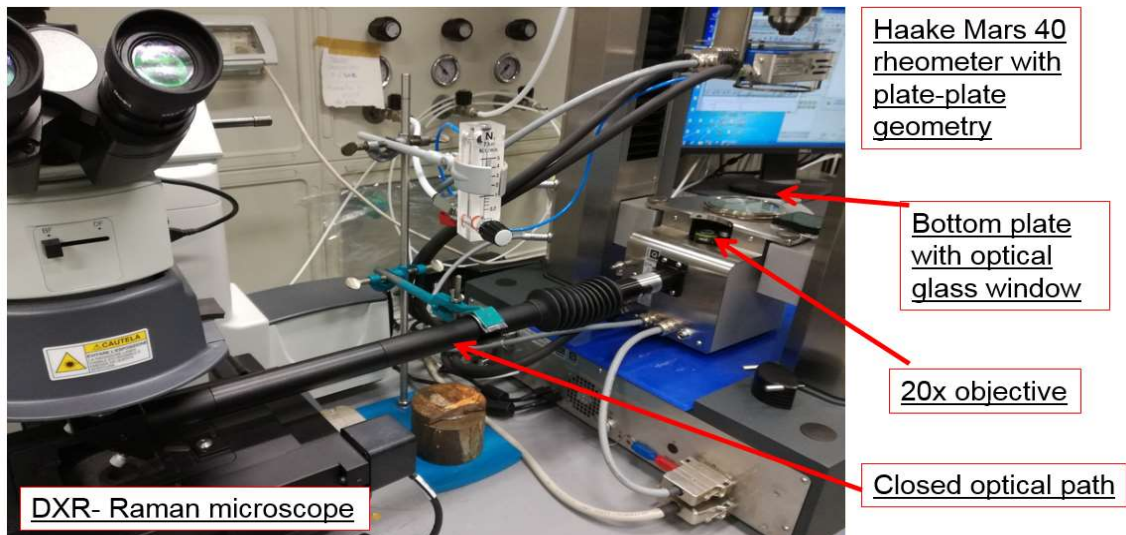
Figure 3.2: Instrument setup.
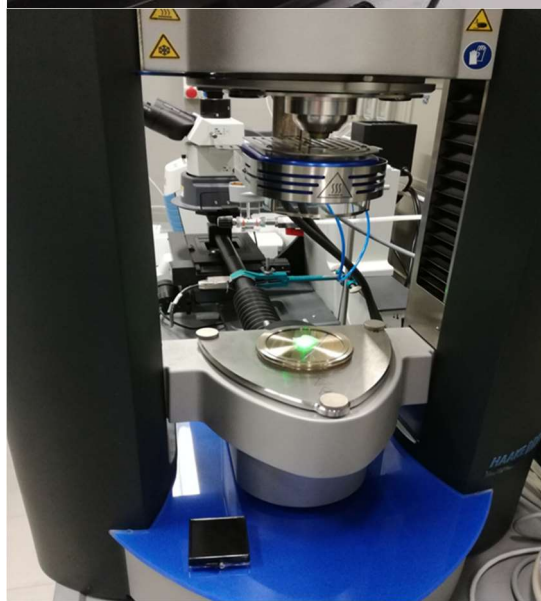
The protocol setup is reported in Figure 3.3: (1) powders of PLLA/PDLA were mixed in a 1:1 weight ratio and loaded between the parallel plates heated at 240; (2) maintain the sample was kept at 240 °C for 2 min to melt the powder; (3) the sample was cooled to 190 °C or 200 °C at the cooling rate of 15 °C/min, and excess of material trimmed out; (4) Pre-shear at a shear rate of 0, 20, 60, 100, 140, 220 s^{-1} was applied for 15 s; (5) The time evolution of the storage modulus (G′) and Raman spectra was followed during the formation and crystallization of PLA sterocomplex process under SAOS' conditions.

To avoid any degradetion due to hydrolysis the experimental setup is carring out under dry nitrogen flow.
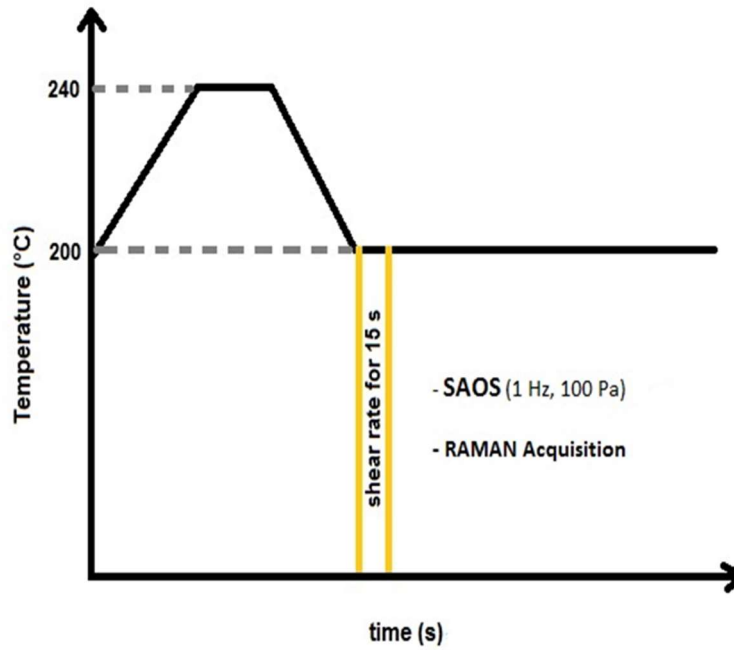
Figure 3.3: Schematic illustration of protocol setup.

Upon completion of the two series of test runs, the sample was removed through glass plate and quenching under liquid nitrogen. All the quenched samples were stored in a desiccator after drying at 60 °C for 24 hours in a vacuum oven. It was further investigated with differential scanning calorimetry DSC.

Rheometer

The rheological properties and isothermal crystallization kinetics for PLLA/PDLA blend samples after shear were performed using a Thermo Scientific HAAKE MARS III rheometer, equipped with a 20 mm diameter stainless steel parallel-plate geometry. In order to determine the linear viscoelastic region (LVER) an amplitude sweep test was performed. The PLA stereocomplex crystallization process after shear was studied by using the rotational rheometer in an oscillatory time sweep mode. This test were performed at 1 Hz with a constant stress of 100 Pa, and data were collected for 30 min (1800 s). The temperature was kept constant throughout the test period.

Time sweep test on PLLA and PDLA samples were run under the same condictions. Plots of complex viscosity (η^*) versus time showed nearly constant values over the time, so degradation reactions during Rheo-Ramen experiment can be ruled out.

Spectrometer

Raman spectroscopy measurements were performed using Thermo Scientific DXR Raman spectrometer. The Raman spectroscopy measurements were performed using 532-nm laser operating with 10-mW power at the sample. Spectral resolution of 5.0 cm^{-1} full width at half maximum (FWHM) is obtained by selecting a 50 μm slit aperture and a ruled grating with a groove density of 900 grooves per mm. This provides an average of 2cm−1 per charge-coupled device (CCD) pixel element, and the spectral range is 200 cm−1 to 3500 cm−1. Alignment of the laser and Raman scatter were all software controlled. The exposure collection time is 5 s, and 2 sample exposures are averaged per spectra collection in all series.

Calorimeter

The melting behaviour of neat PLLA/PDLA and PLA stereocomplex were investigated with differential scanning calorimetry (DSC 6, PerkinElmer, USA) under nitrogen atmosphere.

Sample around 5 mg were heated from 20 °C to 260 °C at a scanning rate of 20° C/min. The glass transition temperature, cold crystallization temperature, homo and stereocomplex melting temperature, the melting enthalpy of homo and stereocomplex, as well as the cold crystallization enthalpy were recorded.

3.2   Results and discussion

Representative Raman spectra for homopolymers and stereocomplex (PLA$_{SC}$) are shown in Figure 3.4.These sharp spectral features suggest a high degree of conformational order, which is indicative of semicrystalline and crystalline structure. Spectral differences of PLA homopolymers and PLA stereocomplex are to be found in the two helical conformations. In the α-form, PLA homopolymer crystallises in an orthorhombic system with two chains per unit cell, each one in a left-handed helical 10$_3$ helix conformation PLA$_{SC}$, on the other hand, adopt a 3$_1$ helix chain conformation, containing a PLLA and a PDLA chain with the same number of L and D units alternatively side by side.
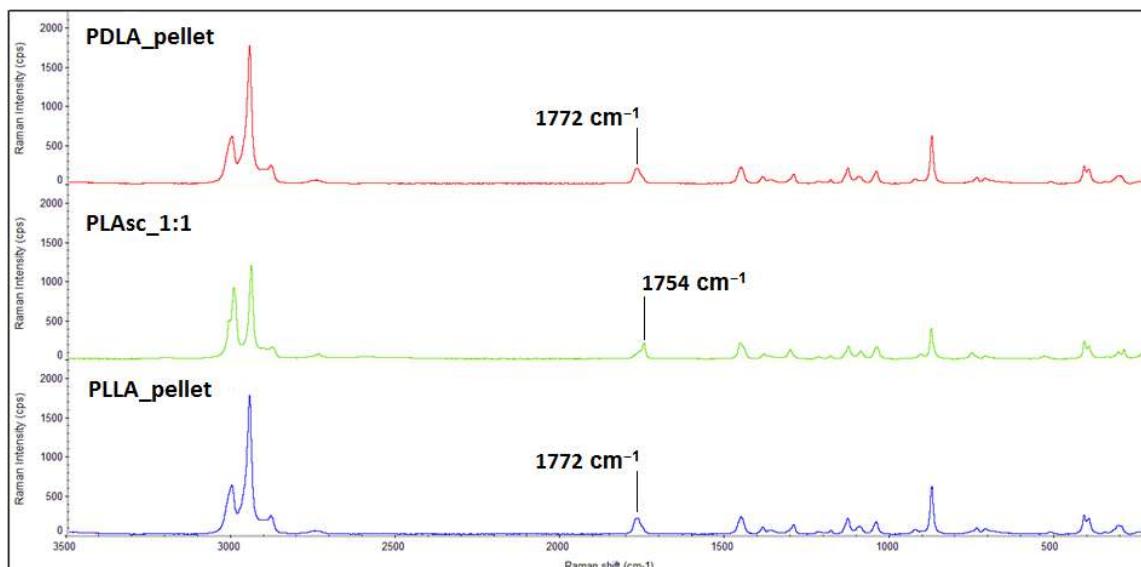
Figure 3.4: Raman spectra for PLLA pellet (red), PLAsc (green), and PDLA pellet (blue).The peaks at 1772 cm^{-1} and 1754 cm^{-1} indicate relevant Raman bands to the stereocomplexation formation.

Specific markers in the Raman spectrums define the difference between PLASC from PLA homopolymers [86]. One of these, is the presence of narrow peaks shifted in frequency, especially from 1772 to 1754 cm^{-1} in the carbonyl stretching region (vC=O) Figure 3.5.
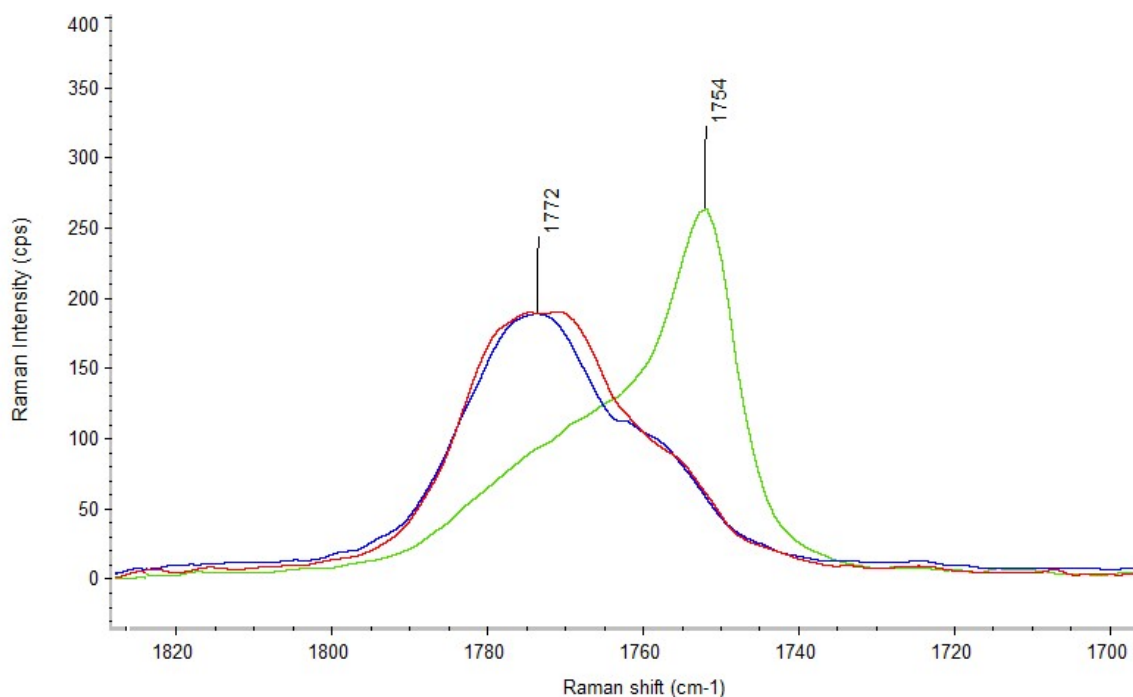

Figure 3.5: Carbonyl stretching region.

In PLASC, the C=O stretching mode is consequently sensitive to the morphology

and the conformation. Furthermore, as reported above, the interaction between the chains of PLLA and PDLA is attributable to the CH3···O=C intermolecular hydrogen bonding or stereoselective Van der Walls forces. This combination is the driving force for forming the PLAsc formation. The peak heights at 1754 cm^{-1} and 1772 cm^{-1} were used as a measure the overall PLAsc formation and crystallization process. In order to observe this development, intensity parameter values were calculated as follows:

$$I' = \frac{(I_{1754} - I_{1772})}{(I_{1754} + I_{1772})}$$

Equation 3.1

At the beginning of the isothermal analysis (Figure 3.6a), the PLLA/PDLA blends were in the molten state, and Raman spectra are representative of homopolymers signal (I' of negative values). However, the peak of PLAsc will get more and more pronounced as time passes. In fact, peak rises when crystallization starts (I' reaches the positive values).
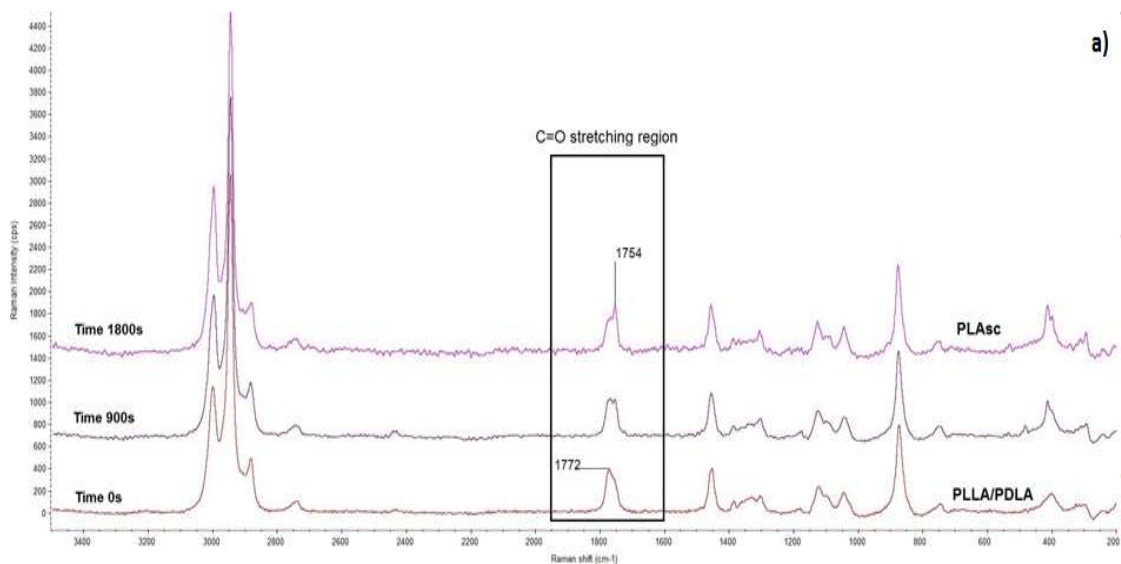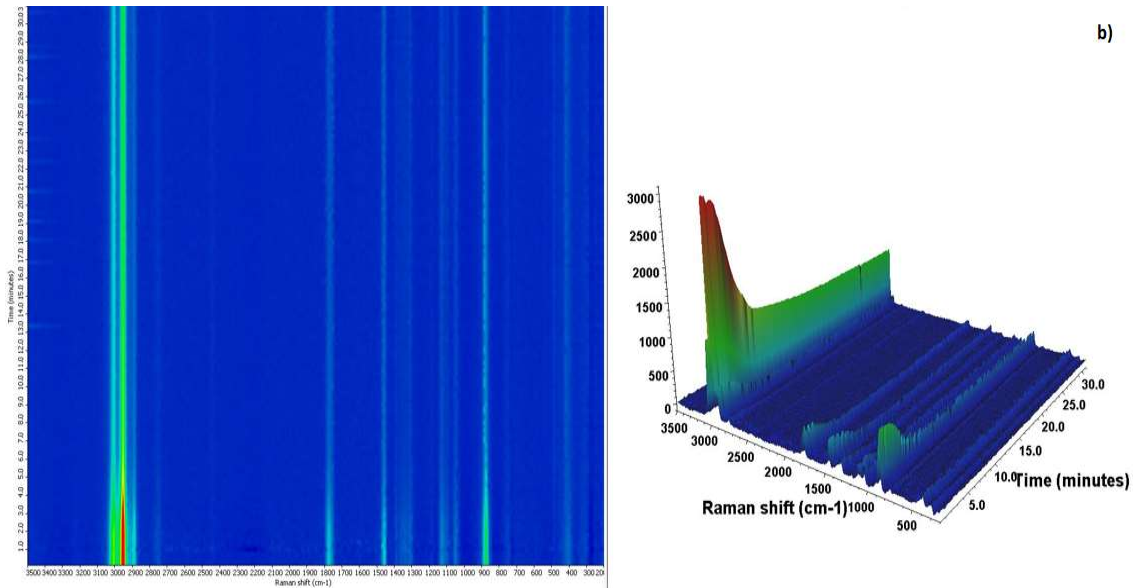
Figure 3.6: a) Raman spectra at the beginning, half time, and final acquisition. b) Software development of all spectra during the time.

Figure 3.6b describe controversial results. Not long after the experiments began, a decrease of intensity of spectral region is observed. It is proposed to be caused by the formation of crystallites of PLA$_{SC}$ matrix [107]. Crystallites with dimension on the same order of magnitude as the wavelength of the incident laser light (532 nm) would scatter light and, as a result, an overall loss in Raman signal can be observed (matrix effect). Peak height ratio was used because data were more consistent respect to peak area ratio for this study. Nevertheless, the decrease of signal is an indication that the crystallization of PLA$_{SC}$ progressed.

The Raman indicators were monitored during time evolution of the Rheometer indicators, storage modulus (G') and loss modulus (G''). G' and G'' are index of material's elastic and viscous behaviour, respectively. At the beginning of test PLLA/PDLA blend is in molten phase and viscous behaviour is predominant (display liquid-like behaviour). In fact G'' is greater than G'. Indeed, as time progressed, G' tends to become constant, reaching a value roughly equal to the absolute value of the relaxation module in the initial instants following the deformation step (Plateau module). On the contrary, G'' goes through a more or less marked maximum and then its values remain below G' values in this area. The response of the material dominated by G' is much more similar to that of an elastic solid (display solid-like behaviour), see Figure 3.7. The crossover point (G' = G'') occur in the moduli as the values of G' and G'' increased over two orders of magnitude.
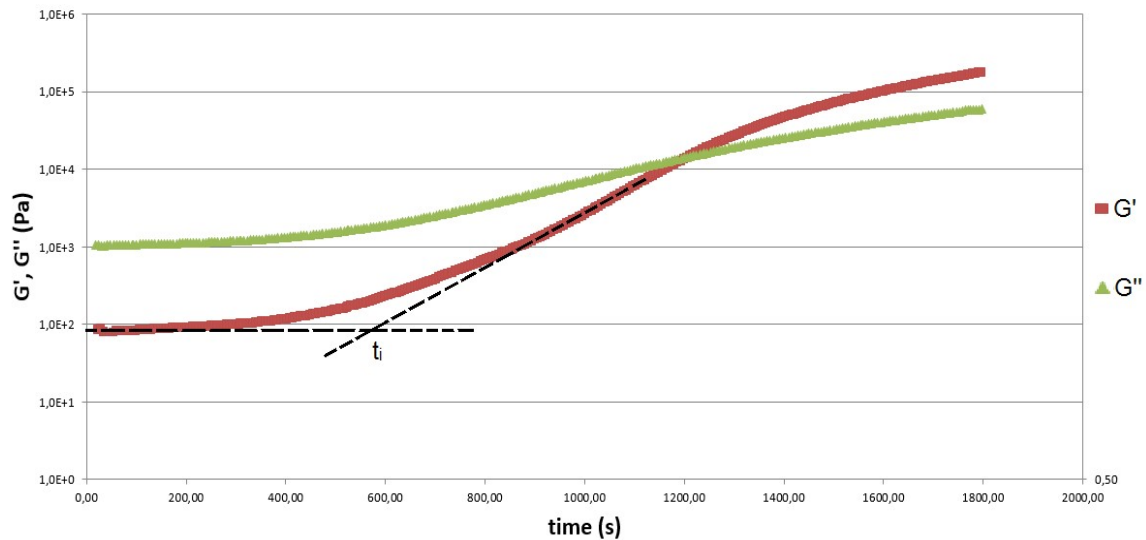
Figure 3.7: Oscillatory parameters during the crystallization PLA$_{SC}$ process, sample PLLA_HW/PDLA_HW measured in isotherm at 200 °C after a pre-shear of 20 s^{-1}.

A sigmoidal shape represents the changes of storage and loss modulus, G' and G'' with time during PLA$_{SC}$ formation and crystallization. In general, the rapid raise of G' can be representative of the nucleation and growth of crystals. For each sigmoidal curve, a different induction times, t$_i$, was calculated. The induction time from the modulus G', can be obtained by taking the intersection time of the two dashed curve lines drawn on the storage modulus−time curve as in Figure 3.7.

The Rheo-Raman results were obtained by combining the G' and I' data. The isothermal formation and crystallization PLA$_{SC}$ process at 190 °C and 200 °C after different pre-shear (0, 20, 60, 100, 140, 220 s-1) were investigated. Results are reported in Figure 3.8 – 3.13 for Low molecular weight PLLA/PDLA samples at 190 °C. Results at 200 °C are reported in Figure 3.14 – 3.19. Figure 3.20 – 3.25 reports the results for High molecular weight PLLA/PDLA samples at 190 °C, while Figure 3.26 – 3.31 reports the results at 200 °C. The temperatures were fixed to 190 and 200°C in order to melt completely the homopolymers (their Tm is 175-180 °C) and to work at temperature below the melting point of the stereocomplex (220 – 230°C).

61
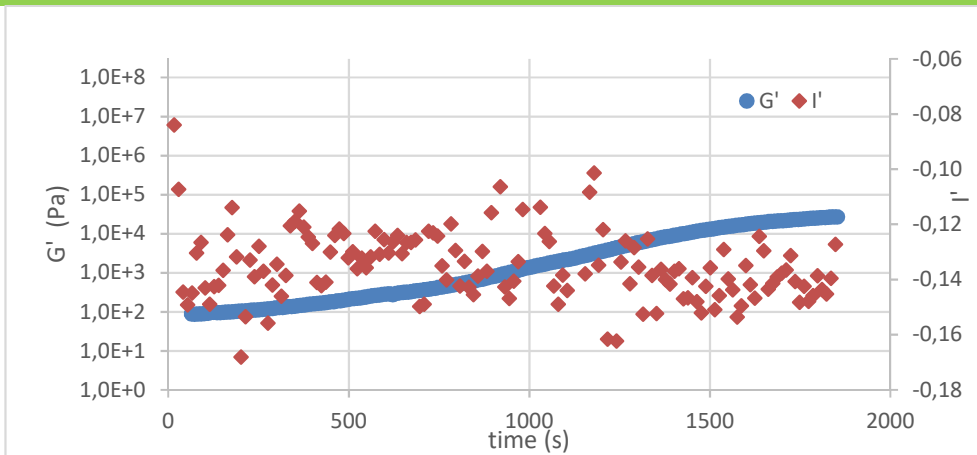
Figure 3.8: Pre-shear 0 s^{-1}.
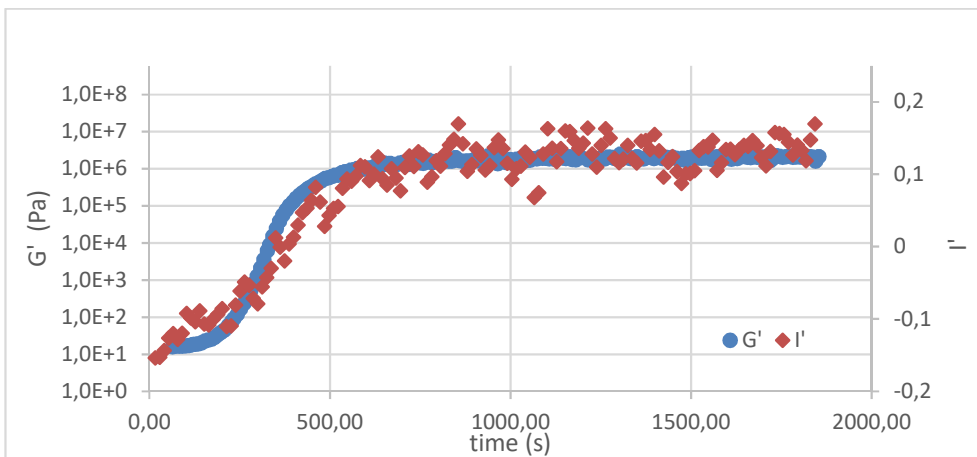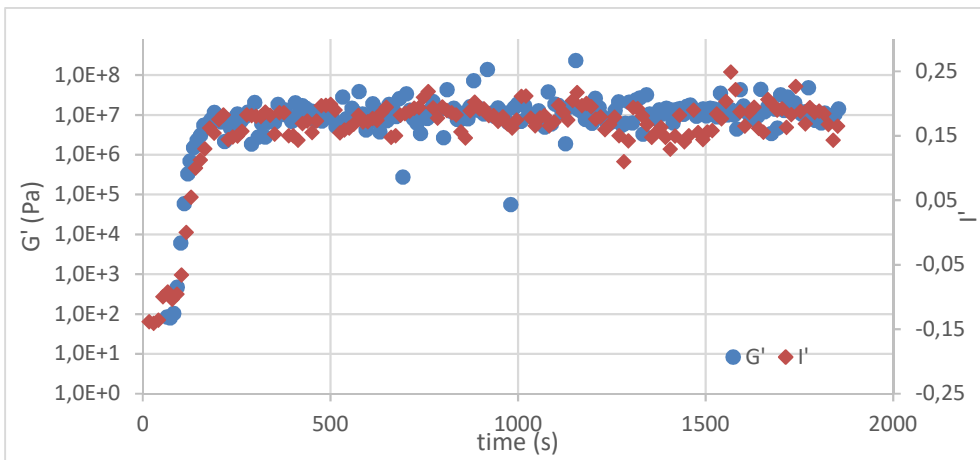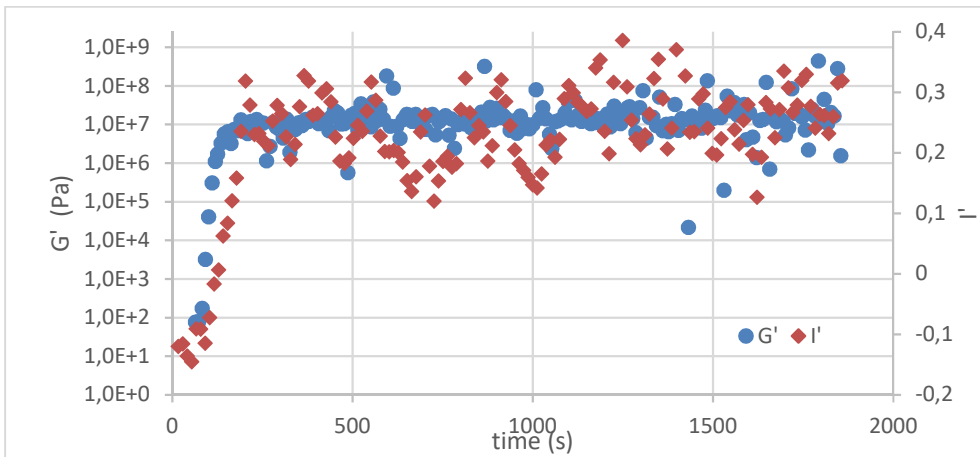

Figure 3.9: Pre-shear 20 s^{-1}.
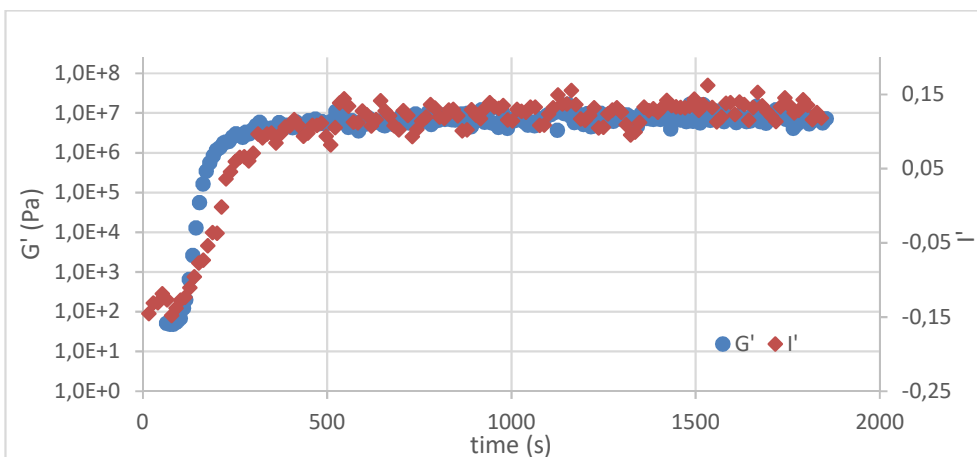
Figure 3.10: Pre-shear 60 s^{-1}.
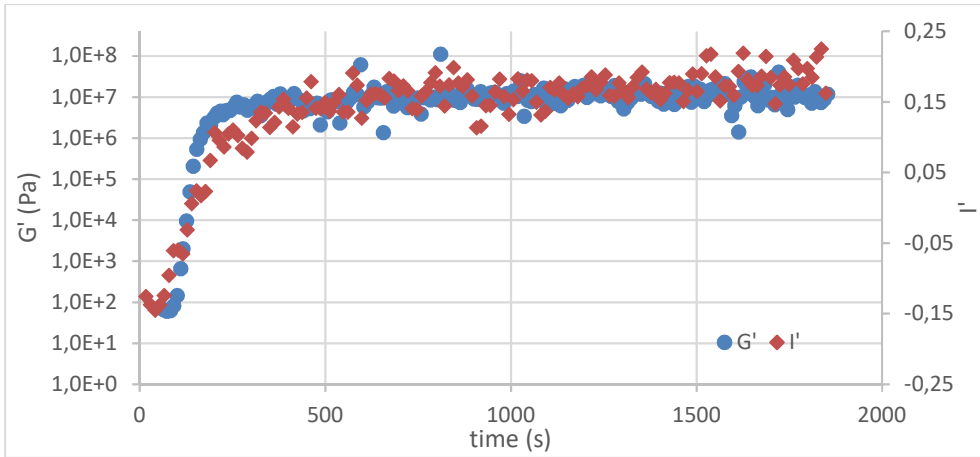
Figure 3.11: Pre-shear 100 s^{-1}.

Figure 3.12: Pre-shear 140 s^{-1}.

Figure 3.13: Pre-shear 220 s^{-1}.
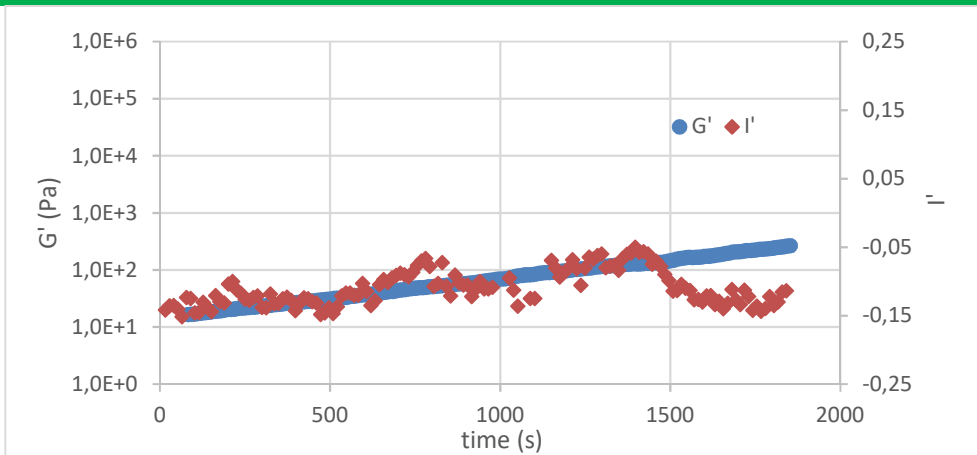
Figure 3.14: Pre-shear 0 s^{-1}.
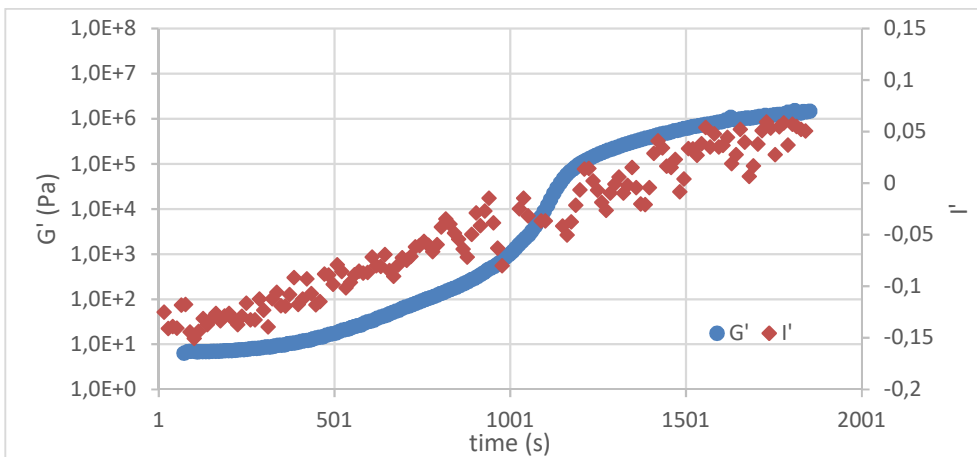
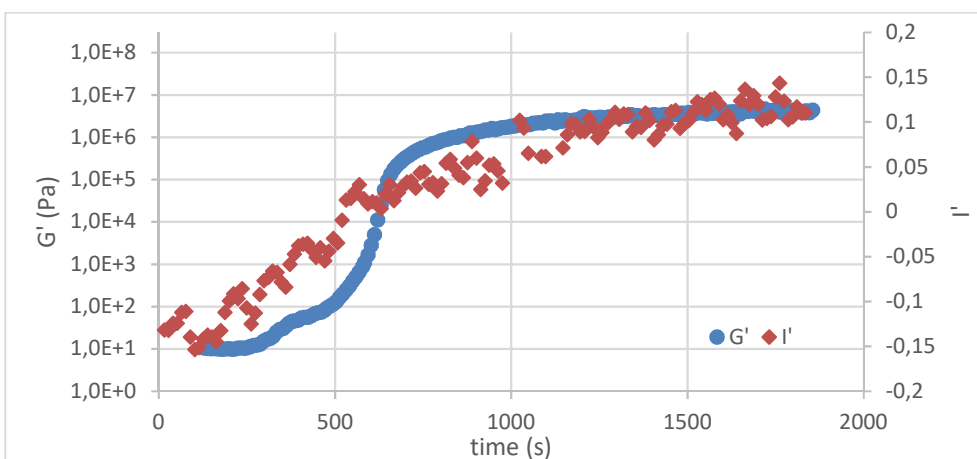**Figure 3.15**: Pre-shear 20 s^{-1}.

Figure 3.16: Pre-shear 60 s^{-1}.
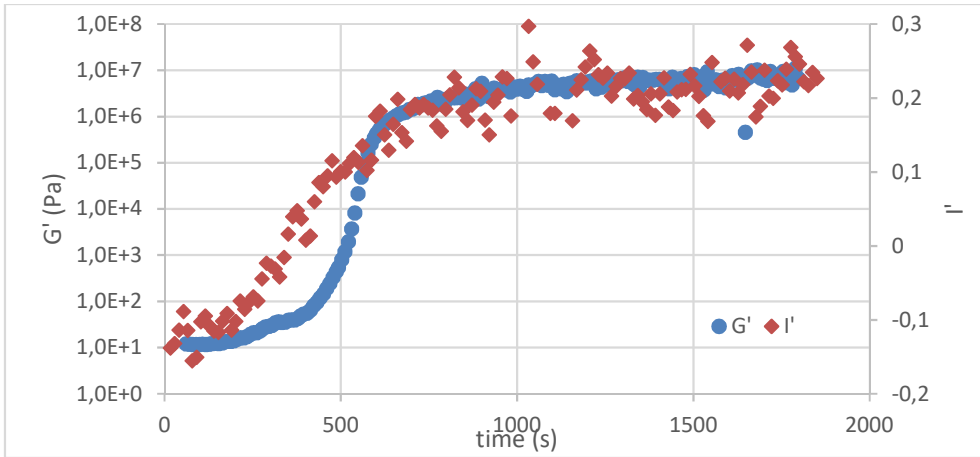
Figure 3.17: Pre-shear 100 s^{-1}.
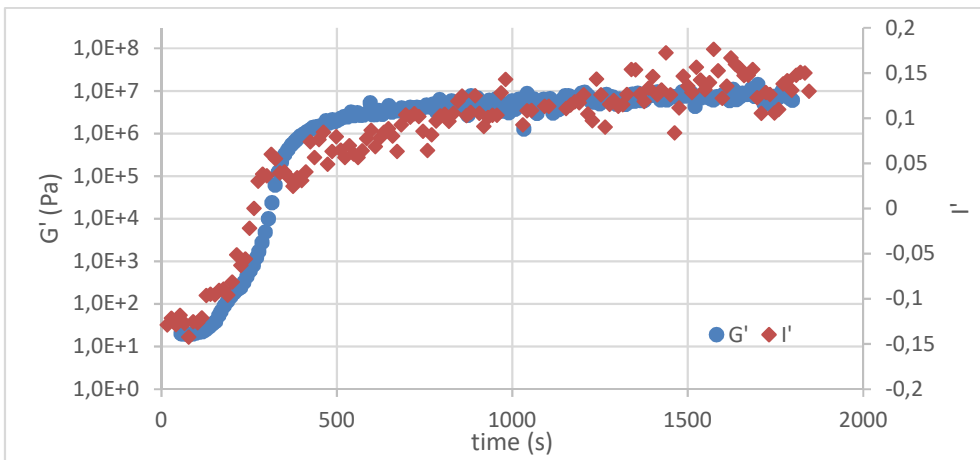
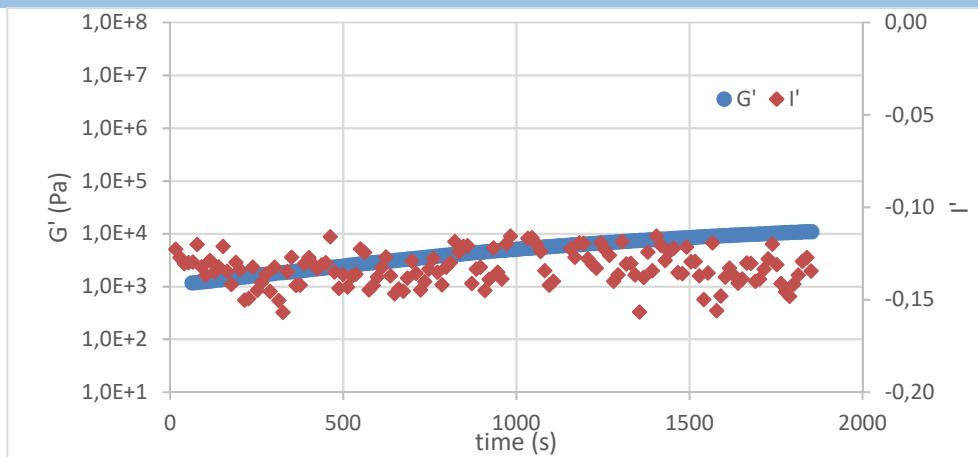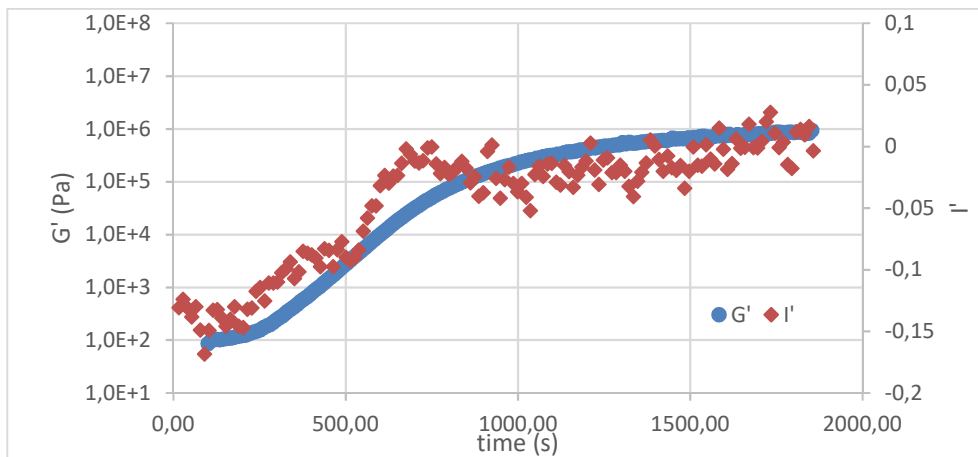**Figure 3.18**: Pre-shear 140 s^{-1}.
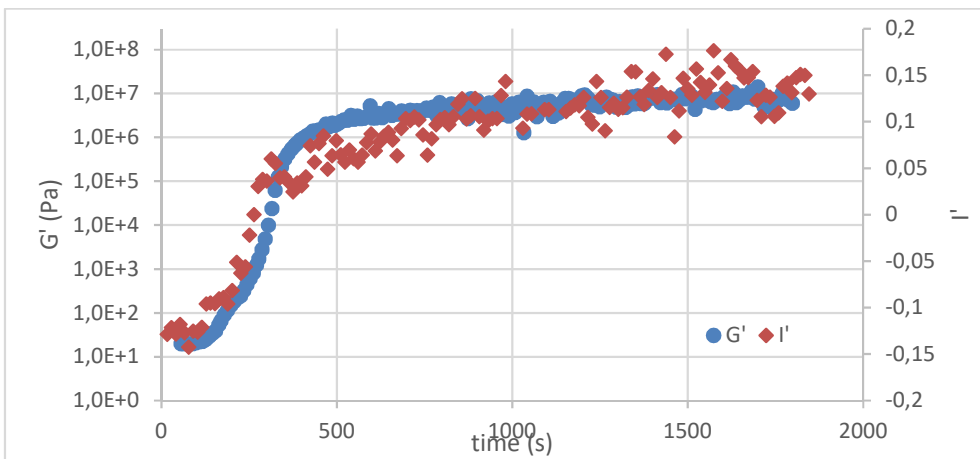
Figure 3.19: Pre-shear 220 s^{-1}.
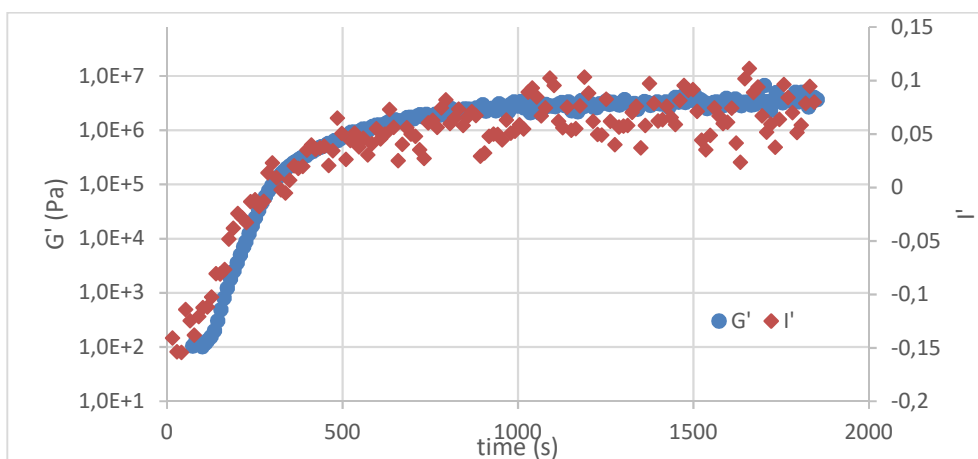
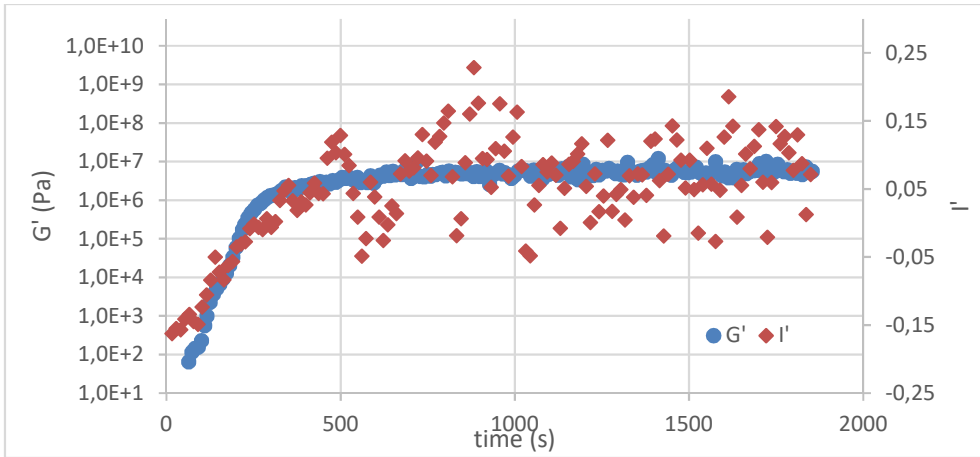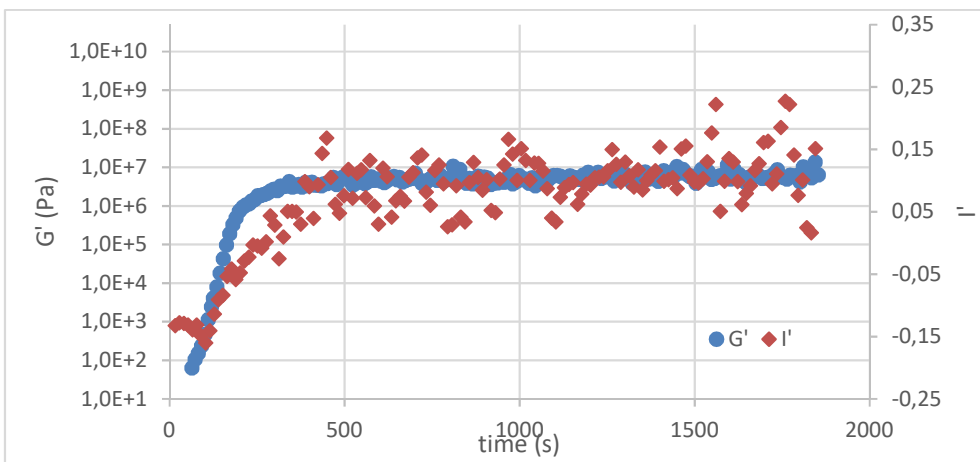Figure 3.20: Pre-shear 0 s⁻¹.

Figure 3.21: Pre-shear 20 s⁻¹.

Figure 3.22: Pre-shear 60 s⁻¹.

Figure 3.23: Pre-shear 100 s^{-1}.

Figure 3.24: Pre-shear 140 s^{-1}.
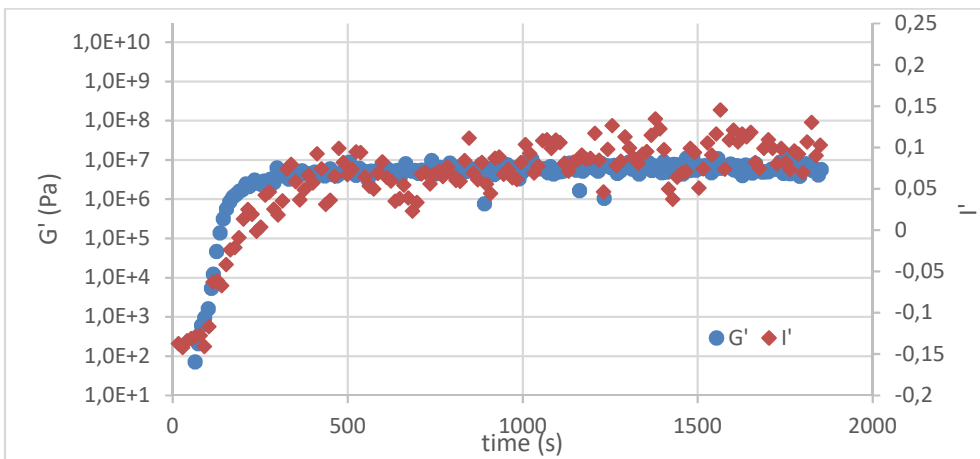
Figure 3.25: Pre-shear 220 s^{-1}.
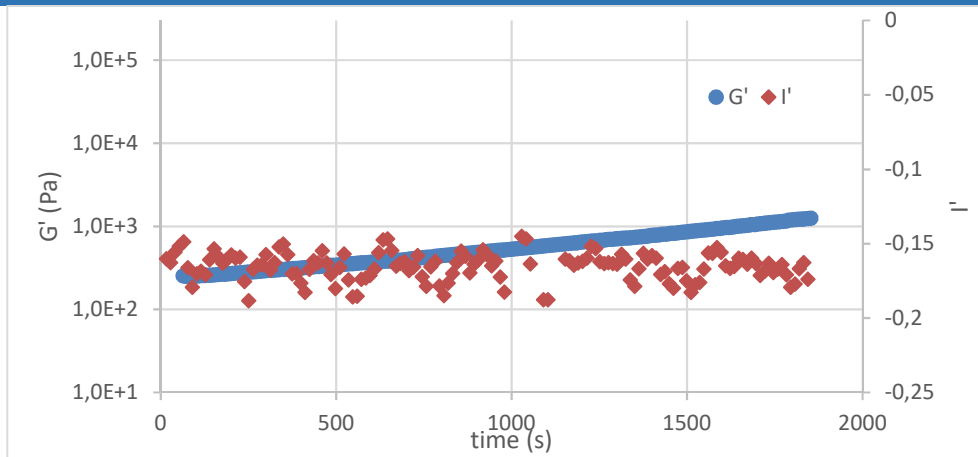
Figure 3.26: Pre-shear 0 s^{-1}.
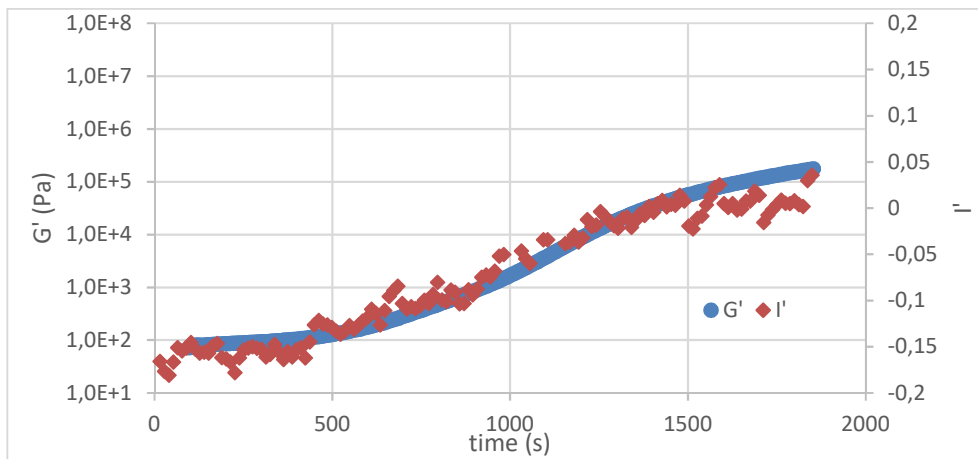
Figure 3.27: Pre-shear 20 s^{-1}.
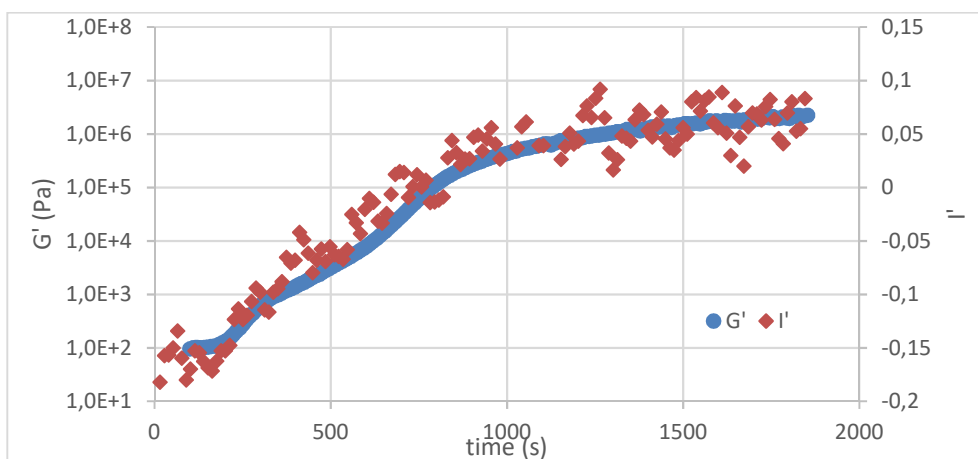
Figure 3.28: Pre-shear 60 s^{-1}.
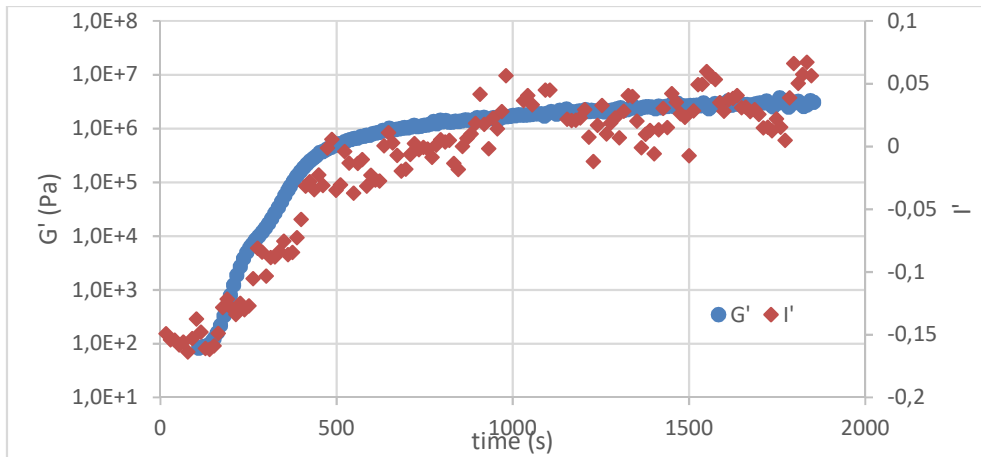
Figure 3.29: Pre-shear 100 s^{-1}.
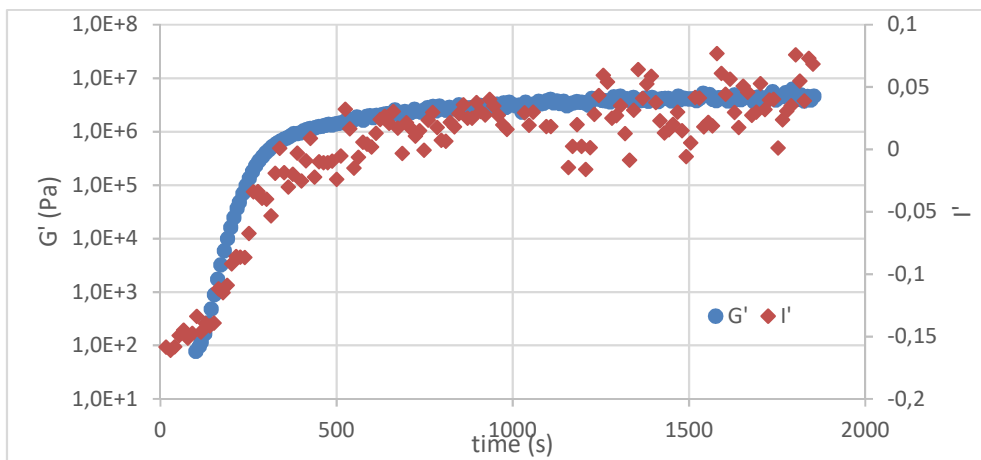
Figure 3.30: Pre-shear 140 s^{-1}.
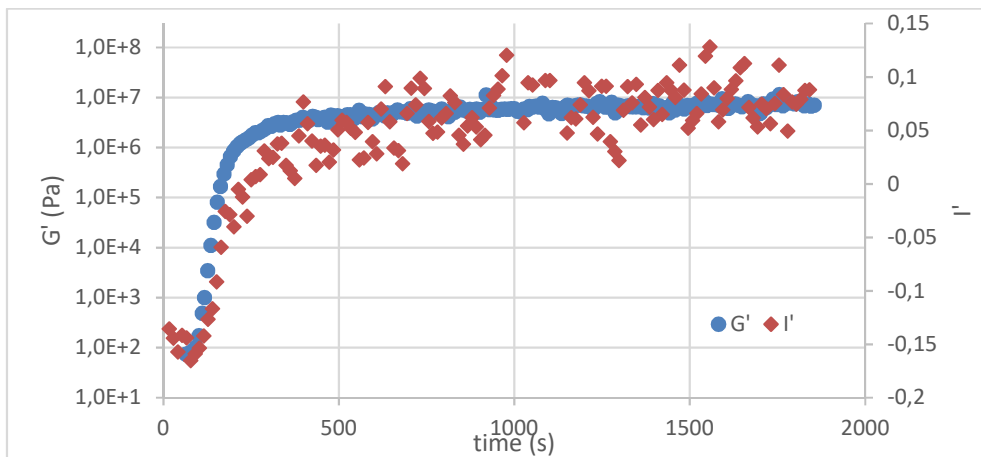
Figure 3.31: Pre-shear 220 s^{-1}.

The in situ Raman spectroscopy data confirm the same behaviour observed for the viscoelastic data. In fact, sigmoidal curves of storage modulus (G') was directly correlated with increase in the peak height ratio (I'). For all fit data, the

development of Raman intensity of bands characteristic of PLA$_{SC}$ scales in agreement with rheological indicator. With the increase of shear rate during pre-shearing, G' and I' curves shift to shorter times and show more rapid evolution towards the solid-like state. The evolution of storage modulus at a single frequency of 1 Hz for different pre-shear are presented from Figure 3.32 to Figure 3.35. For all PLLA_LW/PDLA_LW and PLLA_HW/PDLA_HW the effect of initial modulus difference (a) was removed with the normalized modulus G'$_{norm}$ (b). It can be obtained by logarithmic normalization of G' values [108].

$$G'_{norm} = \frac{\log(\frac{G'(t)}{G'_{min}})}{\log(\frac{G'_{max}}{G'_{min}})} \qquad \textbf{Equation 3.2}$$

where G'$_{min}$ is the storage modulus at the beginning of the test, G'(t) the storage modulus at the time (t) and G'$_{max}$ at the ending plateau.
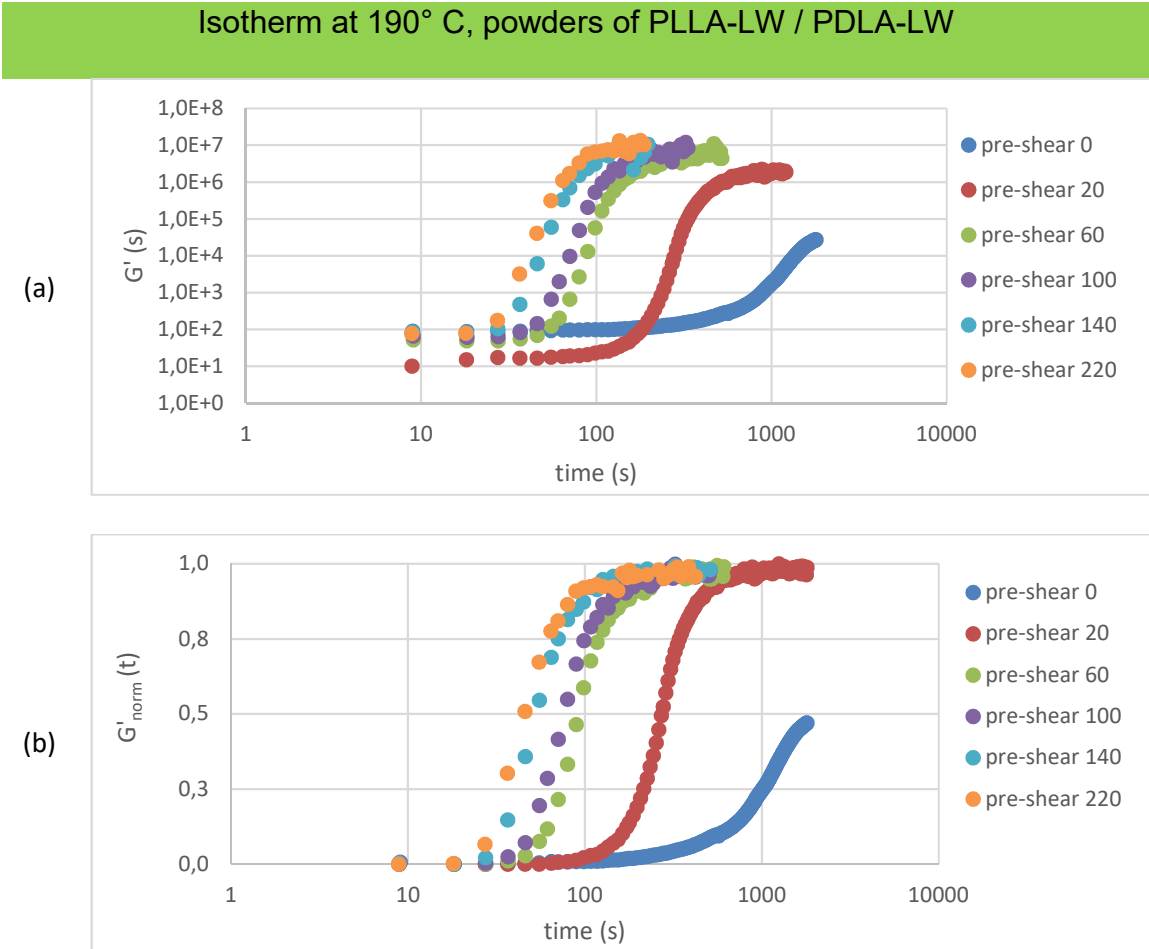
Figure 3.32: (a) Changes of storage modulus, G', with time, (b) changes of normalized modulus, G'$_{norm}$, with time.

Figure 3.33: (a) Changes of storage modulus, G', with time, (b) changes of normalized modulus, G'_{norm}, with time.

Figure 3.34: (a) Changes of storage modulus, G', with time, (b) changes of normalized modulus, G'$_{norm}$, with time.

Figure 3.35: (a) Changes of storage modulus, G', with time, (b) changes of normalized modulus, G'norm, with time.

The normalized modulus G'$_{norm}$ (b) displays the changes of crystallinity of PLA$_{SC}$

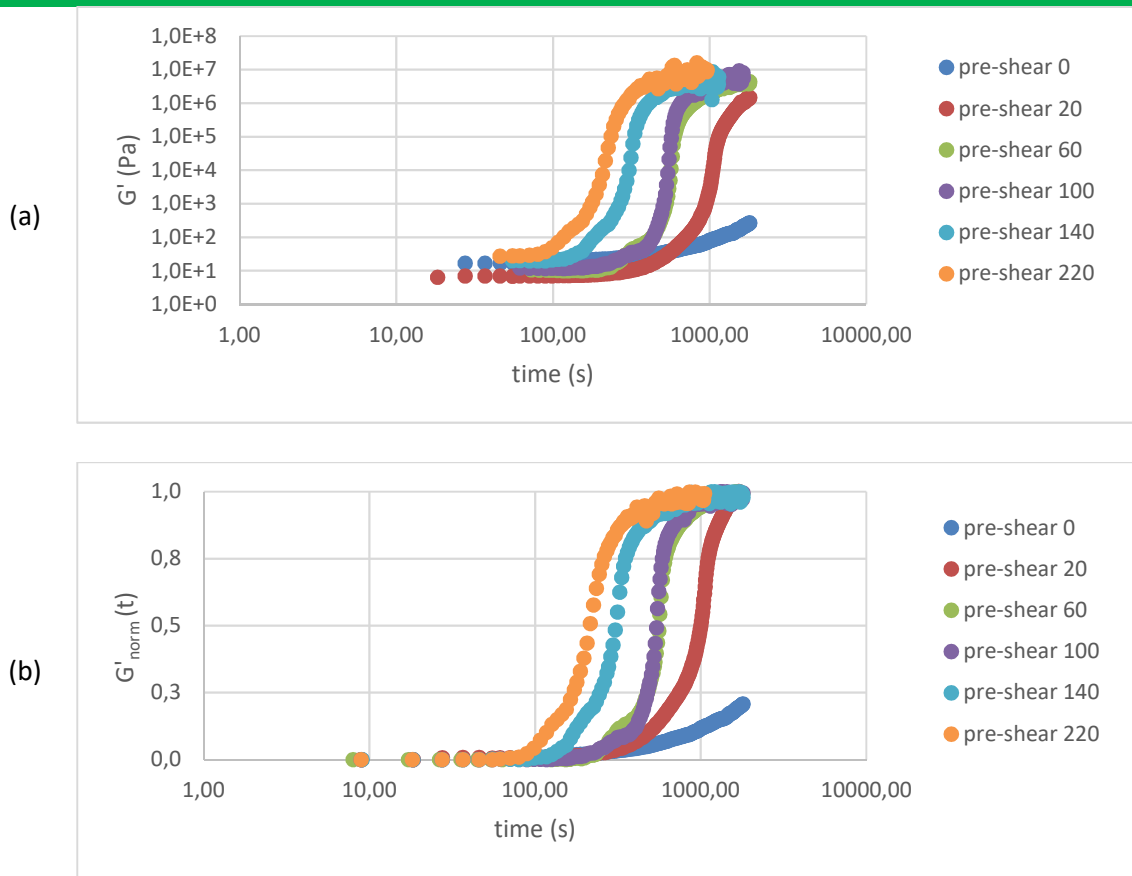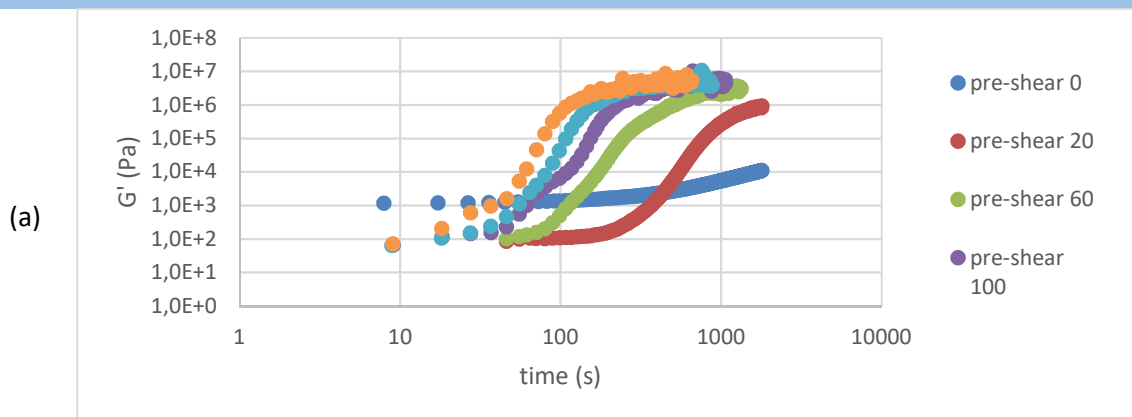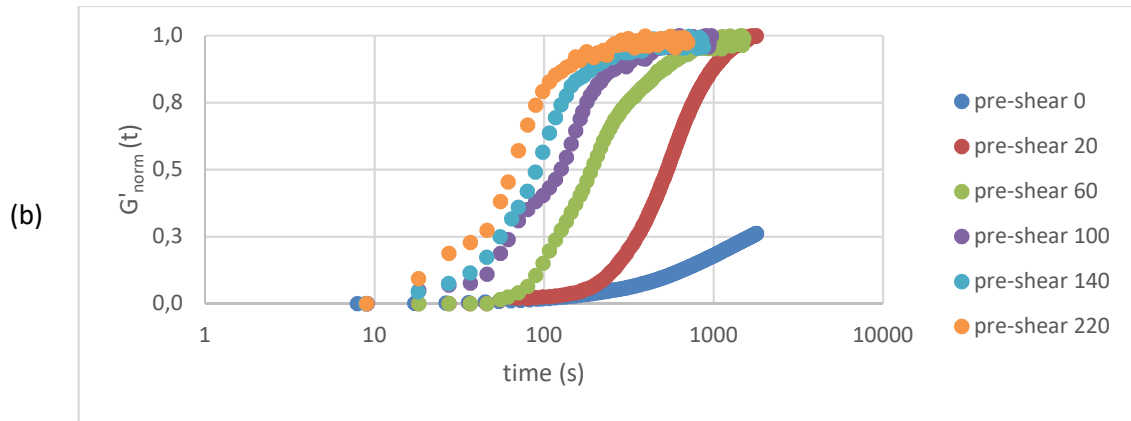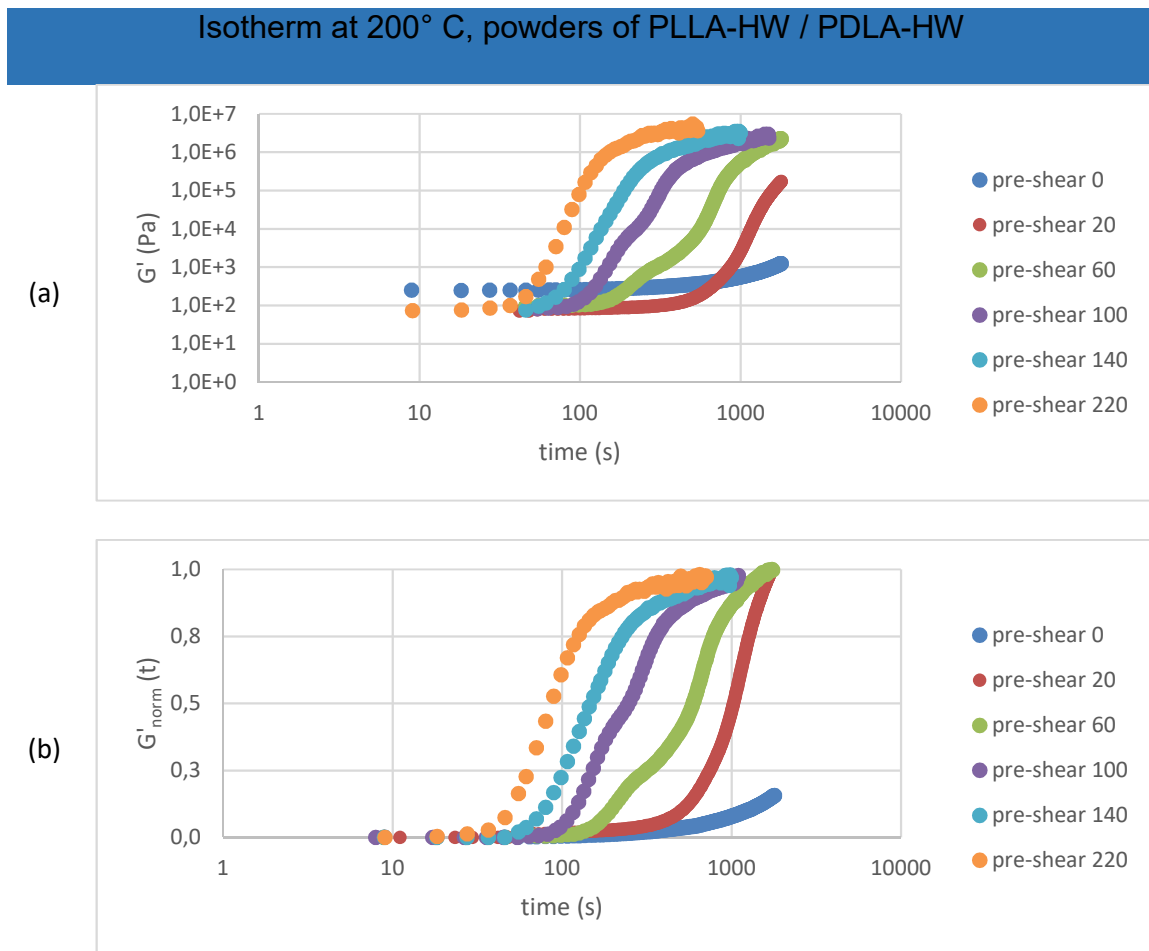during crystallization at experiment temperature. For example, much longer time is needed without pre-shear to complete the crystallization, while the times needed for PLLA/PDLA blends decreases with increasing the pre-shear.

The sigmoidal curves of G' (a) show different initial induction times (t_i) and different initial constant moduli prior to the beginning of crystallization. The time curves shift to the left side, demonstrating reduced induction time with increasing the pre-shear. However, the shift becomes less marked at the sufficiently longer pre-shear, which implies that the acceleration of crystallization kinetics by shear can become saturated after a certain time.

As we have seen above, the phenomenon of crystallization induced by the pre-shear presents important consequences from the rheological point of view. From a technological point of view, the impact is that the application of the shear on a system that is in the amorphous phase can determine dramatic increases in viscosity. Figure 3.36 – 3.39 show the complex viscosities (η^*) of the PLLA/PDLA blends vs time. In the first part of the transient, the polymer appears as liquid, as shown by the relatively low viscosity values. In fact, in this stage, the crystallization has not yet begun. The viscosity surge, at the induction time, is a clear demonstration of the crystallization process.

In the industry process, the increase in viscosity represents a notable problem for injection moulding but not for compression moulding. Indeed, in compression moulding the melt polymer is hot forced through narrow nozzles and gates on the way to field the mould cavity. It seems then possible to design a compression moulding process exploiting a favourable combination of melt cooling, shear rate and residence time in the dosing apparatus. PLA$_{SC}$ with partials crystallized fraction is then inserted into a mould cavity where shaping along with a further, rapid crystallization and final cooling take place. Figures 3.36 –3.39 showed the variation of complex viscosity in the time analysis.
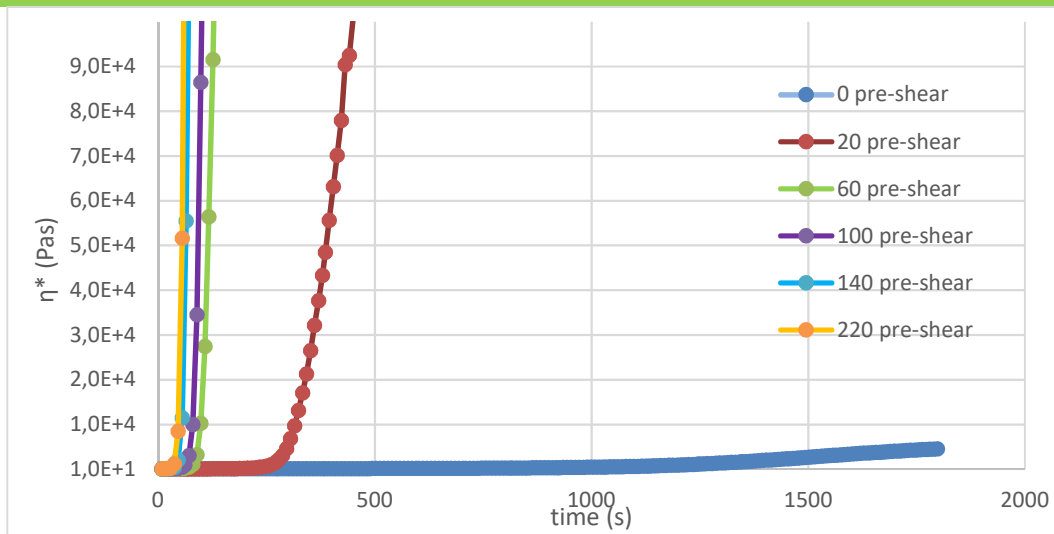
Figure 3.36: Changes complex viscosity, η^*, with time.
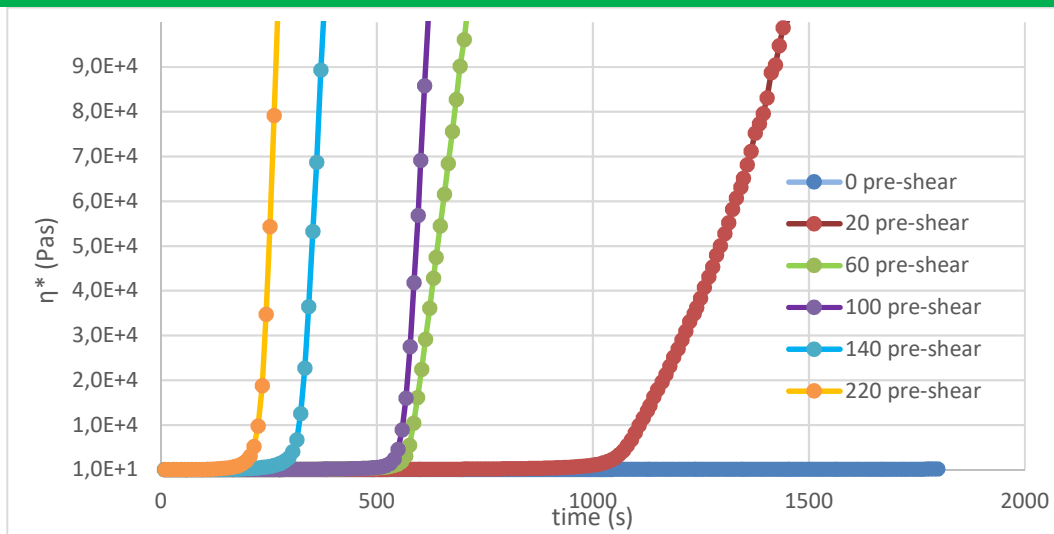
Figure 3.37: Changes complex viscosity, η^*, with time.
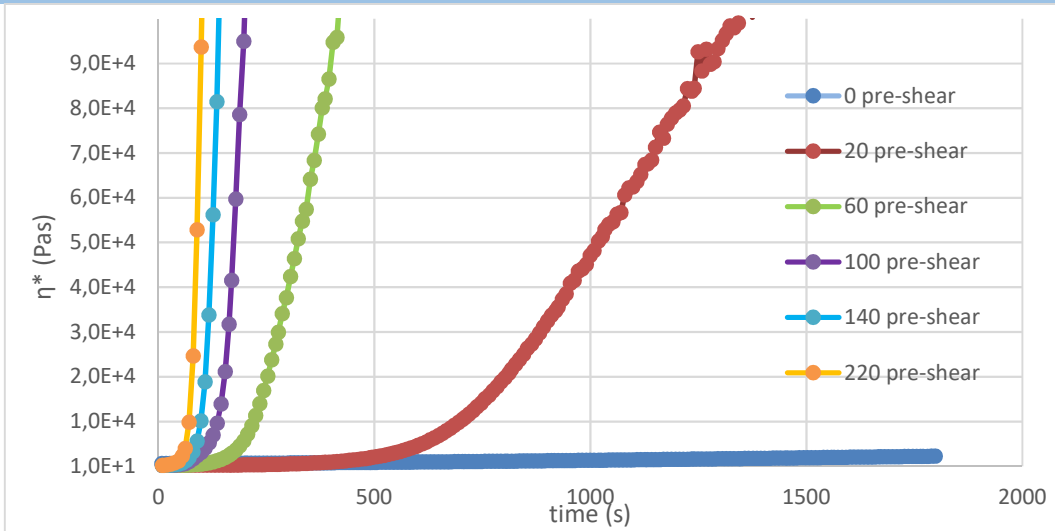
Figure 3.38: Changes complex viscosity, η^*, with time.
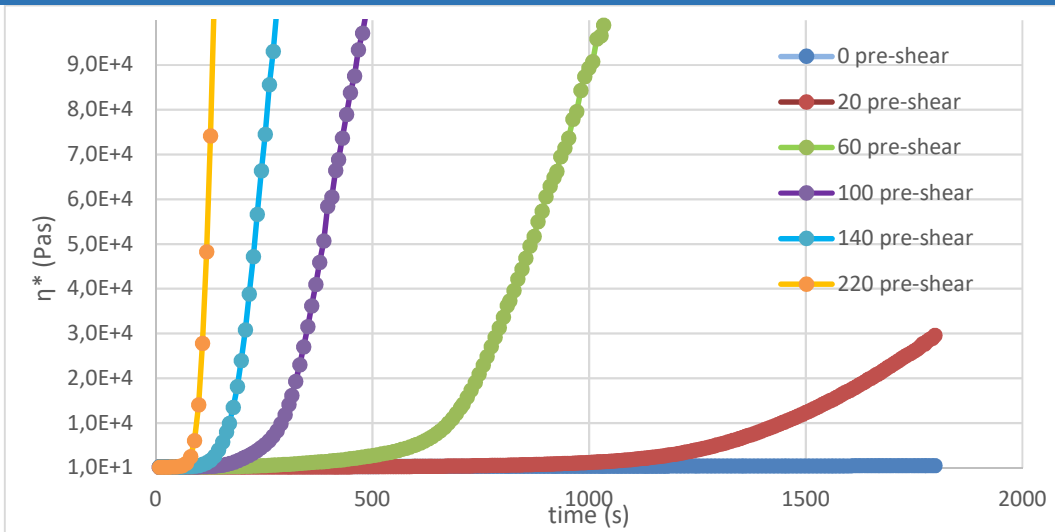
Figure 3.39: Changes complex viscosity, η^*, with time.

The Figures 3.36–3.39 show a direct indication of the phenomenon of crystallization induced by the pre-shear. In fact, as in more intense pre-shear conditions, the crystallization kinetics is strongly accelerated.

Determination of the induction time for different pre-shear conditions makes it possible to derive the quantitative dependence of the crystallization kinetics from the pre-shear conditions. The strong influence of the pre-shear on the acceleration of crystallization can be appreciated, since at very high pre-shear rates (100-200

s^{-1}) the induction time decreases more than the low pre-shear rate (0-60 s^{-1}) Figure 3.40. Song et al. [95][109] showed that the structure and potential properties of PLLA/PDLA blends were further manipulated effectively by shear rate and temperature. The induction time for PLA$_{SC}$ crystallization is greatly enhanced by high shear rate and low temperature, resulting in higher PLA$_{SC}$ nucleation density and higher final PLA$_{SC}$ content after cooling[109].
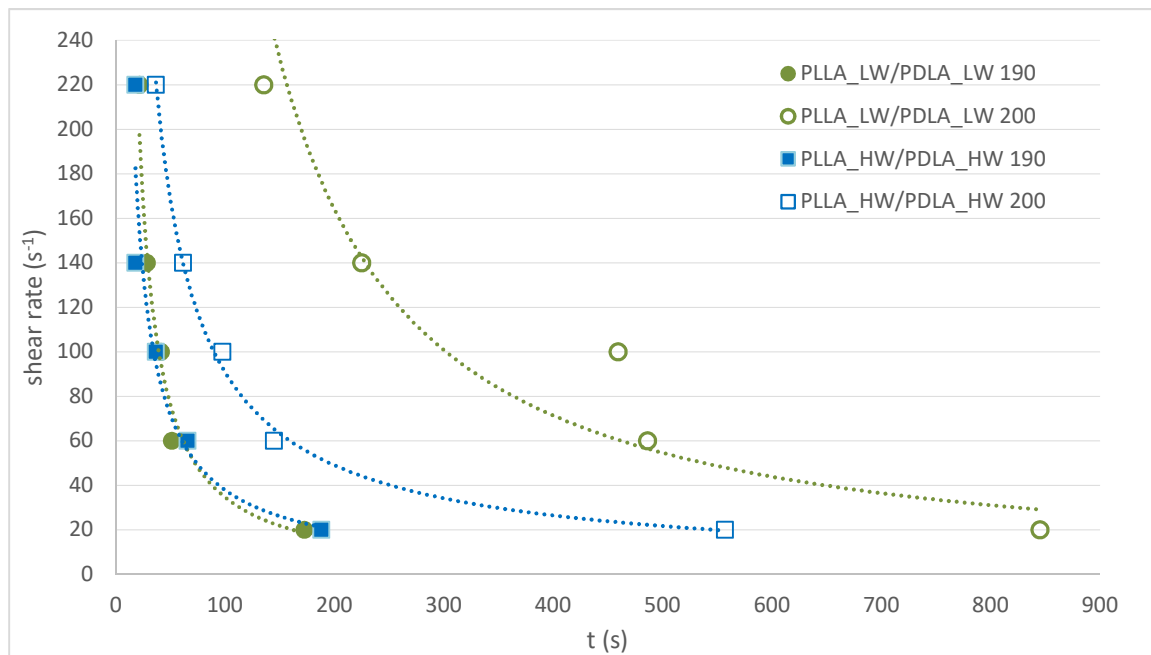
Figure 3.40: Effect of pre-shear rate on induction time.

Comparing the results obtained at 190 and 200 °C, it is possible to observe a different behaviour of the PLA-sc. At 190 °C both polymers showed the same trends; in particular, at low pre-shear, both PLA presented a longer induction time (200 seconds) compared to the results obtained at high pre-shear (<60 seconds). These results can be explained taking into account the difficult for the chains to have an intimate contact to each other, that is necessary for the generation of the interaction that lead the unfolding/folding processes of the chains. The high pre-shear helped not only the mixing of the two melted homopolymers, but also the creation of new interactions/entanglements that promote the crystallization process.

Under these conditions, any relevant variation of the trend is observed with the PLA with low and the high molecular weights. This result suggests that mobility of the chains at 190 °C for both systems is quite similar and the shear helps it to level

out the energy of the systems. The energy supplied by the pre-shear is also used for to generate the interactions as reported before. Increasing the temperature from 190 °C to 200 °C, the effect of the pre-shear is more empathised. It is possible to notice the higher induction times (more than 600 seconds) for both polymers, can be correlated to the higher mobility (entropy) of the chains that retard the crystallization process. Increasing the pre-shear, as observed at 190 °C, a decrease of the induction time is shown, but in this case, there is a strong difference between the results derived from the PLA with low molecular weight with the PLA at high ones. The difference lies, again, on the different mobility (entropy) of the chains. The system with high molecular weight is more constrained than the low one, this favours the crystallization process, that is furtherer helped by the shear; in fact, at very high shear (220 s-1) both PLA treated at 190°C and the one with high MW at 200 °C reach the same induction time. While, for the system with low MW, the higher mobility of the chains reduces the formation of the interactions necessary for the crystallization process.

A quantitative investigation by differential scanning calorimetry (DSC), was carried out on the disk sample obtained at the end of the Rheo-Raman acquisition. In fact, as reported in material and method, the final sample was removed from glass plate and quenched in nitrogen. The DSC heat flow curves for PLLA/PDLA blends are displayed in Figure 3.41.
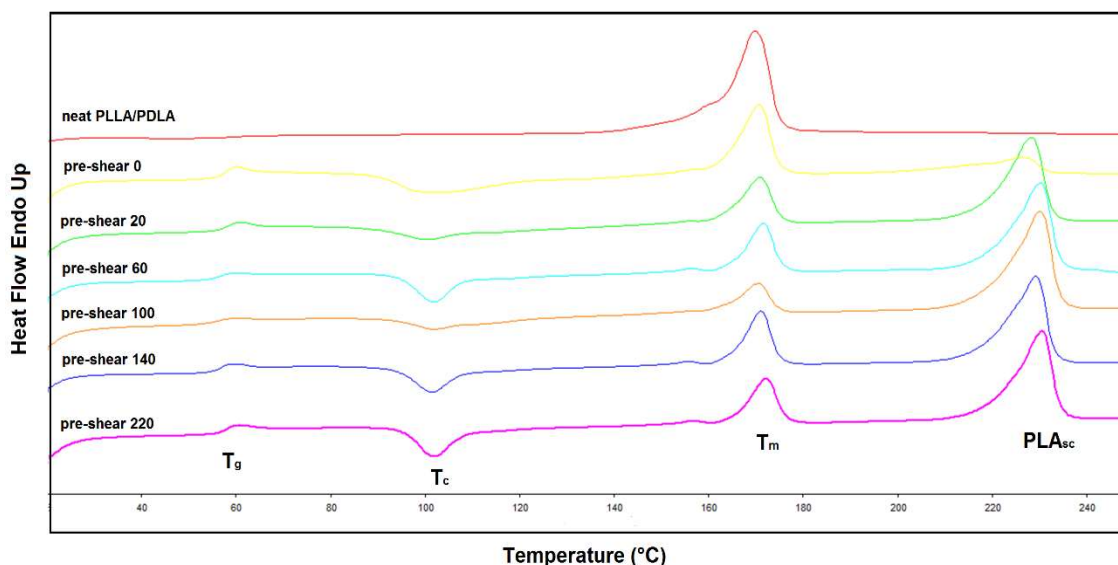
Figure 3.41: DSC heat flow curves during the first heating scan for neat powder PLLA/PDLA without any Rheo-Raman acquisition and PLLA/PDLA blends after different pre-shear. In this Figure was reported only one of the fourth DSC heat flow curves analysed.

Neat PLLA/PDLA refers the two homopolymers mixed in a 1:1 weight ratio and loaded in a DSC. PLA homopolymers, was reported in Table 3.1, are semycrystalline polymers, therefore only two typical physical transitions were observed: glass transition temperature (T_g) and melting temperaure (T_m). The third transition, cold crystallization (T_c), is an exothermic crystallization process. It is observed on heating a polymer that has previously been quenched and had no time to crystallize. This is what happens for fraction homopolymer which did not participate in the formation of the PLA$_{SC}$. Under the test conditions, i.e. isotherm at 190 and 200 ° C, homopolymers are in the molten state. As we saw above, when the pre-shear was applied there was a formation of stereocomplex crystals. These crystals melt at higher temperatures than the homopolymer. This is evidenced by the presence of the melting peak at about 220-230 °C relative to the PLAsc Figure 3.41. In the heat flow curves of PLLA/PDLA blends, the previous exotherm and endotherm transition are related to the homopolymer which did not participate in the formation of the stereocomplex and then remained in the amorphous phase after quenching. Therefore, the contribution of the homopolymer can be subtracted in order to obtain the amount of the sterocomplex that was formed as a result of the pre-shear.

The crystallinity (Xc) of stereocomplexed PLA was calculated using the equation 1.3 reported in chapter 1. The melt enthalpy (ΔH_m^0) of stereocomplexed PLA with 100% crystallinity was reported to be 146 J/g [101]. The amount of PLA$_{SC}$ crystalline phase, Table 3.2, of PLLA/PDLA blends increases with increasing pre-shear, which can be reflected by the increasing melting peak area.

Table 3.2:

PLLA_LW/PDLA_LW								
Isotherm	pre-shear (s-1)	Tc (°C)	ΔHc (J/g)	Tm homo (°C)	ΔH (J/g)	Tm PLAsc (°C)	ΔH (J/g)	Xc PLA$_{SC}$ (%)
190 °C	neat PLLA/PDLA	-	-	170	54	-	-	0
	0	100	-22	171	23	221	10	7
	20	105	-13	170	19	224	36	25
	60	101	-11	172	9	225	40	28
	100	103	-10	172	12	227	43	30
	140	101	-9	172	12	226	47	32
	220	101	-14	172	16	227	45	31
200 °C	neat PLLA/PDLA	-	-	170	51	-	-	0
	0	102	-22	171	23	227	7	5
	20	100	-10	171	14	228	36	25
	60	101	-12	172	13	230	38	26
	100	102	-10	171	8	230	43	30
	140	101	-13	171	16	229	41	28
	220	102	-15	172	17	231	40	28

PLLA_HW/PDLA_HW								
Isotherm	pre-shear (s-1)	Tc (°C)	ΔHc (J/g)	Tm homo (°C)	ΔH (J/g)	Tm PLAsc (°C)	ΔH (J/g)	Xc PLA$_{SC}$ (%)
190 °C	neat PLLA/PDLA	-	-	177	51	-	-	
	0	116	-25	175	30	221	4	2
	20	102	-24	177	23	225	24	16
	60	103	-20	177	19	224	26	18
	100	102	-21	176	20	224	31	21
	140	96	-8	177	11	225	31	21
	220	102	-36	177	38	225	48	33
200 °C	neat PLLA/PDLA	-	-	177	51	-	-	
	0	118	-24	178	31	227	2	1
	20	105	-11	178	23	230	29	20
	60	106	-18	177	19	229	31	21
	100	102	-19	178	22	231	29	20
	140	107	-18	178	19	230	29	20
	220	104	-20	176	20	229	34	23

From all the results obtained by DSC and Rheo-Raman analysis, it was decided to evaluate a possible correlation between the crystallinity and both rheology and spectroscopic results.

Reporting the crystallinity of the stereocomplex samples in function of the logarithm of the storage modulus (G') at the end of the Rheo-Raman analysis at different isotherm temperatures for both low and high molecular weight blends, a linear correlation between the parameters was found, as shown in Figures 3.42 and 3.43
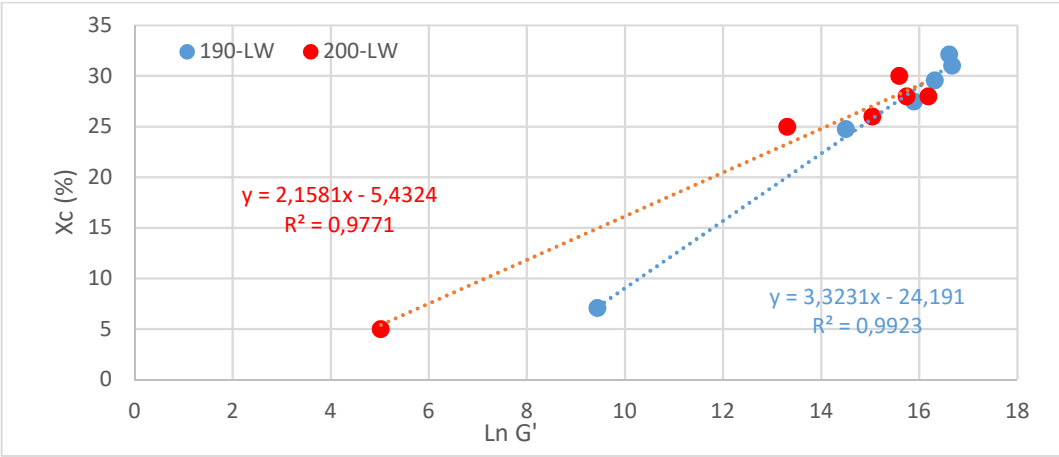
Figure 3.42: Crystallinity of the stereocomplex samples in function of the logarithm of the storage modulus (G') for low molecular weight.
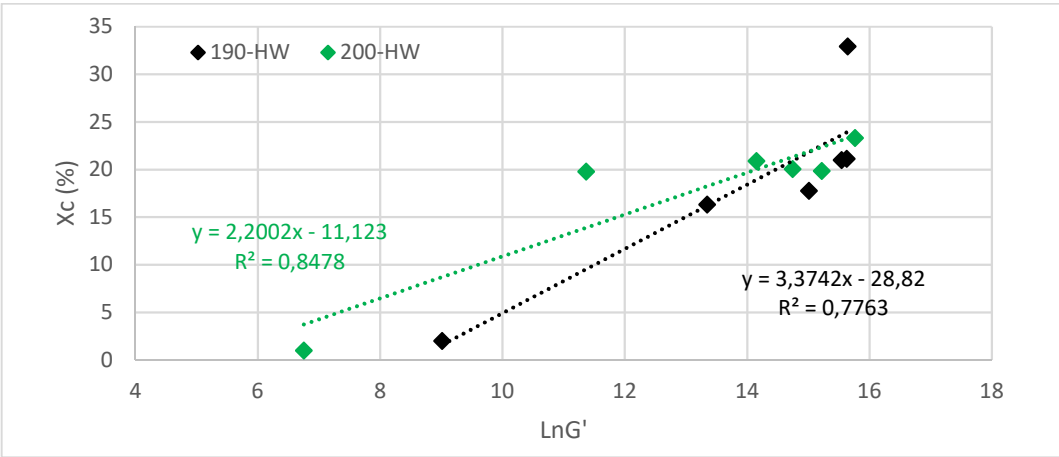
Figure 3.43: Crystallinity of the stereocomplex samples in function of the logarithm of the storage modulus (G') for high molecular weight.

From the Figures 3.42 and 3.43 a linear correlation between crystallinity and lnG' is exhibited. In particular, the correlation between these two parameters is strictly

affected from the operative temperature and the molecular weight of PLLA and PDLA. The first parameter influences the mobility of the amorphous chains that are trapped by the crystalline phase. Increasing even more the crystallinity of the PLA$_{SC}$, by applying a high pre-shear, the amorphous chains are even more constrained and the temperature can affects even less the storage modulus (at high crystallinity, the results obtained at 190 and 200 °C are similar). This effect was observed for both low and high molecular PLA$_{SC}$. As reported from Pantani et al. [110] when crystallinity degree rises from about 5% it was observed the increase of G' of about three orders of magnitude for crystallinities of about 20%.

Figure 3.44: Crystallinity of the stereocomplex samples in function of the logarithm of the storage modulus (G') at the same temperature (190 °C) with different molecular weight.

Figure 3.45: Crystallinity of the stereocomplex samples in function of the logarithm of the storage modulus (G') at the same temperature (200 °C) with different molecular weight.
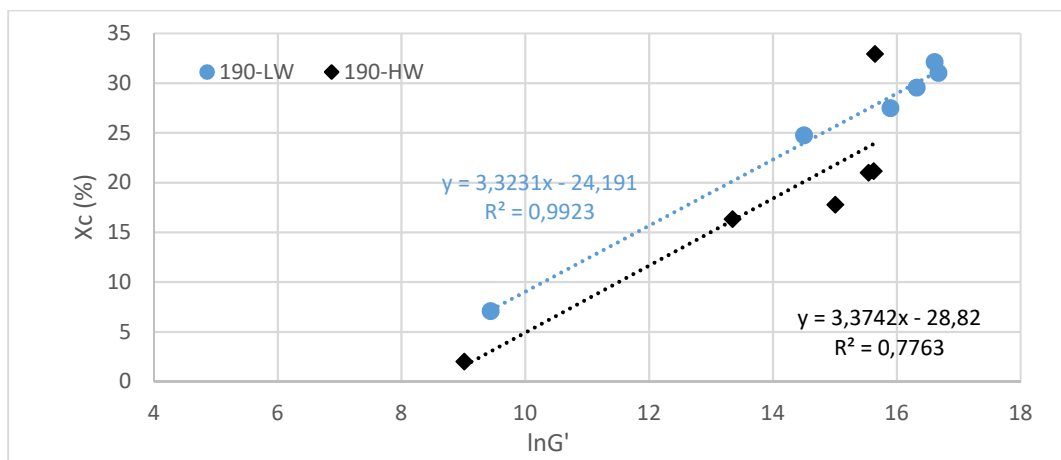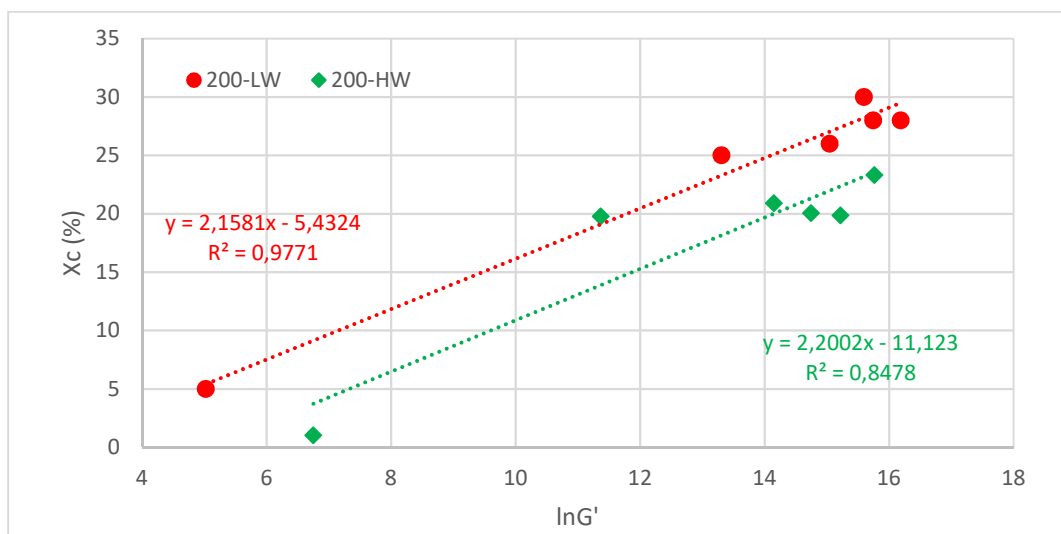
Comparing the results obtained at the same temperature with different molecular weight, as reported in Figure 3.44 and 3.45, showed that at the same crystallinity, PLA_{SC} with higher molecular weight presented a higher storage module. This can be explained taking into account the different amount of the terminal groups of the chains. The terminations chains don't take part to the crystalline domains of the polymer, it is then possible to imagine the amorphous part of a PLA_{SC} with low molecular weight is mainly composed by these groups. On the contrary, for a PLA_{SC} with high molecular weight, the amorphous fraction derives mainly from the not-folded part of the chains. It is then possible to assimilate this system to an elastomeric polymer, where for the PLA_{SC}, the entanglements of the chains in this case derive from the crystalline domains. Under stress, the amorphous domains are deformed, but only the ones that have entanglements can return to its initial state, giving an elastic response.

Differently to what shown before, any correlation between the crystallinity of PLA_{SC} and the Raman signals was found. In fact, Rheo-Raman results show a very good agreement between Raman signal and elastic modulus. However, the impossibility to use the Raman for quantitative analysis derives from the matrix effect of the PLA (as described above).

The possible explanation of these results is proposed in Figure 3.46.
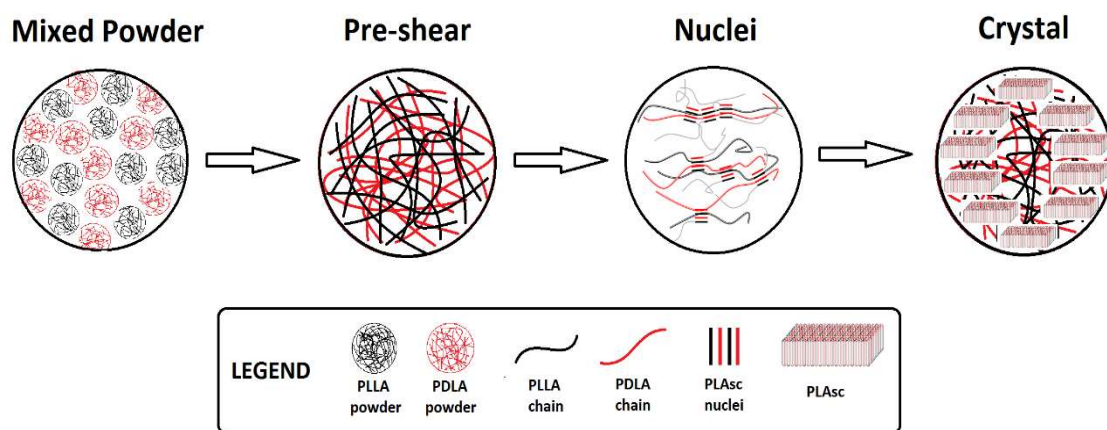
Figure 3.46: Schematics of crystallization PLA_{SC} process from pre-shear to SAOS acquisition[99].

The results obtained can be summarized as follows. The crystallization of PLA_{SC} can be promoted through a pre-shear treatment. It was demonstrated that in a

quiescent state (pre-shear is 0 s^{-1}) at temperature higher than 190 °C, the PLA chains are present in a random coil configuration. Under these conditions, only a very weak interaction between the chains of the PLLA and PDLA occurred disfavouring the formation and crystallization of the stereocomplex. Applying an external force, by shearing, it is not only favoured the mixing of the species but also the engaging of the polymer chains each other. The external energy supplied helps also to generate the interactions (hydrogen bonds or stereoselective interactions) or entanglements that are fundamental for the formation of the nuclei, which are the responsible for the stereocomplex crystallization process. Specifically, the crystallinity of the final stereocomplex is higher in system where a higher pre-shear was applied. The operative temperature plays also an important role in the process. In particular, at 190 °C PLAsc with higher crystallinity was obtained. This can be correlated to the lower mobility of the chains and lower undercooling that helps not only a lower induction time, but also a better growth of the crystallites. On the other hand, the PLAsc obtained at 200 °C presented a higher melting point, that can be correlated to a better arrangement of the chain of the stereocomplex on the melted homopolymer. Molecular weights influence also the crystallinity, in particular, low molecular weight showed a higher crystallinity thanks to their better capability to fold for the formation of the crystallites.

The optimal temperature value for the industrial process to prepare PLA$_{SC}$ can be defined by assessing the effects of the combined crystalline fraction with better crystal perfection, on the performance of the moulded parts

4. **Post-crystallization**

SACMI is an international group manufacturing machines and complete plants for the ceramics, packaging (including beverage and closures-containers), food industries and automation - markets in which it is a recognized worldwide leader. Its strength lies in the application of innovative technology, the outstanding position of the group on international markets and its commitment to research and development and providing customers with top-flight quality and service.

In the recent years, SACMI is pointing to conceptualize the integration of economic activity and environmental wellbeing in a sustainable way of the consumer goods, as well as to strict governmental regulations in the use of non-degradable thermoplastics. SACMI has extended its technological range to the single-serve production sector, offering its skills for the development of new-generation solutions and tools that allow high productivity, energy savings and outstanding final product quality. SACMI is capable of providing individual pods-making machines or creating a complete system that - thanks to close collaboration between SACMI, key partners and subsidiaries - produces the pods, fills it, packages it and places the packs in boxes ready to be palletized. The technological core of the solution is the CCM (continuous compression moulding), the SACMI compression press that, with just 32 cavities, lets manufacturers produce ultra-light pods with outstanding quality/seal characteristics at speeds of up to 800 pods/minute.

The system has several advantages. Above all, energy savings can top 30% compared to the alternative injection technology (thanks to the special, low-temperature extrusion process). The result is a combination of high productivity and the shortest cycle times in the industry (2.4 - 3.2 seconds). Then, there is another key advantage that has attracted manufacturers' attention (and made a key contribution to enhancing process efficiency and lowering costs): with compression, each cavity can be managed independently. This possibility, exclusive to this technology, is a huge plus-point when it comes to both maintenance and quality control; the latter is also aided by the integration of advanced Sacmi vision systems that operate in-line and at ultra-high speeds, allowing real-time identification of faulty podss (and the relative cavity number to ensure immediate identification of the origin of the defect). The outcome is

maximum "opening performance" repeatability and a total guarantee on every pods. In addition, that is not all: being able to process the material at lower temperatures and handle the polymer in a more viscous state has allowed SACMI to develop applications for special, biodegradable materials, PLA.

Although Poly(lactic acid) (PLA) possesses many desirable properties, above all biodegradability and compostability, the physical and mechanical properties of PLA are dependent on the solid-state morphology and its crystallinity. PLA can be either amorphous or semicrystalline depending on its stereochemistry and thermal history. A high crystallinity degree is highly desirable to increase the heat resistance of PLA but is rather difficult to reach during processing technologies due to its low crystallization kinetics. The processing of PLA in a molten state under shear and compression conditions require understanding its thermal and rheological behaviour to optimise the process parameters [93]. To these parameters, we must also add the component linked to the productivity of the completely moulding process. One of these is the time cycle that was closely linked whit crystallization kinetics of PLA. In order to achieve the best value of crystallinity with the lowest cycle time, the study of compression moulded PLA coffee pods was carried by a complete study divided in four main parts, starting from the analytical method to the optimization of the operative parameters for the compression moulding. Specifically, the steps were:

1. Develop of a method to measure crystallinity by DSC, avoiding the effect of cold-crystallization during scanning rate instrument (HyperDSC).
2. Assess the impact of the process parameters, the nucleating agents and PLA molecular weigh on the crystallinity of PLA in moulded coffee pods.
3. Develop a thermal treatment by DSC in order to reach the crystallinity of PLA required by final application (post-crystallization/annealing).
4. Transfer the optimized thermal annealing cycle to a post-moulding device.

PLA coffee pods were prepared by SACMI continuous compression moulding (CCM) with different thermal histories. The main process parameters that affect the post-crystallization and then, the final product are:

- The temperature of Melt Cooler, that is a thermostatic mixer in which the melted polymer, coming out from the extruder unit, is cooled down in the range of temperature (typically from 160 to 210 °C). The material is then

moulded into the mould at a temperature, where the polymer is closer to transition from the liquid-like to solid-like viscoelastic behaviours [111]. Moreover, this apparatus reduces drastically the cycle time required for the cooling of the moulded object from its working temperature. This helps also the extraction of the object from the mould without being damaged [112].

- The effect of nucleating agent (Lak-301) compounded with the PLA, in order to provide high crystallinity and allows to decrease the onset of cold crystallization at lower temperature [53].
- Effect of different grade of PLA (in terms of different molecular weight) used by SACMI to produce coffee pods.

The target value for the crystallinity of the final product (for its application as coffee pods) has to be at least 35-40 %. These values were obtained from results of specific tests (patented by the company) on the coffee machines. For example with low values of crystallinity, (20 %) the pod bottom has a low resistance to tearing so that the performance of the pod during coffee serve is not acceptable. All these tests were not presented in the thesis work.

4.1. Experimental section

4.1.1 Material

As reported in Table 4.1, different grade of Poly (lactic acid) was applied for the post-crystallization of coffee pods. Commercial PLA was supplied by NatureWorks to Sacmi .

Table 4.1: PLA grades available from NatureWorks.

PLA	Sample ID	T_m [°C]	MFR [g/10 min]	D– Isomer [%]
2500HP	PLA_HW	165-180	8 *	< 0.5
3100HP	PLA_LW	165-180	24 *	< 0.5

* 210 °C / 2.16 Kg [104]
HV = High Molecular Weight
LV = Low Molecular Weight

Before any test or processing, the coffee pods ware dried under vacuum at the

temperature of 60°C overnight. The analysis of post-crystallization was consequently conducted on coffee pods taken from compression moulded specimens. The commercial product LAK-301 (LAK) was used as nucleating agent [113]. It is an aromatic sulfonate derivative produced by Takemoto, Japan and currently employed in Ingeo (TM) 2500HP and 3100HP formulation as nucleating agent.

4.1.2 Sample preparation

Continuous compression moulding (CCM)

The compression moulding machine, SACMI continuous compression moulding (CCM), is a complex but more precious process with high advantages Figure 4.1. All processing parameters such temperature (separate for extruder, and every cap-forming unit), compression pressure and duration, punch closing speed, and rotary speed were controlled from human machine interface (HMI).
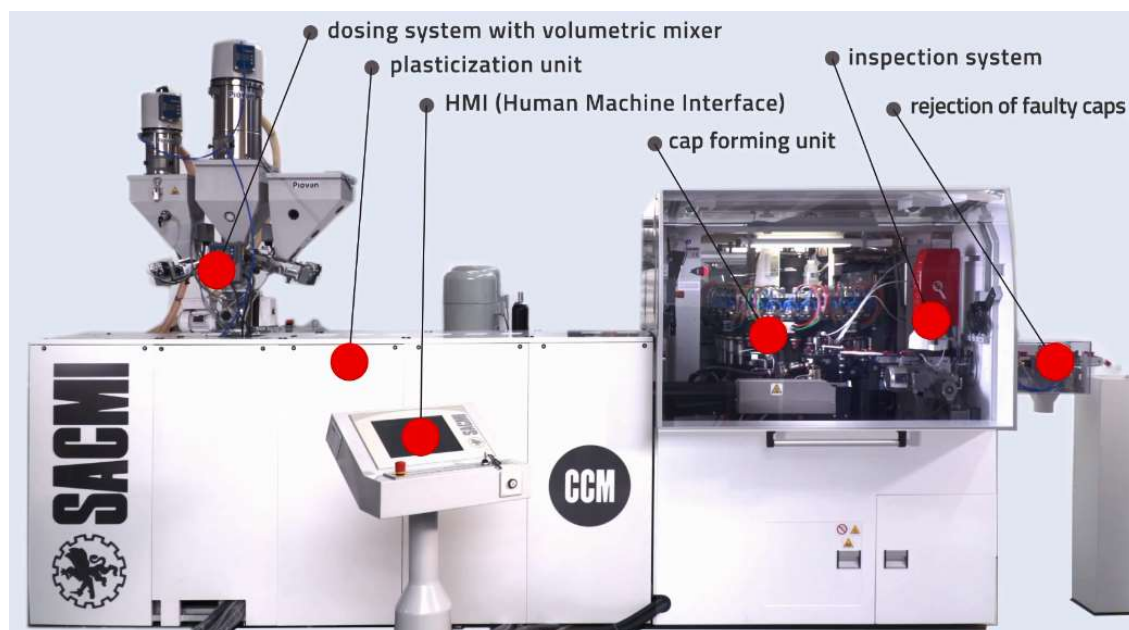
Figure 4.1: Continuous compression moulding (CCM) .

A continuous work cycle is carried out, during which the PLA material is fed by a plasticization unit, cut into suitably sized pellets and then inserted in the cavities. A hydraulic system clamps the moulds at a pressure that can be adjusted even while the production cycle is in progress Figure 4.2.
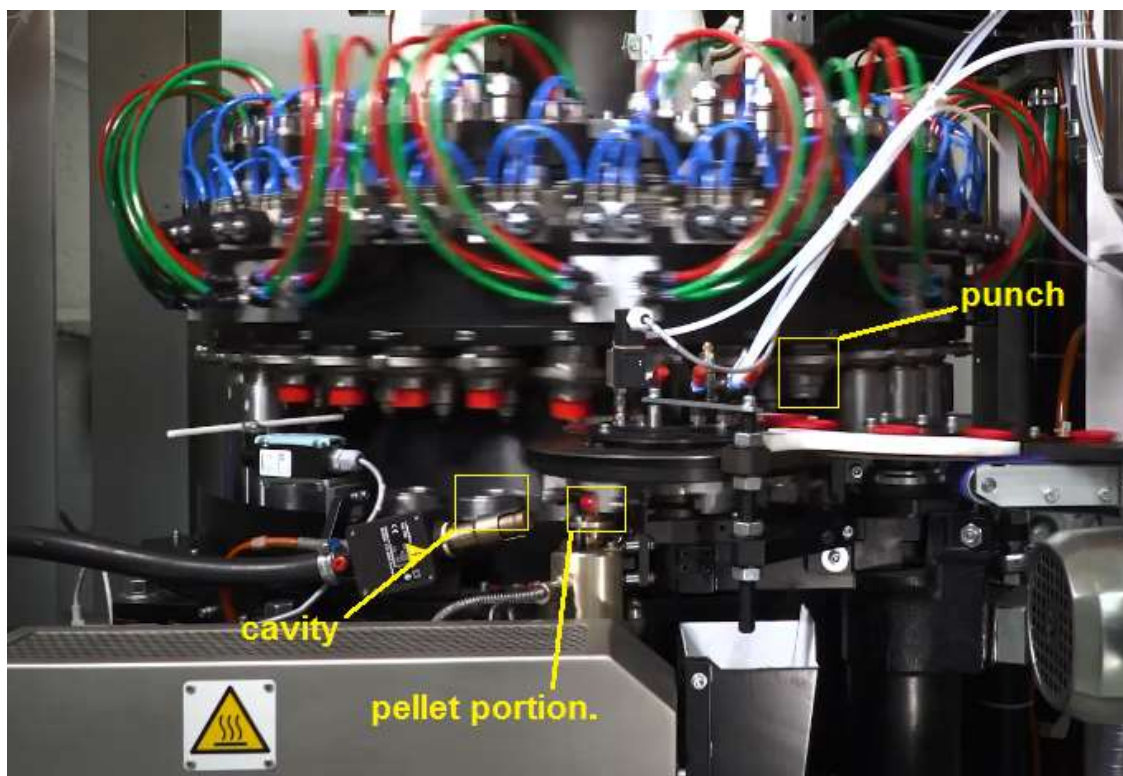
Figure 4.2: Rotary moulding system.

To avoid degradation due to hydrolysis and prevent the formation of voids during processing, PLA pellets were dried at 80 °C with in-line drying system placed before the dosing system.

In Table 4.2, were reported the processing condition adopted to obtain the best dimensional stability of coffee pods.

Table 4.2

Coffee pod	polymer	LAK	T_{mc}* [°C]	t cycle [s]	T punch [°C]	T cavity [°C]	Pressure [bar]
PLA_HW_1	HP2500	YES	170	4,8	20	20	110
PLA_HW_2	HP2500	YES	190	4,8	20	20	100
PLA_LW_1	HP3100	YES	170	4,8	20	20	100
PLA_LW_2	HP3100	YES	190	4,8	20	20	100
PLA_LW_3	HP3100	NO	170	4,8	20	20	100
PLA_LW_4	HP3100	NO	190	4,8	20	20	100
PLA_LW_5	HP3100	NO	210**	4,8	20	20	100

* T_{mc} = temperature meltcooler.
** Same temperature as extruder outlet.

4.1.3 Test Methods

Calorimeter

The melting behaviour of PLA coffee pods were performed using a rapid scanning calorimeter (DSC 8500, PerkinElmer, USA) under nitrogen atmosphere. Small sample pans with a diameter of 1.6 mm were used for the tests in order to minimize the effect of thermal gradients at the rapid scanning rates. Sample sizes of 0.1 - 0.2 mg were prepared by cutting a wall section of the coffee pods. The sample was heated from -50 °C to crystallization temperature, T_{iso} (100, 120 °C), at 600 °C/min and held isothermally (12, 30, 60 s). The sample was quenched at 20 °C and heated back at 20 °C/min to examine the effect of given isothermal history. The crystallinity (Xc) of PLA was calculated using the equation 1.3, chapter 1, and by subtracting the enthalpy of cold crystallization. The melt enthalpy (ΔH_m^0, equation 1.3 in chapter 1) of PLA with 100% crystallinity was reported to be 93 J/g [53].

4.2.   Results and Discussion

The DSC heat flow of coffee pods before the post-crystallization process was reported in Figure 4.3 and the results in Table 4.3.
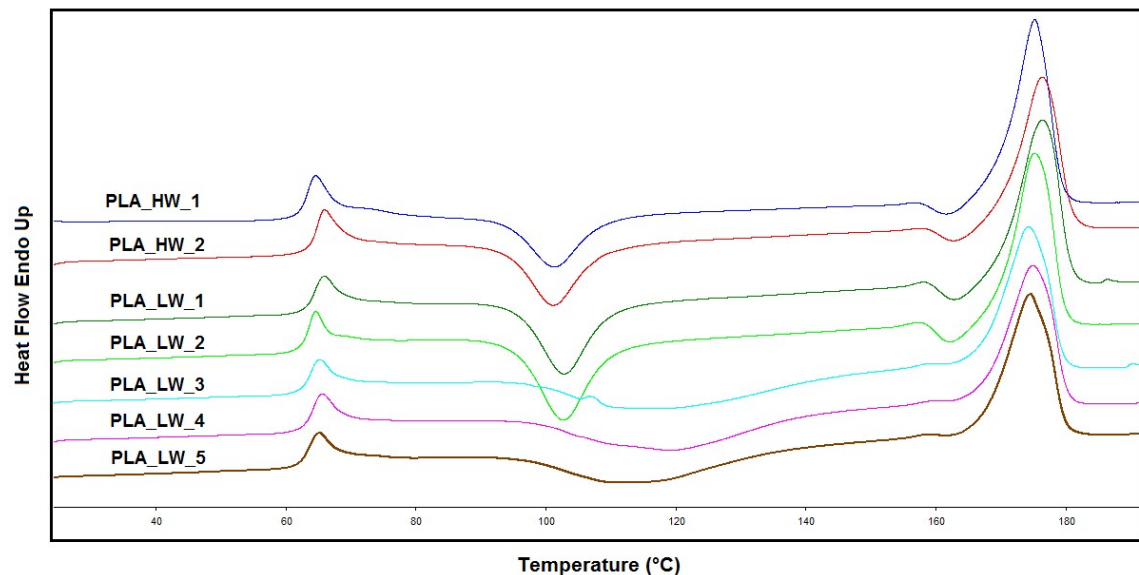
Figure 4.3: DSC heat flow curves during the first heating scan for coffee pods after CCM process.

In Figure 4.3 although coffee pods were moulded with different materials and different process parameters, all coffee pods show typically three physical transitions. These are: glass transition (Tg), cold crystallization (Tc), and melting of crystals (Tm), consistent with our previous study in chapter 3. The most interesting feature is the shift of cold crystallization for the pods (PLA_HW _1,2 and PLA LW_1,2) moulded with nucleating agents. They show that both the maximum rate of crystallisation and the time taken to achieve the total possible crystallinity are reduced by the presence of the nucleating agent. In particular, neat PLA coffee pods (PLA_LW_3,4,5) exhibits a broad crystallization peak at about 115 °C. For nucleated PLA samples (PLA_LW_1,2), the corresponding peak becomes much sharper and moves to lower temperature (101 °C) with nucleation agents.

Table 4.3:

Coffee pod	Tc (°C)	ΔHc (J/g)	Tm (°C)	ΔH (J/g)	Xc(%)
PLA_HW_1	101	-19	176	38	20
PLA_HW_2	101	-19	176	33	15
PLA_LW_1	103	-24	176	38	15
PLA_LW_2	103	-25	176	35	10
PLA_LW_3	118	-21	174	35	15
PLA_LW_4	118	-25	175	37	12
PLA_LW_5	115	-30	175	36	6

The resulting values were used to identify the temperatures for the post crystallization study. Two temperatures, 100 and 120 °C that cover all the cold crystallization range seen in Figure 4.3 were selected.

A first assess from Table 4.3 is that the meltcooler temperature affected the crystallinity values. Indeed, by comparing PLA_HW_1 Vs PLA_HW_2, PLA_LW_1 Vs PLA_LW_2, and PLA_LW_3 Vs PLA_LW_4 the lower was the meltcooler temperature in the process, the higher was the initial crystallinity.

The effects of isothermal annealing at the different times for all coffee pods previously moulding are reported from Figure 4.4 to Figure 4.7.
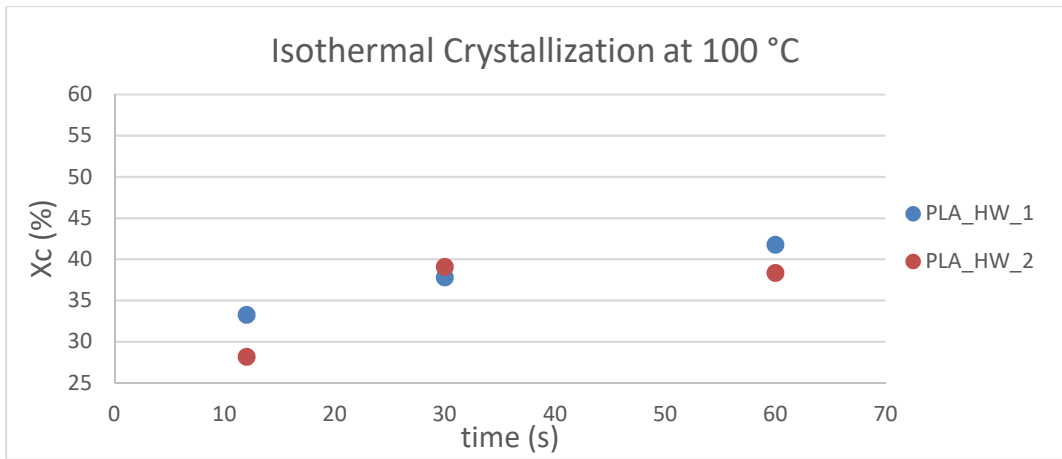
Figure 4.4: Isothermal crystallization at 100 °C for coffee pods moulding with nucleating agent and high molecular weight.
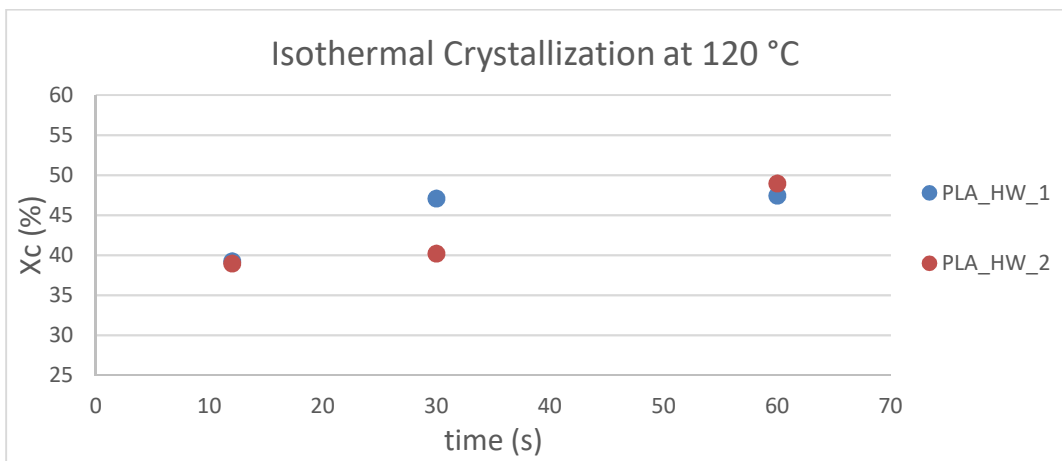
Figure 4.5: Isothermal crystallization at 120 °C for coffee pods moulding with nucleating agent and high molecular weight.
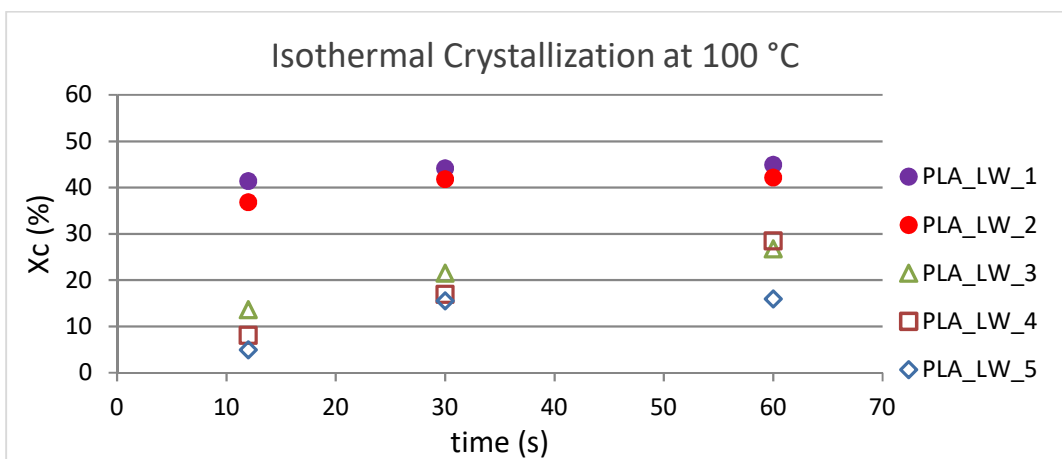
Figure 4.6: Isothermal crystallization at 100 °C for coffee pods moulding with/without nucleating agent and high/low molecular weight.
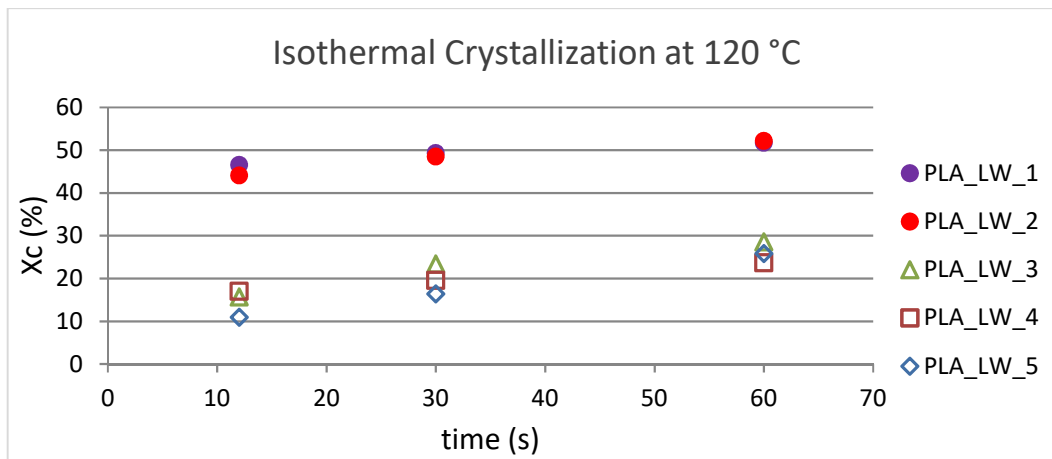
Figure 4.7: Isothermal crystallization at 120 °C for coffee pods moulding with/without nucleating agent and high/low molecular weight.

From these results, it can be observed how annealing for short periods greatly influences the crystallinity of the pods. For all the tests, the crystallinity response to annealing has an increasing trend with time. For the coffee pods moulded with nucleated material, the effect is more evident. The crystallinity values are twice the values of to the starting material. In fact, the starting materials have a crystallinity about 20 % while the final crystallinity after 60 s is about 45- 50 %. These values are conform to the standard for test in coffee machine. For the pods without nucleating agent, crystallinity increased to a much lower extent than that nucleated coffee pods. These results demonstrate how nucleating agent influenced the crystallization kinetics of the pods. In particular, the nucleating agent is more efficient during the annealing than the compression moulding process. This behaviour derived from concatenation of items induced by compression moulding process. These items are the temperature of the cavity/punch (20 ° C), the temperature of meltcooler, and the cycle time (4,8 s). In the continuous work cycle, the melt polymer was cut into suitably sized doses and then inserted in the cavities. The dose at the melting temperature, were transported inside the cavities of the rotary mould. The material is very rapidly cooled due to the stretching of the materials and the contact with the cold walls of the punch and cavity. The coffee pods leave the rotary mould in less than 5 seconds at a temperature lower than Tg. In this short time, there is no effect of nucleating, because the pods did not remain at the crystallization temperature for sufficient time to favour the crystallization. This explains why similar crystallinity values for pods of same

polymer grade but with and without nucleating agent were observed (Table 3.3). The results revealed that elongation deformation transformed an amorphous PLA into a crystalline fibrillary texture oriented in the flow direction [114].

The variables that influenced the post-crystallization of coffee pods were analysed separately in HyperDSC experiments. All the results obtained at t=0 seconds corresponded to the crystallinity of the coffee pods subsequently to the compression moulding step.

The influence of molecular weight
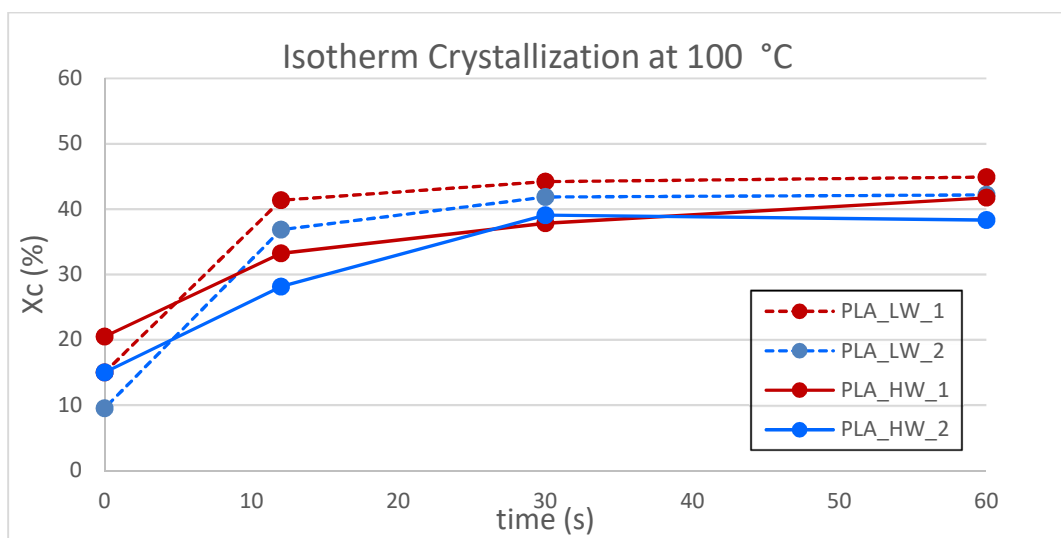
Figure 4.8: Effect of isotherm crystallization temperature (100 °C) on two grade of PLA with nucleating agent.
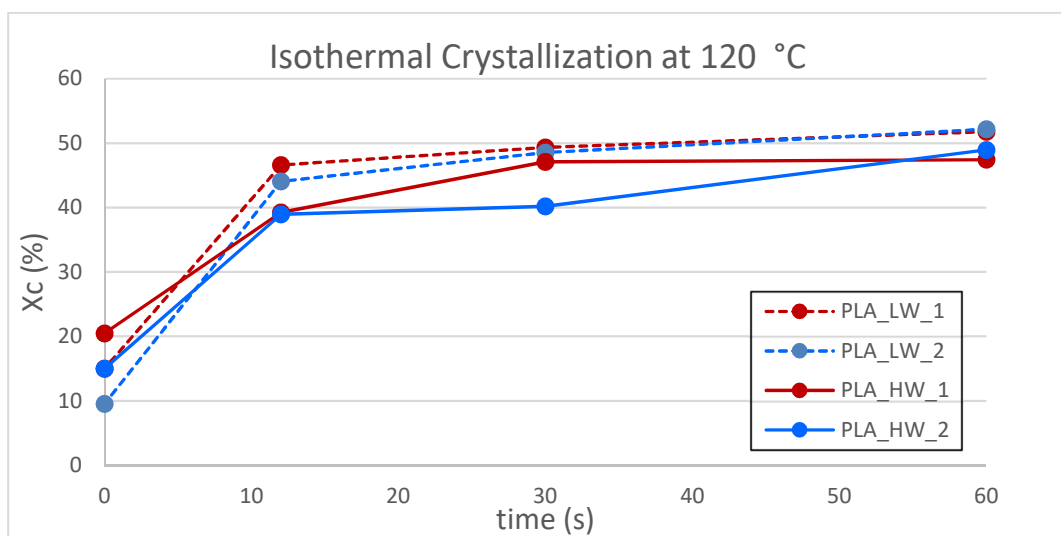
Figure 4.9: Effect of isotherm crystallization temperature (120 °C) on two grade of PLA with nucleating agent.

The influence of molecular weight (PLA_HW_1 and PLA_LW_1 related to 170 °C of melt cooler and PLA_HW _2 and PLA_LW_2 related to 190 °C of temperature), at different isothermal temperature are reported in Figure 4.8 and Figure 4.9.

In Figure 4.8 is possible to observe the polymers with higher molecular weights presented a higher initial crystallinity that is correlated to the lower mobility of the chains during the moulding step. During the annealing, due to this lower mobility, the crystallization rate is slower for higher molecular weight respect to the polymers with lower molecular weight (after 12 second the first reached values close to 28-30%, while the second values near 40%). After 30 seconds, for both polymers, the crystallization reached a plateau, with values' levelling off at 45 % for the samples with lower molecular weight.

In Figure 4.9 is possible to observed the same behaviour that was obtained from Figure 4.8 but there is an increase of crystallinity values.

The influence of nucleating agent
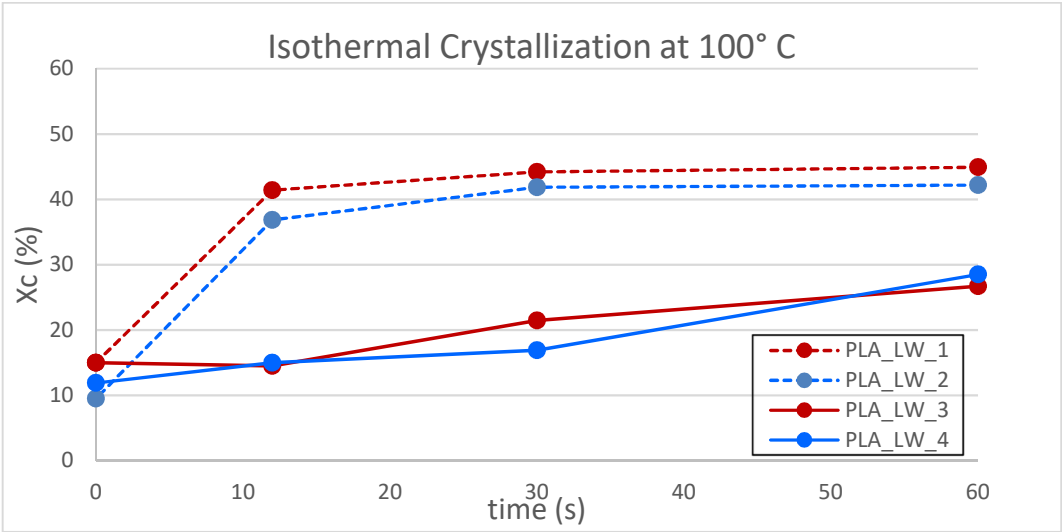
Figure 4.10: Effect of isotherm crystallization temperature (100 °C) on of PLA with or without nucleating agent.
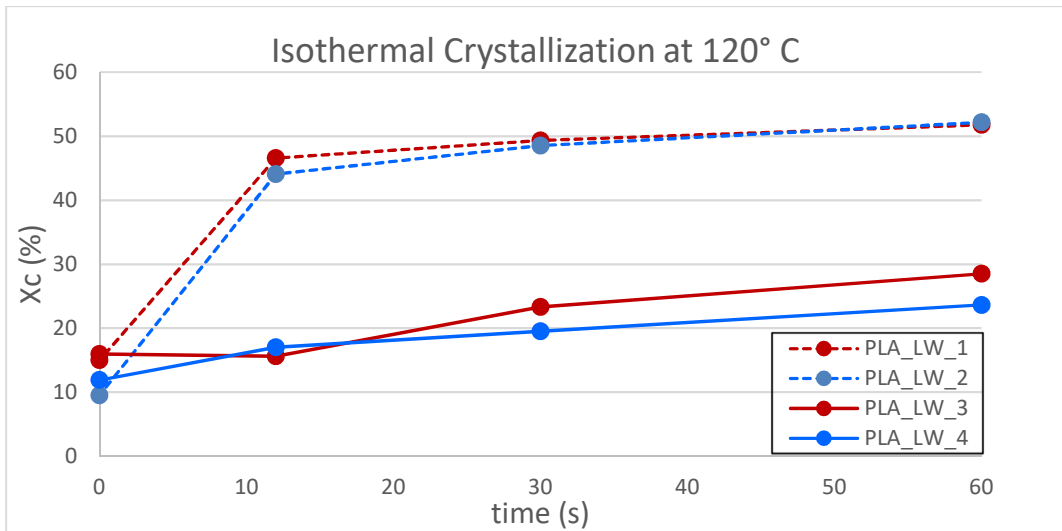
Figure 4.11: Effect of isotherm crystallization temperature (120 °C) on of PLA with or without nucleating agent.

From the results reported in figures 4.10 and 4.11 it is possible to observe the strong influence of the nucleating agent on the crystallization process of PLA. Already after 12 seconds, in presence of the LAK301, the crystallinity reached values higher than 40% (that is target value). After that time and reaching the 40%, the "free" chains present less mobility avoiding the folding process that lead the crystallization. This aspect is emphasized comparing the maximum crystallinity obtained during the isothermal treatment at 100 and 120 °C. Higher temperature favours the mobility and then the folding, reaching a crystallinity close to the 52%. As observed in the figures 4.8 and 4.9, the influence of the annealing step by meltcooler doesn't affect notably the performance of the final product.

The influence of meltcooler
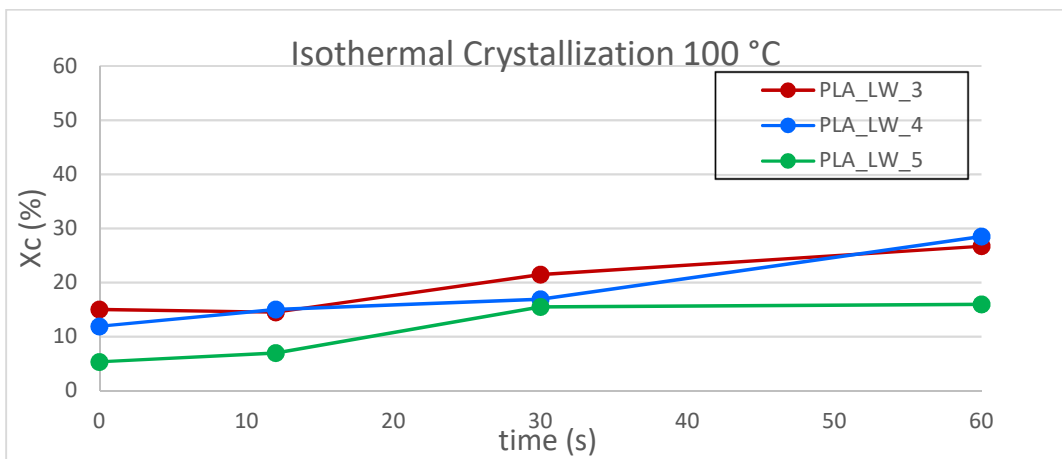
Figure 4.12: Effect of isotherm crystallization temperature (120 °C) on of PLA without nucleating agent and different melt cooling temperature.

95

Figure 4.13: Effect of isotherm crystallization temperature (120 °C) on of PLA with melt cooling temperature.

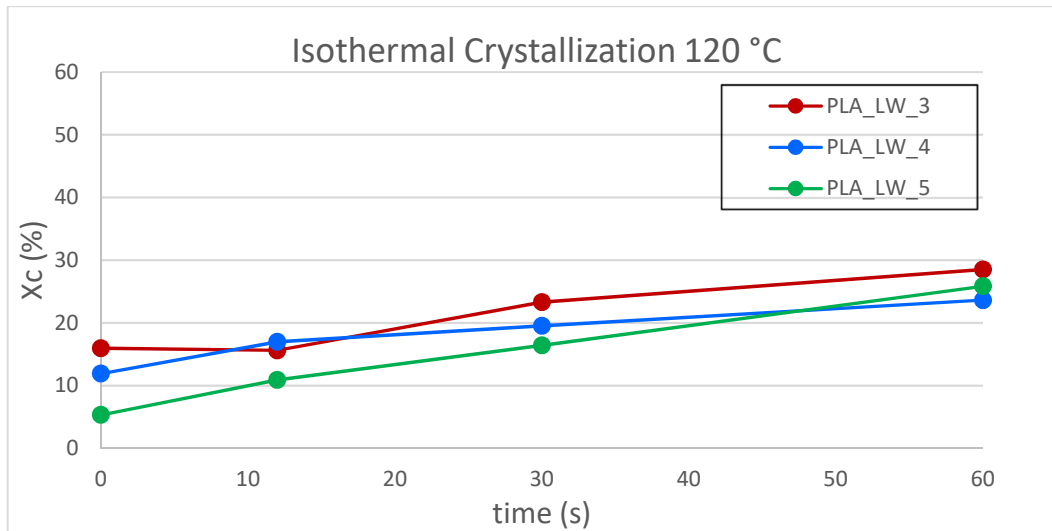The influence of melt cooler was reported respect the coffee pods moulding with PLA low molecular weight and without the nucleating agent. In Figure 4.12, the pods obtained with a meltcooling of 170 and 190 ° C, showed similar crystallinity values. The same result was also reported in the figures from 3.8 to 3.11. On the other hand, the pods obtained with meltcooling at 210 °C, have lower percentage of crystallinity. These differences can be correlated to the different trend of the polymers to their nucleation and growth processes (that is strictly correlated to the mobility of the chains as reported also in the chapter 3). Comparing the crystallization rates obtained during the isotherm at 100 °C, both the PLA_LW_3 and PLA_LW_4 presented the same values (where is reached the Xc close to the 30%). PLA_LW_5 showed a lower Xc, underlining even more the important effect of the annealing.

Increasing the temperature of the isotherm from 100 to 120 °C, a different behaviour was observed about the crystallinity rates. PLA_LW_5 showed the highest variation, reaching a crystallinity close to the 25%, that is similar to the results obtained with the PLA obtained after the annealing at lower temperatures. The different behaviour reported in Figure 4.13, compared to the one in figure 4.12, PLA_LW_3 and PLA_LW_4 presented the same trends, suggesting a lower influence of the isotherm treatment on the crystallinity. While, PLA_LW_5, showed a different behaviour, that can be explained taking into account the different amount and dimension of the spherulites.

In conclusion, at isotherm of 120 °C a successful crystallinity (45-50%) was observed. Moreover, the times to obtain these values are relatively low, around 12-30 seconds. From the point of view of the material, the fundamental role of nucleating in favouring the crystallization kinetics was evident. In fact, the crystallinity of coffee pods with nucleating agent is 20-25% higher than the non-nucleating material.

Starting from these results a post-moulding oven was designed in the collaboration of SACMI technical office. The purpose of this post-moulding oven is to reproduce, as better as possible, the post-crystallization step, investigated by means HyperDSC analysis on the coffee pods. The entire coffee pods are subjected to an isothermal treatment for different time. The result obtained from the design of the post-crystallization oven are shown in Figure 4.14.

Front Profile   Cross Profile   Rear Profile   Cross Profile
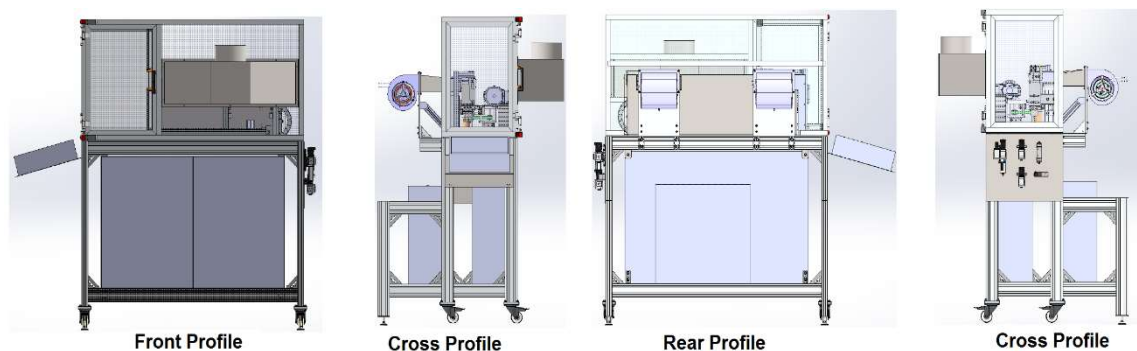
Figure 4.14: Post-crystallization oven.

In Figure 4.15 is reported the internal part of the oven that can be divided into two different areas. Area A is the core of the oven, where the pods (leaving the rotary mould at T<<Tg) reach the desired temperature by means a series of infrared lamps and heated for the necessary time. The quick heating helps to avoid the possible cold-crystallization processes that can occur when the system is heated. In the area B the pods are cooled down to room temperature.
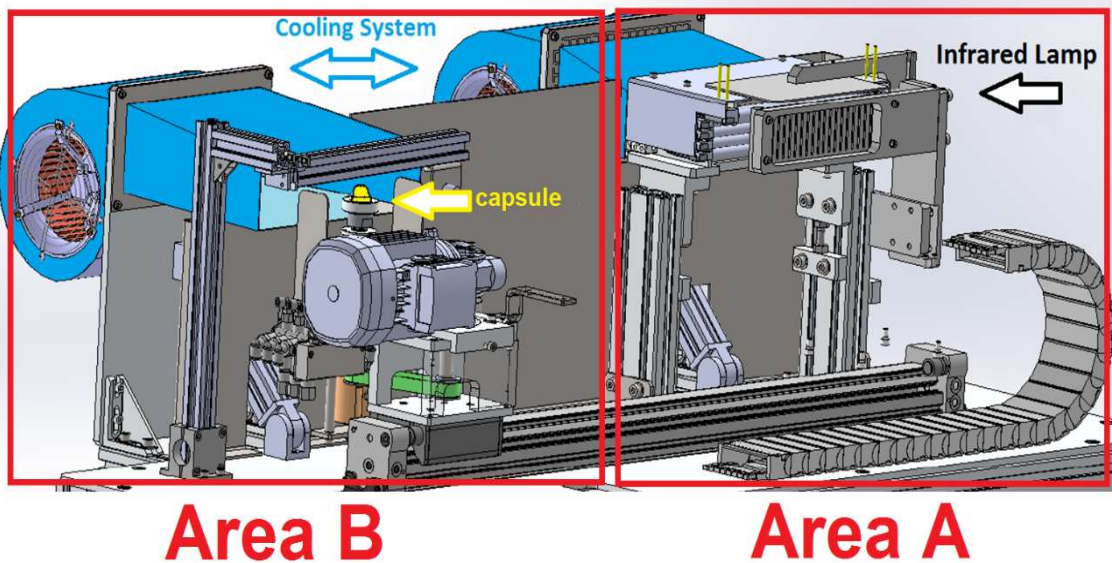
Figure 4.15: The internal profile of post-crystallization oven

A preliminary test was carried out by using the post-moulding oven on coffee pods obtained with the best operative parameters (reported in the previously results).
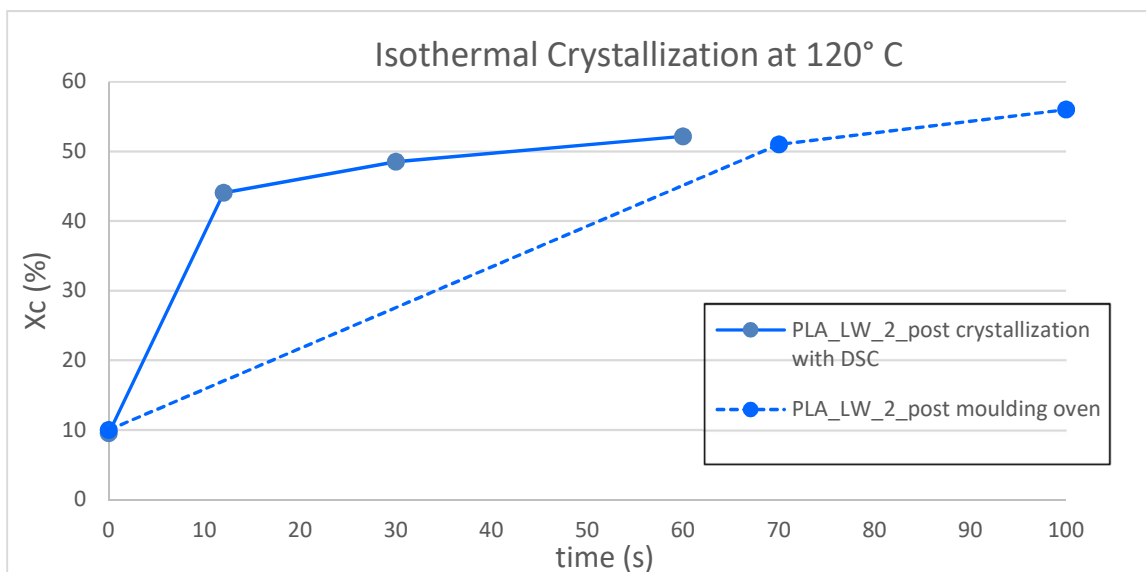
Figure 4.16: Isothermal crystallization at 120 °C of coffee pods analysed with Hyper DSC or post-moulding oven.

In Figure 4.16 are summarized the crystallinities of PLA_LW_2 obtained both with HyperDSC analysis and the post-moulding oven. For long times, the results show a good reproducibility of the results obtained by the oven and the HyperDSC. However, at shorter times there was not any appreciable improve of the crystallinity of the PLA was observed with the treatment by the oven (the results

are not reported). This discrepancy is correlated to the different heating exchange processes of the that take place when the PLA is heated by the oven and the DSC. With this latter, the polymer is placed inside a closed chamber, heated uniformly and where all the heating exchange resistances are reduced. While, for the scale up of the process, the heating exchanges are the rate-determinant step, because it is also necessary to minimize the sizes of the entire equipment. Another limitation to this process is correlated to the maximum operative temperature of the oven, because it is necessary to avoid reaching temperatures higher than 130 °C in order to minimize the possible deformation that can occur on the PLA coffee pods. Therefore, order to optimize the post-moulding oven further investigation will be performed.

However, the results obtained with post-moulding oven were encouraging. Indeed, SACMI will pursue this project in order to implement process line with this post-moulding oven.

5. **Conclusion**

The physical, mechanical and barrier properties of PLA depend on the solid-state morphology and its crystallinity. PLA can be either amorphous or semicrystalline depending on its stereochemistry and thermal history. A high crystallinity degree is desirable to increase the heat resistance of PLA but it is rather difficult to reach high values during compression moulding due to its very slow crystallization kinetics. For these reasons a in my thesis project I study two different approach in order to improve the thermal stability, crystallinity, and mechanical properties leading to reach the target value requested for the industrial application.

The results of first strategy came from the study of PLASC formation and crystallization by coupling Rheo-Raman technique. The coupling not only increases the information content from a single measurement, but also enables a direct comparison between rheological properties, fundamental in industry process, and their underlying physical changes associated with shifts in the viscoelastic profile. Since all measurements were performed simultaneously, experimental conditions such as temperature and pre-shear rate are identical for Raman spectroscopy and rheometer. This multimodal method allowed to correlate the bulk properties of obtained PLAsc to the pre-shear applied. The results have demonstrated that, applying a pre-shear, the crystallization kinetics is strongly affected. Determination of the induction time for different pre-shear conditions makes it possible to derive the quantitative dependence of the crystallization kinetics from the pre-shear conditions. In particular, the induction time is lower at high pre-shear (100-200 s^{-1}), but decreased more rapidly in the low shear rate range (0-60 s^{-1}). This means that with increasing shear rate it becomes more and more difficult to further accelerate the crystallization kinetics. Moreover, the operative temperature plays also an important role in the process, in particular, at 190 °C PLAsc with higher crystallinity was obtained. This can be correlated to the lower mobility of the chains that helps not only a lower induction time, but also a better growth of the crystallites. Comparing the results obtained with PLA with different molecular weight, it was shown the PLAsc with lower molecular weight presented a higher crystallinity thanks to their better capability to fold for the formation of the crystallites.

In the second strategy, the optimization of the industrial compression moulding process was done starting from the definition of a specific DSC method that simulate the industrial thermal treatments that the PLA undergoes. It was possible to determine the main parameters that affect post-crystallization of coffee-pods. In particular, the possibility of post crystallization of the coffee pods by annealing treatment was studied. The results of HyperDSC showed that the effect of the annealing temperature is more evident on coffee pods moulded with nucleated material. The crystallinity values are twice as compared to the starting material values. In fact, if the starting materials have a crystallinity about 20 % while the final crystallinity after 60 s is about 45- 50 %. These values are conform to the standard for test in coffee machine. For the coffee pods without nucleating agent, crystallinity increased to a much lower extent than that nucleated coffee pods. These results demonstrate how nucleating agent influenced the crystallization kinetics of the pods. In particular, the nucleating agent is more efficient during the annealing than the compression moulding process.

The crystallization kinetics obtained by DSC was adopted to design a post-moulding oven in order to implement process line of compression moulding. It was found that the predictions were accurate for samples treated according to protocol developed by HyperDSC. The predictions underestimated the crystallinity of the samples subjected to the post-moulding step. This was ascribed to the flow-induced crystallization, which enhances the crystallization kinetics of the material moulded in the cold mould. By adopting the post moulding step procedure, it was possible to producing crystalline samples with high crystallinity percentage respect the level required by final application. However, the time required (70-100 s) to increase the crystallinity, does not yet fall within the optimal process parameters.

Bibliography

[1]   R. Auras, B. Harte, and S. Selke, "An overview of polylactides as packaging materials," *Macromol. Biosci.*, vol. 4, no. 9, pp. 835–864, 2004.

[2]   M. Belgacem and A. Gandini, *Monomers, Polymers and Composites from Renewable Resources*. 2008.

[3]   PlasticsEurope Market Research Group (PEMRG) / Consultic Marketing & Industrieberatung GmbH, "Plastics – the Facts 2017," p. 16, 2017.

[4]   M. Niaounakis, *Biopolymers: Applycations and Trends*. Elsevier, 2015.

[5]   H. Benninga, *A History of Lactic Acid Making*, Springer., vol. 11. New York, 1990.

[6]   W. H. Carothers, G. L. Dorough, and F. J. van Natta, "Studies of Polymerization and ring formation. X. Reversible polymerization of six-membered cyclic esters," *Am. Chem. Soc.*, vol. 54, pp. 761–772, 1932.

[7]   M. Singh, B. Shirley, K. Bajwa, E. Samara, M. Hora, and D. O. Hagan, "Controlled release of recombinant insulin-like growth factor from a novel formulation of polylactide-co-glycolide microparticles," vol. 70, pp. 21–28, 2001.

[8]   Y. Baimark, R. Molloy, N. Molloy, J. Siripitayananon, and W. Punyodom, "Synthesis , characterization and melt spinning of a block copolymer of L-lactide and ε -caprolactone for potential use as an absorbable monofilament," vol. 6, pp. 699–707, 2005.

[9]   D. Benson *et al.*, "U.S. Patent," 5,357,035, 1994.

[10]   C. W. Scheele, "Kgl. Vetenskaps-Academiens nya Handlingar," vol. 1, Stockholm, pp. 116–124, 1780.

[11]   C. H. Holten, A. Müller, and D. Rehbinder, "Lactic Acid: Properties and Chemistry of Lactic Acid and Derivates," *Weinheim: Verlag Chemie*, p. 1971, 1971.

[12]   C. E. AVERY, "MANUFACTURE OF LACTATES," 1881.

[13]   H. Benninga, "A History of Lactic Acid Making." Kluwer Academic Publishers, Dordrecht, 1990.

[14]   A. Jimenez, M. Peltzer, and R. Ruseckaite, *Poly(lactic acid) Science and Technology Processing, Properties, Additives and Applications*. Cambridge: The Royal Society of Chemistry, 2015.

[15]   R. Auras, L.-T. Lim, S. E. M. Selke, and H. Tsuji, *Poly (lactic Acid) Synthesis, Structure, Properties, Processing, and Application*. Hoboken, NJ, USA, 2010.

[16]   J. Van Krieken, "Method for the purification of α -hydroxy acids on an industrial scale," WO0222544 (A1), 2002.

[17]   O. Kandler, "Carbohydrate metabolism in lactic acid bacteria," *Antonie Van Leeuwenhoek*, vol. 49, no. 3, pp. 209–224, 1983.

[18]   S. Ding and T. Tan, "l-lactic acid production by Lactobacillus casei fermentation using different fed-batch feeding strategies," *Process Biochem.*, vol. 41, no. 6, pp. 1451–1454, 2006.

[19]   A. Aeschlimann, L. Di Stasi, and U. Von Stockar, "Continuous production of lactic acid from whey permeate by Lactobacillus helveticus in two chemostats in series," vol. 12, pp. 811–816, 2000.

[20]   "Corbion (2015) Corbion Purac successfully develops PLA resin from second generation feedstocks.," 2016. [Online]. Available:

http://www.corbion.com/media/press-releases?newsI.

[21] J. Pelouze, "Ueber die Milchsäure," *European J. Org. Chem.*, vol. 53, pp. 112–124, 1845.

[22] R. Grueter and H. Pohl, "Manufacture of lactid.," US1095205 A, 1914.

[23] R. G. Sinclair, R. A. Markle, and R. K. Smith, "Lactide production from dehydration of aqueous lactic acid feed," US1095205 A, 1992.

[24] M. H. Hartmann, "High molecular weight polylactic acid polymers.," *Biopolym. from Renew. Resour.*, pp. 367–411, 1998.

[25] P. R. Gruber, J. J. Kolstad, E. S. Hall, R. S. E. Conn, and C. M. Ryan, "Melt- stable lactide polymer composition and process for manufacture thereof," US5338822 A, 1994.

[26] P. Gruber, E. Hall, J. Kolstad, M. L. Iwen, R. Benson, and R. Borchardt, "Continuous process for manufacture of lactide polymers with controlled optical purity," US5258488 A, 1993.

[27] I. D. Fridman and J. Kwok, "Lactide melt recrystallization," US5264592 A, 1993.

[28] P. Coszach, J. C. Bogaert, and F. Van Gansberghe, "Method for the productiion of polylactide from a solution of lactic acid or one of the derivatives thereof," US20060014975 A1, 2006.

[29] R. U. Scholz and D. S. R. P. Van, "Purification of lactide rich streams," WO2007148975 A3, 2008.

[30] D. K. Yoo, D. Kim, and D. S. Lee, "Reaction kinetics for the synthesis of oligomeric poly(lactic acid)," *Macromol. Res.*, vol. 13, no. 1, pp. 68–72, 2005.

[31] S. I. Moon, C. W. Lee, M. Miyamoto, and Y. Kimura, "Melt polycondensation of L-lactic acid with Sn(II) catalysts activated by various proton acids: A direct manufacturing route to high molecular weight Poly(L-lactic acid)," *J. Polym. Sci. Part A Polym. Chem.*, vol. 38, no. 9, pp. 1673–1679, 2000.

[32] J. Nieuwenhuis, "Synthesis of Polylactides, Polyglycolides and Their Copolymers," *Clin. Mater.*, vol. 10, no. 1–2, pp. 59–67, 1992.

[33] A. J. Nijenhuis, D. W. Grijpma, and A. J. Pennings, "Lewis acid catalyzed polymerization of L-lactide. Kinetics and mechanism of the bulk polymerization," *Macromolecules*, vol. 25, no. 24, pp. 6419–6424, 1992.

[34] H. R. Kricheldorf and B. Fechner, "Polylactones. 59. Biodegradable Networks via Ring-Expansion Polymerization of Lactones and Lactides with a Spirocyclic Tin Initiator," *Biomacromolecules*, vol. 3, no. 4, pp. 691–695, 2002.

[35] P. Dubois, C. Jacobs, R. Jerome, and P. Teyssie, "Macromolecular engineering of polylactones and polylactides. 4. Mechanism and kinetics of lactide homopolymerization by aluminum isopropoxide," *Macromolecules*, vol. 24, no. 9, pp. 2266–2270, 1991.

[36] Z. Zhong, P. J. Dijkstra, and J. Feijen, "Controlled and Stereoselective Polymerization of Lactide: Kinetics, Selectivity, and Microstructures," *J. Am. Chem. Soc.*, vol. 125, no. 37, pp. 11291–11298, 2003.

[37] A. Kowalski, A. Duda, and S. Penczek, "Mechanism of Cyclic Ester Polymerization Initiated with Tin(II) Octoate. 2. [†] Macromolecules Fitted with Tin(II) Alkoxide Species Observed Directly in MALDI−TOF Spectra," *Macromolecules*, vol. 33, no. 3, pp. 689–695, 2000.

[38] Y. Ikada, K. Jamshidi, H. Tsuji, and S. H. Hyon, "Stereocomplex Formation

between Enantiomeric Poly(lactides),” *Macromolecules*, vol. 20, no. 3, pp. 904–906, 1987.

[39] H. Tsuji, “Poly (lactic acid) stereocomplexes : A decade of progress ☆,” *Adv. Drug Deliv. Rev.*, vol. 107, pp. 97–135, 2016.

[40] T. Ke and X. Sun, “Melting behavior and crystallization kinetics of starch and poly(lactic acid) composites.,” *J. Appl. Polym. Sci.*, vol. 89, no. 5, pp. 1203–1211, 2003.

[41] P. De Santis and A. J. Kovacs, “Molecular conformation of poly(S- lactic acid).,” *Biopolymers*. pp. 299–306, 1968.

[42] B. Kalb and A. J. Pennings, “GENERAL CRYSTALLIZATION BEHAVIOUR OF POLY(L-LACTIC ACID).,” *Polymer*, vol. 21. pp. 607–612, 1980.

[43] J. Kobayashi *et al.*, “Structural and optical properties of poly lactic acids.,” *Journal of Applied Physics*, vol. 77. pp. 2957–2973, 1995.

[44] J. Zhang *et al.*, “Crystal modifications and thermal behavior of poly(L-lactic acid) revealed by infrared spectroscopy.,” *Macromolecules,* vol. 38. pp. 8012–8021, 2005.

[45] J. Zhang, K. Tashiro, H. Tsuji, and A. J. Domb, “Disorder-to-order phase transition and multiple melting behavior of poly(L-lactide) investigated by simultaneous measurements of WAXD and DSC.,” *Macromolecules*, vol. 41. pp. 1352–1357, 2008.

[46] M. Cocca, M. L. D. Lorenzo, M. Malinconico, and V. Frezza, “Influence of crystal polymorphism on mechanical and barrier properties of poly(l-lactic acid).,” *European Polymer Journal*, vol. 47. pp. 1073–1080, 2011.

[47] L. Cartier, T. Okihara, Y. Ikada, H. Tsuji, J. Puiggali, and B. Lotz, “Epitaxial crystallization and crystalline polymorphism of polylactides,” *Polymer (Guildf).*, vol. 41, no. 25, pp. 8909–8919, 2000.

[48] K. Aou and S. L. Hsu, “Trichroic vibrational analysis on the α-form of poly (lactic acid) crystals using highly oriented fibers and spherulites,” *Macromolecules*, vol. 39, pp. 3337–3344, 2006.

[49] B. Eling, S. Gogolewski, and A. J. Pennings, “BIODEGRADABLE MATERIALS OF POLY(L-LACTIC ACID) - 1. MELT-SPUN AND SOLUTION-SPUN FIBRES.,” *Polymer*, vol. 23. pp. 1587–1593, 1982.

[50] J. Puiggali, Y. Ikada, H. Tsuji, L. Cartier, T. Okihara, and B. Lotz, “The frustrated structure of poly(L-lactide).,” *Polymer*, vol. 41. pp. 8921–8930, 2000.

[51] J.-R. Sarasua, R. E. Prud’homme, M. Wisniewski, A. Le Borgne, and N. Spassky, “Crystallization and melting behavior of polylactides,” *Macromolecules*, vol. 31. pp. 3895–3905, 1998.

[52] F. Chabot, M. Vert, S. Chapelle, and P. Granger, “CONFIGURATIONAL STRUCTURES OF LACTIC ACID STEREOCOPOLYMERS AS DETERMINED BY 13C-{1H} n.m.r.,” *Polymer*, vol. 24. pp. 53–59, 1983.

[53] Z. Gui, C. Lu, and S. Cheng, “Comparison of the effects of commercial nucleation agents on the crystallization and melting behaviour of polylactide,” *Polym. Test.*, vol. 32, no. 1, pp. 15–21, 2013.

[54] H. Abe, Y. Kikkawa, Y. Inoue, and Y. Doi, “Morphological and Kinetic Analyses of Regime Transition for Poly[(S)-lactide] Crystal Growth.,” *Biomacromolecules*, vol. 2. pp. 1007–1014, 2001.

[55] J. R. Dorgan, J. Janzen, M. P. Clayton, S. B. Hait, and D. M. Knauss, “Melt rheology of variable L-content poly(lactic acid).,” *J. Rheol. (N. Y. N. Y).*, vol. 49, pp. 607–619, 2005.

[56] K. Jamshidi, S. H. Hyon, and Y. Ikada, "Thermal characterization of polylactides.," *Polymer*, vol. 29. pp. 2229–2234, 1988.

[57] D. R. Witzke, "Introduction to properties, engineering, and prospects of polylactide polymers." Michigan State University: Michigan., 1997.

[58] J. Huang *et al.*, "Crystallization and Microstructure of Poly(L-lactide-co-meso-lactide) Copolymers," *Macromolecules*, vol. 31, no. 8, pp. 2593–2599, 1998.

[59] M. L. Di Lorenzo, "Determination of spherulite growth rates of poly(L-lactic acid) using combined isothermal and non-isothermal procedures," *Polymer (Guildf).*, vol. 42, no. 23, pp. 9441–9446, 2001.

[60] T. Miyata and T. Masuko, "Crystallization behaviour of poly(L-lactide)," *Polymer (Guildf).*, vol. 39, no. 22, pp. 5515–5521, 1998.

[61] S. Saeidlou, M. A. Huneault, H. Li, and C. B. Park, "Poly(lactic acid) crystallization," *Prog. Polym. Sci.*, vol. 37, no. 12, pp. 1657–1677, 2012.

[62] D. Garlotta, "A literature review of poly(Lactic Acid).," *J. Polym. Environ.*, vol. 9, no. 2, pp. 63–84, 2001.

[63] Q. Fang and M. A. Hanna, "Rheological properties of amorphous and semicrystalline polylactic acid polymers.," *Ind. Crop. Prod.*, vol. 10, pp. 47–53, 1999.

[64] J. J. Cooper-white and M. E. Mackay, "Rheological Properties of Poly (lactides). Effect of Molecular Weight and Temperature on the Viscoelasticity of Poly (l-lactic acid)," pp. 1803–1814, 1999.

[65] H. Tsuji and Y. Ikada, "Properties and morphologies of poly(L-lactide): 1. Annealing condition effects on properties and morphologies of poly(L-lactide)," *Polymer (Guildf).*, vol. 36, no. 14, pp. 2709–2716, 1995.

[66] I. Pillin, N. Montrelay, and Y. Grohens, "Thermo- mechanical characterization of plasticized PLA: Is the miscibility the only significant factor?," *Polymer*, vol. 47. pp. 4676–4682, 2006.

[67] O. Martin and L. Avérous, "Poly (lactic acid): plasticization and properties of biodegradable multiphase systems," *Polymer*, vol. 42. pp. 6209–6219, 2001.

[68] Z. Kulinski, E. Piorkowska, K. Gadzinowska, and M. Stasiak, "Plasticization of poly(L-lactide) with poly(propylene glycol).," *Biomacromolecules*, vol. 7, pp. 2128–2135, 2006.

[69] K. Sungsanit, N. Kao, and S. N. Bhattacharya, "Properties of linear poly(lactic acid)/polyethylene glycol blends.," *Polym. Eng. Sci.*, vol. 52, pp. 108–116, 2012.

[70] R. Legras, J. P. Mercier, and E. Nield, "Polymer crystallization by chemical nucleation.," *Nature*, vol. 304, pp. 432–434, 1983.

[71] H. Li and M. A. Huneault, "Effect of nucleation and plasticization on the crystallization of poly(lactic acid).," *Polymer*, vol. 48. pp. 6855–6866, 2007.

[72] J. J. Kolstad, "Crystallization kinetics of poly(L-lactide-co- meso-lactide).," *J. Appl. Polym. Sci.*, vol. 62, pp. 1079–1091, 1996.

[73] J. Y. Nam, M. Okamoto, H. Okamoto, M. Nakano, A. Usuki, and M. Matsuda, "Morphology and crystallization kinetics in a mixture of low-molecular weight aliphatic amide and polylactide.," *Polymer*, vol. 47. pp. 1340–1347, 2006.

[74] D. M. Bigg, "Controlling the performance and rate of degradation of polylactide copolymers.in 61st Annual Technical Conference ANTEC 2003, May 4, 2003 - May 8, 2003. 2003. Nashville, TN, United states: Society of

Plastics Engineers.," 2003.

[75] S. Brochu, R. E. Prud'homme, I. Barakat, and R. Jérôme, "Stereocomplexation and Morphology of Polylactides," *Macromolecules*, vol. 28, no. 15, pp. 5230–5239, 1995.

[76] K. S. Anderson and M. A. Hillmyer, "Melt preparation and nucleation efficiency of polylactide stereocomplex crystallites," *Polymer (Guildf).*, vol. 47, no. 6, pp. 2030–2035, 2006.

[77] S. C. Schmidt and M. A. Hillmyer, "Polylactide Stereocomplex Crystallites as Nucleating Agents for Isotactic Polylactide," pp. 300–313, 2000.

[78] H. Tsuji, H. Takai, and S. K. Saha, "Isothermal and non-isothermal crystallization behavior of poly(l-lactic acid): Effects of stereocomplex as nucleating agent.," *Polymer (Guildf).*, vol. 47, pp. 3826–3837, 2006.

[79] T. Okihara *et al.*, "Crystal structure of stereocomplex of poly(L-lactide) and poly(D-lactide).," *Macromol. Sci. - Phys.*, vol. 30, pp. 119–140, 1991.

[80] H. Tsuji, "Poly (lactide) Stereocomplexes : Formation , Structure , Properties , Degradation , and Applications," *Macromol. Biosci.*, vol. 5, pp. 569–597, 2005.

[81] D. Brizzolara, H. J. Cantow, K. Diederichs, E. Keller, and A. J. Domb, "Mechanism of the stereocomplex formation between enantiomeric poly(lactide)s," *Macromolecules*, vol. 29, no. 1, pp. 191–197, 1996.

[82] K. Jamshidi, S. Hyon, and Y. Ikada, "Thermal Characterization of polylactides," *Polym. Mater.*, vol. 29, pp. 2229–2234, 1988.

[83] H. Tsuji and Y. Ikada, "Stereocomplex formation between enantiomeric poly (lactic acid) s . XI . Mechanical properties and morphology of solution-cast films," *Polymer (Guildf).*, vol. 40, pp. 6699–6708, 1999.

[84] H. Tsuji, S. Hyon, and Y. Ikada, "Stereocomplex Formation between Enantiomeric Poly (1actic acid) s . 4 . Differential Scanning Calorimetric Studies on Precipitates from Mixed Solutions of Poly (D-lactic acid) and Poly (L-lactic acid)," *Macromolecules*, pp. 5657–5662, 1991.

[85] H. Tsuji, S. H. Hyon, and Y. Ikada, "Stereocomplex formation between enantiomeric poly(lactic acid)s. 3. Calorimetric studies on blend films cast from dilute solution.," *Macromolecules*, vol. 24, pp. 5651–5656, 1991.

[86] G. Kister, G. Cassanas, and M. Vert, "Effects of morphology , conformation and configuration on the IR and Raman spectra of various poly (lactic acid) s," *Polymer (Guildf).*, vol. 39, no. 2, pp. 267–273, 1998.

[87] J. Zhang, H. Tsuji, I. Noda, and Y. Ozaki, "Structural changes and crystallization dynamics of poly(L-lactide) during the cold-crystallization process investigated by infrared and two-dimensional infrared correlation spectroscopy," *Macromolecules*, vol. 37, no. 17, pp. 6433–6439, 2004.

[88] H. Tsuji and I. Yoshito, "Stereocomplex formation between enantiomeric poly(lactic acid)s. 9. Stereocomplexation from the melt.," *Macromolecules*, vol. 26, pp. 6918–6926, 1993.

[89] M. Thielen, "Eco-centric mobile phone," *Bioplastics Mag.*, vol. 4, no. 6, p. 27, 2009.

[90] "Regulation No 1935/2004 of the European Parliament and of the Council of 27 October 2004 on materials and articles intended to come in contact with food and repealing Directives 80/590/EEC and 89/109/EEC," *Official Journal of the European Union*. 2009.

[91] N. S. Oliveira, J. Oliveira, T. Gomes, A. Ferreira, J. Dorgan, and I. M. Marrucho, "Gas sorption in poly(lactic acid) and packaging materials," *Fluid*

Phase Equilib., vol. 222–223, pp. 317–324, 2004.

[92] S. Shang, A. Ro, S. J. Huang, and R. A. Weiss, *Functional Polymers From Renewable Resources*. 2006.

[93] L. T. Lim, R. Auras, and M. Rubino, "Processing technologies for poly(lactic acid)," *Prog. Polym. Sci.*, vol. 33, no. 8, pp. 820–852, 2008.

[94] S. Saeidlou, M. A. Huneault, H. Li, and C. B. Park, "Poly (lactic acid) Stereocomplex Formation : Application to PLA Rheological Property Modification," vol. 41073, pp. 1–8, 2014.

[95] J. Bai *et al.*, "Stereocomplex Crystallite-Assisted Shear-Induced Crystallization Kinetics at a High Temperature for Asymmetric Biodegradable PLLA/ PDLA Blends," *Am. Chem. Soc.*, vol. 4, pp. 273–283, 2016.

[96] J. Xu *et al.*, "Shear-induced stereocomplex cylindrites in polylactic acid racemic blends : Morphology control and interfacial performance," vol. 140, pp. 179–187, 2018.

[97] J. Ahmed, S. K. Varshney, and F. Janvier, "Rheological and thermal properties of stereocomplexed polylactide films," pp. 2053–2061, 2014.

[98] X. Wei, R. Bao, Z. Cao, W. Yang, B. Xie, and M. Yang, "Stereocomplex Crystallite Network in Asymmetric PLLA/PDLA Blends: Formation, Structure, and Con fi ning E ff ect on the Crystallization Rate of Homocrystallites," 2014.

[99] Z. Zhang *et al.*, "Enhanced Heat Deflection Resistance via Shear Flow-Induced Stereocomplex Crystallization of Polylactide Systems," 2017.

[100] Y. Liu *et al.*, "Melt stereocomplexation from poly (L -lactic acid) and poly (D -lactic acid) with different optical purity," *Polym. Degrad. Stab.*, vol. 98, no. 4, pp. 844–852, 2013.

[101] E. M. Woo and L. Chang, "Crystallization and morphology of stereocomplexes in nonequimolar mixtures of poly (L -lactic acid) with excess poly (D -lactic acid)," *Polymer (Guildf).*, vol. 52, no. 26, pp. 6080–6089, 2011.

[102] D. Qin and R. T. Kean, "Crystallinity determination of polylactide by FT-Raman spectrometry," *Appl. Spectrosc.*, vol. 52, no. 4, pp. 488–495, 1998.

[103] G. Kister, G. Cassanas, M. Bergounhon, D. Hoarau, and M. Vert, "Structural characterization and hydrolytic degradation of solid copolymers of d,l-lactide-co-ε-caprolactone by Raman spectroscopy," *Polymer (Guildf).*, vol. 41, no. 3, pp. 925–932, 2000.

[104] "ASTM D1238 - Standard Test Method for Melt Flow Rates of Thermoplastics by Extrusion Plastometer," *Annual Book of ASTM Standards*, no. August. pp. 1–16, 2013.

[105] A. P. Kotula *et al.*, "The rheo-Raman microscope : Simultaneous chemical , conformational , mechanical , and microstructural measures of soft materials," *Rev. Sci. Instrum.*, vol. 87, p. 105105, 2016.

[106] R. B. Bird, R. C. Armstrong, and O. Hassager, *Dynamics of Polymeric Liquids, Volume 1: Fluid Mechanics*, vol. 1. 1987.

[107] D. Drapcho, J. P. Plog, and N. Crawford, "Monitoring Polymer Phase Transitions by Combining Rheoloy and Raman Spectroscopy," *Spectroscopy*, vol. 32, no. 6, pp. 18–28, 2017.

[108] N. V. Pogodina, H. H. Winter, and S. Srinivas, "Strain effects on physical gelation of crystallizing isotactic polypropylene," *J. Polym. Sci. Part B Polym. Phys.*, vol. 37, no. 24, pp. 3512–3519, 1999.

[109] Y. Song *et al.*, "Enhancement of stereocomplex formation in poly (L - lactide)/ poly (D -lactide) mixture by shear," *Polymer (Guildf).*, vol. 72, pp. 185–192, 2015.

[110] R. Pantani, V. Speranza, and G. Titomanlio, "Simultaneous morphological and rheological measurements on polypropylene : Effect of crystallinity on viscoelastic parameters," vol. 377, pp. 0–14, 2015.

[111] H. H. Winter and M. Mours, "Rheology of Polymers Near Liquid-Solid Transitions," vol. 134, 1997.

[112] F. Parinello and F. Pucci, "A METHOD AND AN APPARATUS FOR COMPRESSION MOULDING AN OBJECT MADE OF POLYMERIC MATERIAL," 20180117803, 2018.

[113] M. K. Fehri *et al.*, "Composition dependence of the synergistic effect of nucleating agent and plasticizer in poly(lactic acid): A mixture design study," *Express Polym. Lett.*, vol. 10, no. 4, pp. 274–288, 2016.

[114] M. Pluta and A. Galeski, "Plastic deformation of amorphous poly(L/DL-lactide): Structure evolution and physical properties," *Biomacromolecules*, vol. 8, no. 6, pp. 1836–1843, 2007.